EFFECTS OF SUSPENSION AND STEERING PARAMETERS ON HANDLING OF A LIGHT COMMERCIAL VEHICLE

by

Artuğ Acar

B.S., M.E., Ege University, 2003

Submitted to the Institute for Graduate Studies in
Science and Engineering in partial fulfillment of
the requirements for the degree of
Master of Science

Graduate Program in FBE Program for which the Thesis is Submitted
Boğaziçi University
2006

ACKNOWLEDGEMENTS

I would like to thank my advisor, Dr. Günay Anlaş for his academic support that made this thesis possible, and for his patience in correcting my errors.

I thank Dr. Emre Aksan with whom I had the opportunity to work as a teaching assistant for his concern, tolerance, encouragement and for all his valuable helps during this two years.

I would also like to thank Mrs. Banu Sinanoğlu for supplying all measurements data used here and her valuable academic advice.

I thank Mr. Aydın Kuntay, Bias Inc., for allowing me to attend their professional ADAMS seminars and conferences.

Finally, I would like to thank my parents, my brother and my grandmother for their encouragement and understanding during this study.

ABSTRACT

EFFECTS OF SUSPENSION AND STEERING PARAMETERS ON HANDLING OF A LIGHT COMMERCIAL VEHICLE

The influence of suspension and steering geometry parameters on lateral drift of a light commercial vehicle is investigated by using Automatic Dynamic Analysis of Mechanical Systems (ADAMS). The aim of this study is to order the effect of suspension parameters on lateral drift. The vehicle that is used in this study is produced in Turkey and is widely used as a light commercial vehicle.

Front and rear suspension parameters of the vehicle such as toe, camber and caster are modified in a range in ADAMS/Chassis to calculate their effect on lateral drift. Road tests are done using a real vehicle to compare road test results to computational ones. The effect of suspension parameters on lateral drift of the vehicle are measured to decide which parameters dominate lateral displacement under suitable road conditions without any external input such as wind or unsteady road crown. The suspension parameters that dominate lateral drift of the vehicle the most are determined using a DOE analysis.

As a result of statistical analysis, front toe, front caster and rear toe are together dominant parameters that affect lateral drift of the vehicle. The third important parameter group includes front camber and rear toe. It has only two parameters to be equally aligned for the left and right handsides. So, in the assembly of this vehicle front camber and rear toe angles should be perfectly aligned to overcome lateral drift problem.

ÖZET

HAFİF TİCARİ ARAÇ ASKI DONANIMI PARAMETRELERİNİN YOL TUTUŞUNA ETKİLERİ

Bu çalışmada ADAMS/Chassis 2005 çoklu cisim dinamiği yazılımı kullanılarak, var olan bir araç sanal ortamda modellenmiş, süspansiyon ve direksiyon geometrilerinin aracın yol üzerindeki yanal hareketine etkileri incelenmiştir. Bu çalışmada kullanılan hafif ticari araç Türkiye'de üretilmektedir ve yaygın olarak kullanılmaktadır.

Aracın askı donanımı parametreleri tolerans değerleri arasında değiştirilerek araç ADAMS/Chassis yazılımı ile analiz edilmiştir. Gerçek araç kullanılarak yapılan yol testleri bilgisayar sonuçları ile karşlaştırılmıştır. Süspansiyon parametrelerinin yanal yerdeğiştirmeye etkileri ölçülerek hangi parametrenin daha etkin olduğu saptanmıştır.

ADAMS/Chassis yazılımı kullanılarak süspansiyon parametrelerinin steady state drift hareketi analiz edilmiştir. Analizler gerçek araç paramtreleri kullanılarak yapılmıştır ve yol testleri ile karşılaştırılmıştır. Süspansiyon parametrelerinin etkinliği DOE analizi ile saptanmıştır.

İstatistik analizler sonucunda ön toe, ön caster ve arka toe açıları birarada yanal kayma üzerinde en etkili parametrelerdir. Üçüncü derecede önemli parametre grubu ön kamber ve arka toe açılarıdır. Bu grupta sadece iki parametre yer almaktadır ve etkisi birinci gruptakilere çok yakındır. Daha az parametre ile ilgilenmek avantajlı olacağı için üçüncü grupta yer alan parametrelerin doğru şekilde ayarlanması yanal kayma problemini ortadan kaldıracaktır.

TABLE OF CONTENTS

ACKNOWLEDGEMENTS iii
ABSTRACT iv
ÖZET v
LIST OF FIGURES vii
LIST OF TABLES xii
LIST OF SYMBOLS/ABBREVIATIONS xiv
1. INTRODUCTION xvi
1.1. Statement of The Problem xvi
1.1.1. Scope and Objective xvi
1.1.2. Overview of the Thesis xvi
1.2. Literature Survey 1
1.3. Various Vehicle Models 6
1.3.1. 2-DOF Single Track Model 6
1.3.2. 3-DOF Yaw-Roll Model 11
1.3.3. 7-DOF Vehicle Model 17
1.3.4. 13-DOF Vehicle Model 28
2. ADAMS MODEL OF A LIGHT COMMERCIAL VEHICLE 43
2.1. ADAMS Solution Methodology 43
2.2. ADAMS Model 45
2.3. Front and Rear Suspension Model Parts and Suspension Geometries . . 51
3. RESULTS 58
3.1. Field Test Procedures and Results 58
3.2. Individual Effects of Suspension Parameter Analysis in ADAMS 61
3.3. Steady State Drift Tests in ADAMS 67
3.4. Comparison of Road Test and ADAMS Results 77
3.5. Statistical Analysis of Steady State Drift Tests 79
4. CONCLUSIONS 84
REFERENCES 86

LIST OF FIGURES

Figure 1.1. Single track model 7

Figure 1.2. Single track simulink model 10

Figure 1.3. 2-dof model time response data 10

Figure 1.4. Yaw-roll model car 11

Figure 1.5. Yaw-roll model time response data 17

Figure 1.6. 7-dof vehicle model 19

Figure 1.7. 7-dof model time response data 27

Figure 1.8. 7-dof model time response data 27

Figure 1.9. 13-dof vehicle model 29

Figure 1.10. 13-dof vehicle simulink model 36

Figure 1.11. Subsystem 1 37

Figure 1.12. Subsystem 2 37

Figure 1.13. Subsystem 3 38

Figure 1.14. Subsystem 4 38

Figure 1.15. Subsystem 5 39

Figure 1.16. Subsystem 6 39

Figure 1.17. Steering input for 13-dof model 40

Figure 1.18. Comparison of yaw velocity time response between 13-dof model, single track model and yaw-roll model 40

Figure 1.19. Comparison of roll velocity time response between 13-dof model, 7-dof model and 3-dof model 41

Figure 1.20. 13-dof longitudinal velocity change time response 41

Figure 1.21. Comparison of rear right tire and rear left tire slip angles time response in 13-dof model 42

Figure 1.22. Comparison of front right tire and front left tire slip angles time response in 13-dof model 42

Figure 2.1. Double wishbone suspension model 44

Figure 2.2. ADAMS configuration of two rigid parts connected to each other . 45

Figure 2.3. Front suspension, steering and tire model in ADAMS 49

Figure 2.4. Rear suspension and tire model in ADAMS 49

Figure 2.5. Full vehicle model in ADAMS 50

Figure 2.6. Full vehicle model in IDEAS 50

Figure 2.7. Suspension and steering components of the vehicle 51

Figure 2.8. Front suspension components and camber angle. (1- Shock absorber spring plate, 2- Ball-joint, 3- Ball-joint, 4- Heat shield, 5- Bearing, 6- Gaitor, 7- Ball-joint) 51

Figure 2.9. Front suspension components. (1- Top mount, 2- Shock absorber, 3- Tie rod, 4- Knuckle, 5- Hub, 6- Toe adjuster, 7- Cross-member, 8- Anti-Roll bar, 9- Steering column, 10- L-arm) 52

Figure 2.10. Front suspension caster angle 52

Figure 2.11. Rear suspension components.(1- Shackle, 2- Bush, 3- Leaf spring, 4- Hub, 5- Clamp plate, 6- Shock absorber, 7- Front eye, 8- Bush, 9- Rear axle, 10- Bump stop, 11- Anti-roll bar, 12- Spindle) 53

Figure 2.12. Rear suspension side view 53

Figure 2.13. Rear suspension camber angle 54

Figure 2.14. Rear suspension bottom view 54

Figure 2.15. Toe adjustment process with a fastened steering wheel 55

Figure 2.16. Front wheel toe adjustment 55

Figure 2.17. Front suspension L-arm 56

Figure 2.18. Front wheel alignment 56

Figure 3.1. Test road 58

Figure 3.2. Steady state drift test front camber effect 67

Figure 3.3. Steady state drift test front caster effect 68

Figure 3.4. Steady state drift test front toe effect 69

Figure 3.5. Steady state drift test rear camber effect 69

Figure 3.6. Steady state drift rear toe effect 70

Figure 3.7. Steady state drift road crown effect 70

Figure 3.8. Steady state drift test for vehicles 1-2-3-4-5-6 71

Figure 3.9. Steady state drift test for vehicles 7-8-9-10-11-12 71

Figure 3.10. Steady state drift test for vehicles 13-14-15-16-17-18 72

Figure 3.11. Steady state drift test for vehicles 19-20-21-22-23-24 72

Figure 3.12. Steady state drift test for vehicles 25-26-27-28-29-30 73

Figure 3.13. Steady state drift test for vehicles 31-32-33-34-35-36 73

Figure 3.14. Steady state drift test for vehicles 37-38-39-40-41-42 74

Figure 3.15. Steady state drift test for vehicles 43-44-45-46-47-48 74

Figure 3.16. Steady state drift test for vehicles 49-50*51-52-53-54 75

Figure 3.17. Steady state drift test for vehicles 55-56-57-58-59-60 75

Figure 3.18. Steady state drift test for vehicles 61-62-63-64-65 76

Figure 3.19. Comparison of ADAMS data and experimental data 78

Figure 3.20. Comparison of ADAMS data and experimental data 78

Figure 3.21. Comparison of road test results and regression results 81

LIST OF TABLES

Table 2.1. Vehicle body hardpoint locations 46

Table 2.2. Front suspension hardpoint locations 47

Table 2.3. Rear suspension hardpoint locations 48

Table 3.1. Vehicle parameters 59

Table 3.2. Vehicle parameters 60

Table 3.3. Vehicle parameters 61

Table 3.4. Vehicle parameters 62

Table 3.5. Vehicle parameters 63

Table 3.6. Vehicle parameters 64

Table 3.7. Drift time/lane change (sec) 65

Table 3.8. Drift time/lane change (sec) 66

Table 3.9. Drift time/lane change (sec) 67

Table 3.10. Nominal suspension values and tolerance range 68

Table 3.11. Estimated effects and coefficients for drift time 80

Table 3.12. Analysis of variance for drift time 81

Table 3.13. Stepwise regression table 82

Table 3.14. Stepwise regression 83

LIST OF SYMBOLS/ABBREVIATIONS

a	Distance from CG to front of the vehicle
a_r	Rolling mass acceleration vector
a_{NR}	Non-rolling mass acceleration vector
a_y	Lateral acceleration
a_{y_p}	Peak Lateral Acceleration
a_{sy}	Sprung mass lateral acceleration
a_{uy}	Unsprung mass lateral acceleration
b	Distance from CG to rear of the vehicle
C_f	Front tire cornering stiffness
C_r	Rear tire cornering stiffness
F_r	Rated Load
F_y	Tire lateral force
F_z	Vertical force
F_x	Longitudinal force
G_{acc}	Lateral acceleration gain
G_{yaw}	Yaw velocity gain
H	Center of gravity height
h_{cg}	Center of gravity
J	Moment of inertia
K_ϕ	Roll gradient
L	Wheelbase of the vehicle
m_s	Sprung mass
m_u	Unsprung mass
M_x	Overturning moment
M_y	Rolling resistance moment
M_z	Aligning moment
r	Yaw rate
$\dot{r}$	Yaw acceleration

$\vec{r_r}$	Sprung mass position vector
r_{NR}	Non-rolling mass position vector
R_e	Effective tire rolling radius
T	Track width
u	Longitudinal velocity
U	Speed of the vehicle
v	Lateral velocity
V_{NR}	Non-rolling mass velocity vector
$\vec{V_r}$	Sprung mass velocity vector
$\dot{v}$	Lateral acceleration
$Y_{\delta_w}, N_{\delta_w}$	Control derivatives
y_{cg}	Half of the track width
β	Roll angle
δ_w	Front wheel steering
μ_{yp}	Friction of tire
$\triangle R$	Change in loaded radius of the tire
ω_{NR}	Non-rolling mass yaw rate
ω_U	Unsprung mass yaw rate
ω_R	Rolling mass yaw rate
ω_S	Sprung mass yaw rate
κ	Slip ration
α	Lateral slip
γ	Camber angle
CG	Center of gravity
SSD	Steady state drift

1. INTRODUCTION

1.1. Statement of The Problem

1.1.1. Scope and Objective

The objective of this work is to study the influence of suspension and steering geometry parameters on lateral dynamics of a light commercial vehicle. The parameters that are studied in this study are front caster, front camber, rear camber, front toe, and rear toe. The effects of these parameters on steady state drift are analyzed. The effect of each parameter is studied in combination with other. The use of multibody dynamics model has an advantage over previous results that have used single track model, yaw-roll model, 7-DOF freedom model or 13-DOF model that are only valid in the linear range of vehicle dynamics.

Drift is the lateral displacement of a vehicle when the steering wheel is released. Typically, drift is measured in lane change/seconds. The vehicle must not drift excessively to one side of the road in the allowable range of alignment settings. Acceptance criteria for constant drift is, time to change one lane must be bigger than 10 seconds when hands are off the steering wheel.

1.1.2. Overview of the Thesis

The influence of suspension parameters is identified. A light commercial vehicle is chosen in order to investigate the lateral dynamics. Input data for this study include the following:

Suspension and chassis parameters: front caster, front and rear camber, front left/right toe, rear left/right toe. Initial conditions: constant speed (80 kph), initially zero steering angle. Tire model: Pacejka 2002 195/65R-15. For parameter variation studies a range is selected for the variation of each parameter from its nominal value.

The range is limited to 0.5 degree for caster, 0.5 degree for rear camber, 1.0 degree for front camber, 0.14 degree for front toe, 0.15 degree for rear toe.

To understand the effect of parameters, a virtual model of a light commercial vehicle is built in ADAMS/Chassis. ADAMS/Chassis is used together with Insight module in ADAMS for a number of response data to get the response change as a result of collective variation of the suspension parameters. Regression/DOE analysis techniques are used to determine the effect of all factors and interactions. Regression/DOE techniques establish a functional relationship between lateral displacement and any factor or interaction which is shown to be significant.

In the introduction part a brief history of vehicle dynamics from the very beginning of basic models is told. Then some of the linear vehicle models are introduced and compared to each other. In the fourth chapter, the methodology of ADAMS multibody dynamics software that is used in this study is explained in detail. In the next chapter, ADAMS model of the light commercial vehicle that is studied in this work is introduced. Last chapter is about the results of field tests, analysis and their comparison. Finally, this work is concluded by explaining the parameters that dominate lateral drift of the vehicle.

1.2. Literature Survey

A general theory for ride dynamics of an automobile was first established in 1925. However, very little progress has been made in static and dynamic directional motion. This is because of need in understanding the mechanism for lateral force generation by tires. In 1925, Broulheit proposed a basic concept for side-slip and slip angle. In 1931 Becker, Fromm and Maruhn examined the role of the tire in steering system vibrations [1]. During 1930s Cadillac suspension group of General Motors, under the direction of Maurice Olley, developed the first independent suspension. During their studies certain steering geometries led the vehicle to an unsafe position. They called this situation as oversteer. Then it was realized that not only steering geometries but also overloading or under inflating were the causes of oversteer. In 1934, Olley wrote a report about the idea of critical speed which initiates oversteer or understeer [2]. After this report, Goodyear Tire and Rubber Company began rolling drum tests to determine tire characteristics. In 1950, Lind Walker introduced the concept of the neutral steer and stability margin which are still used for the state of directional motion in automobiles.

In 1956, William F. Milliken, David W. Whitcomb and Leonard Segel presented the first major quantitative and theoretical analysis of vehicle handling in a series of papers. These papers still constitute a reference for automobile motion and control. Milliken's paper provides a historical overview in this field. Milliken also noted that, the effects of tire design on handling are unknown because of the need to test passenger car tires to determine the effects of various design parameters.

The second paper of the series was written by Leonard Segel [3]. Segel derived linearized three degree of freedom equations for lateral and directional motion. The bounce and pitch degrees of freedom of the chassis were ignored and a fixed longitudinal roll axis parallel to the ground was used. Segel also made several other simplifying assumptions including constant forward velocity, fixed driving thrust divided equally between the rear wheels. The unsprung mass was modeled as a single non-rolling mass. An experimental validation of the model was performed using a 1953 Buick Super four-door sedan. The vehicle was put through different steering input tests and the response of the three degrees of freedom model (lateral displacement, yaw and roll) was measured at different constant forward velocities. The theoretical predictions of the model were compared to experimental data.

The final paper of the series was written by D.W. Whitcomb [4]. Whitcomb established a two degree of freedom model (yaw and side slip) with experimentally determined parameters. The model didn't include roll motion. That is why Whitcomb assumed that the vehicle had no width and the tires laid on the centerline of the vehicle. That is why this model is also called as "bicycle model". A set of linearized differential equations was derived using stability derivatives and the responses was studied.

In 1960, H.S. Radt and W.G. Milliken Jr. explored the motions of a skidding automobile [5]. They used a relatively simple vehicle model with yaw and lateral velocity as the only degrees of freedom. In 1961, Martin Goland and Frederick Jindra published a paper where they used a two degree of freedom (yaw and sideslip) vehicle model to study the directional motion and control of a four wheeled vehicle [6]. The model is a simplified version of Segel's model. Results showed that the motion of a vehicle changed as the center of mass moved, the tire inflation pressure and the tire tread width changed. In 1968 D.H. Weir, C.P. Shortwell and W.A. Johnson published a paper in which they explored the role of vehicle dynamics on controllability [7]. They used experimental data and simulated a model which combined elements of a nonlinear model developed by H.S. Radt in 1964 and Segel's earlier model. Their model consisted of two unsprung masses representing the front and rear suspension assemblies respectively, and a single sprung mass representing the body of the vehicle. The vehicle was modeled using a four degrees of freedom model (roll of the sprung mass about a fixed axis, lateral velocity, yaw rate and axial velocity).

In 1970s, simulations of vehicle became more complex and realistic. Digital computers allowed researchers to create nonlinear models. At Bendix Corporation Research Laboratories, a vehicle dynamics simulation for a hybrid computer was created [8]. The model was a ten degree of freedom model created by R.R. Mc Henry and N.J. Deleys at Cornell Aeronautics Laboratory [9]. In 1973, T. Okada described a seven degree of freedom model for vehicle simulation [10]. The model was used to simulate vehicle handling at the first stage of vehicle design. Five of the degrees of freedom were used to model the vehicle (roll, yaw, pitch, lift and lateral position). The remaining two degrees of freedom were used to model the steering system. The effects of roll steer, axle steer, caster, camber, toe-in were approximated based on wheel travel, steer angle. In 1973 Frank H. Speckhart published a paper in which he presented a vehicle model containing fourteen degrees of freedom [11]. Six degrees of freedom were assigned to the sprung mass, four degrees of freedom were associated with the suspension movement at the four corners of the vehicle, and four rotational degrees of freedom were assigned to wheels. He used a Lagrangian approach in deriving his equations. In 1977 Kenneth N. Mormon presented a paper containing a detailed three degree of freedom model of the front suspension in Ford Motor Company [12]. In the model all of the springs, dampers and bushings were assumed to be linear.

In 1981, W. Riley Garrot described a vehicle simulation developed at University of Michigan. The model had seven degrees of freedom. In 1986, R. Wade Allen from system Technology Inc. performed experimental tests and correlated the results with a computer model to validate a simplified lateral vehicle dynamics and tire modeling procedure [13]. The tests were performed on a rear wheel driven car, 1980 Datsun 210, and a front wheel drive 1984 Honda Accord. Several types of tires were used on the Datsun including both radial and bias ply tires. A good correlation was obtained with experimentally obtained data. In 1987, Andrez Nalecz presented the results of an investigation of suspension design that affects the handling of vehicles [14]. Twenty-five suspension types were considered. A typical three-degree-of-freedom lateral dynamics model was used with the addition of quasi-static pitch degree of freedom. In 1992, Nalecz published a second paper in which he described an eight degree of freedom model called LVDS (Light Vehicle Dynamics Simulation)[15]. The model consisted of a three degree of freedom lateral dynamics model coupled to a five degree of freedom planar rollover model. In the beginning of 1990s, R. Wade Allen at Systems Technology Inc. published number of papers in which he validated his VNDAL (Vehicle Dynamics Analysis: Non-Linear) code [16]. The experimental studies and simulation runs on vehicle handling were presented by R. Wade Allen [18]. VDANL was also put through a validation process by Gary J. Heydinger at Ohio State University [19]. The validation process was carried out by comparing experimental data to simulations in time and frequency domains. Heydinger explored the use of pulse inputs which require shorter test runs, and by this method he did the tests in the same frequency range [20]. Also Clover and Bernard wrote another paper by using VDANL software. They took the effects of braking and acceleration into account [21]. The details of updated vehicle dynamics model VDANL were presented by R. Wade Allen [22].

In the early 1980s, the demand for accurate vehicle dynamics models combined with the difficulty in deriving the equations of motion for large multibody systems led to the use of general multibody simulation codes. The first code was NEWEUL.

It generates equations of motion in symbolic form with FORTRAN code output. The second program was MEDYNA. It generates the equations of motion in numerical form.

In 1993, W. Körtüm and R.S. Sharp studied multibody simulation codes such as ADAMS, MEDYNA, NEWEUL, DADS, AUTOSIM and SIMPACK. In 1994, R.S. Sharp wrote a paper in which he compared the capabilities of the major multibody computer codes. In particular he noted the limitations of each code. In 1986, R.J. Antoun discussed a vehicle dynamic handling computer simulation created using the multibody code ADAMS (Automatic Dynamic Analysis of Mechanical Systems) in a paper [23]. A model of a 1985 Ford Ranger pickup truck was created in ADAMS. The simulation results and the experimental data were in good correlation. In 1991, Yoshinori Mori at Toyota described a model created for simulation of active suspension control systems in a paper [24]. The vehicle model control algorithms were coded in FORTRAN. The vehicle model contained twenty degrees of freedom. The vehicle was modeled as front wheel drive, rear wheel drive, and four wheel drive.

In 1996, Michael R. Petersen and John M. Starkey described a relatively detailed straight line acceleration vehicle model for predicting vehicle performance. The model included longitudinal weight transfer effects, tire slip, aerodynamic drag, aerodynamic lift, transmission and driveline losses and rotational inertias of the wheels, engine and driveline components.

Sayers and Han compared time history responses for a step steer input at three vehicle speeds. The plots show a correlation between the detailed model and 18-DOF model. This might be because of the difference between the full suspension system in the detailed model and the simplified one. S. Hegazy, H. Rahnejat and K. Hussain studied on multibody dynamics in full-vehicle handling analysis [25]. The model consisted of double-wishbone front and rear suspensions, rack and pinion steering system, vehicle body, road wheels and tyres. The model had 94 degree of freedom. The components of the model had non-linear characteristics. The vehicle model was created in ADAMS. The model was used for the purpose of vehicle handling analysis. Simulations were done under ISO and British Standards. R.W. Allen, T.J. Rosenthal, D.H.

Klyde, and J.R. Hogue from Systems Technology Inc. studied computer simulation analysis of light vehicle lateral/directional motion [26]. Their study is to investigate the vehicle and tire characteristics and maneuvering conditions that affect directional motion. The simulation that they have used included lateral and directional dynamics. The simulation also included a detailed tire model that generates lateral longitudinal forces They used a SUV (Sport Utility Vehicles) as a model vehicle.

1.3. Various Vehicle Models

1.3.1. 2-DOF Single Track Model

The basic analytical study of vehicle dynamics begins with the formulation of the single track model [27]. It is also called the bicycle model. It models a four-wheeled vehicle by using a planar two-wheeled model. In this model, δ represents the steering angle, F_{SF} and F_{SR} are front and rear tire lateral forces, F_{LF} and F_{LR} are front and rear tractive forces, αf and αr are front and rear slip angles, r is yaw velocity, C.G. is the vehicle center of gravity or mass center. In this model, the vehicle does not make pitch or roll motions. It has only two degrees of freedom.

The track width of this model is zero. The tires in this model are assumed to generate lateral forces directly proportional to the slip angle α relative to the direction of travel of the wheel. If C_f and C_r are the cornering stiffness values for the front and rear axles for small slip angles, then [27]:

$$F_{yf} = C_f \alpha_f$$
$$F_{yr} = C_r \alpha_r \tag{1.1}$$

The two equations of motion related to vehicle handling can be written in the

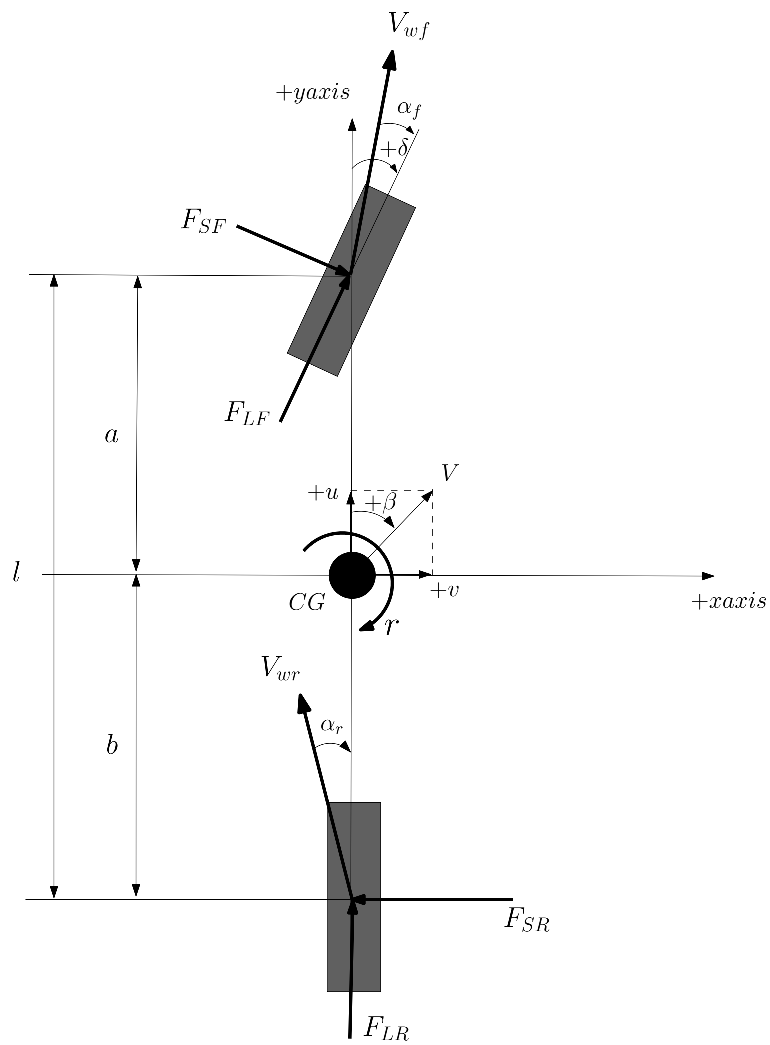

Figure 1.1. Single track model

following form:

$$\sum F_y = ma_y \tag{1.2}$$

$$m(\dot{v} + Ur) = C_f\alpha_f + C_r\alpha_r \tag{1.3}$$

$$\sum M_{CG} = I\alpha \tag{1.4}$$

$$J\dot{r} = aC_f\alpha_f - bC_r\alpha_r \tag{1.5}$$

It should be noted that cornering stiffness values are assumed to be negative.

The slip angles α_f and α_r can be written from Figure 1.1 as:

$$\alpha_f = \frac{v + ar}{U} - \delta \tag{1.6}$$

and

$$\alpha_r = \frac{v - br}{U} \tag{1.7}$$

Inserting the above values into the equations 1.3 and 1.5:

$$m(\dot{v} + Ur) = (C_f + C_r)\frac{v}{U} + (aC_f - bC_r)\frac{r}{U} - C_f\delta \tag{1.8}$$

and

$$J\dot{r} = (aC_f - bC_r)\frac{v}{U} + (a^2C_f + b^2C_r)\frac{r}{U} - aC_f\delta \tag{1.9}$$

The above equations can be put into the general state space form:

$$\{\dot{x}(t)\} = [A]\{x(t)\} + [B]\{u(t)\} \tag{1.10}$$

$$\begin{Bmatrix} \dot{v} \\ \dot{r} \end{Bmatrix} = \begin{bmatrix} \frac{C_f+C_r}{mU} & \frac{aC_f-bCr}{mU} - U \\ \frac{aC_f-bC_r}{JU} & \frac{a^2C_f+b^2C_r}{JU} \end{bmatrix} \begin{Bmatrix} v \\ r \end{Bmatrix} + \begin{Bmatrix} -\frac{C_f}{m} \\ -\frac{aC_f}{J} \end{Bmatrix} \delta \tag{1.11}$$

If we assume that a steady state angle of steer, δ, is applied and held, in a steady state turn.

The state space equation of a single track model is set up in Matlab as a Simulink Model as shown in Figure 1.2. The steering input is a step function. The outputs of this model are yaw veloctity, lateral acceleration, and lateral velocity.

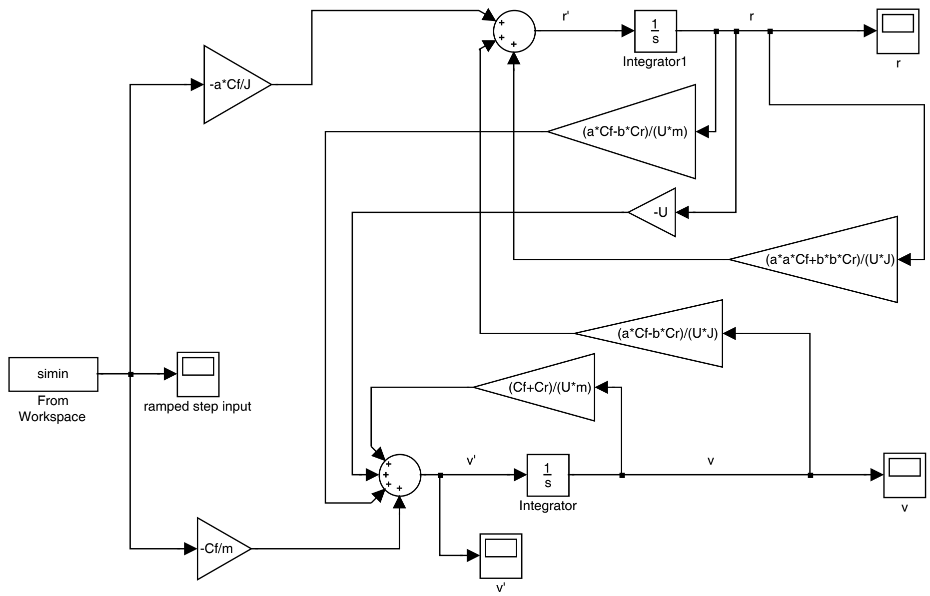

Figure 1.2. Single track simulink model

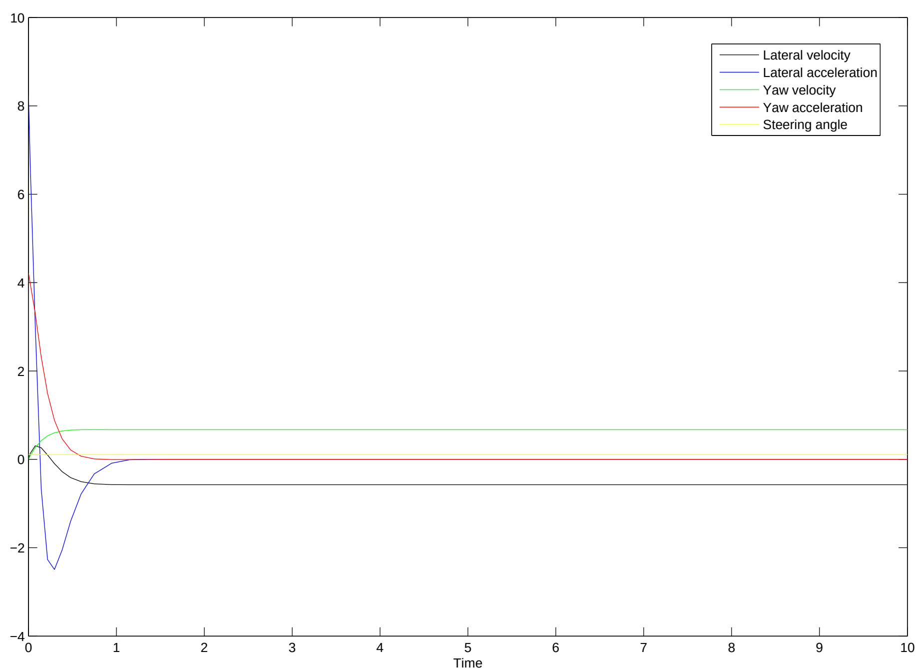

Figure 1.3. 2-dof model time response data

1.3.2. 3-DOF Yaw-Roll Model

Yaw-roll model was developed by Segel in 1957 [28]. This linear model includes a roll degree of freedom, two translational degrees of freedom in X and Y directions, and a yaw degree of freedom. The unsprung mass is non-rolling and the sprung mass is rolling. The velocity is constant.

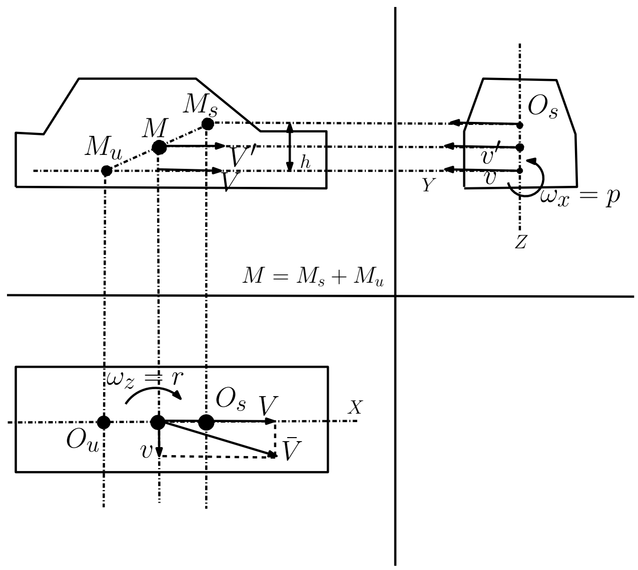

Figure 1.4. Yaw-roll model car

For sprung mass the position vector of the CG is found to be as follows:

$$\vec{r}_r = \vec{r}_a = \vec{r}_0 + c\vec{i} + h.sin\phi.\vec{j} - h.cos\phi.\vec{k} \tag{1.12}$$

$$\vec{r}_{NR} = \vec{r}_u = \vec{r}_0 - e.\vec{i} \tag{1.13}$$

Since $\vec{V}_r = \vec{V}_s = dr_s/dt$ then, The velocity of the sprung mass is as follows:

$$\vec{V_r} = \vec{V_s} = \vec{V_0} + c\dot{\vec{i}} + h.cos\phi.\dot{\phi}\vec{j} + h.sin\phi.\dot{\phi}\dot{\vec{j}} + h.sin\phi.\dot{\phi}\vec{k} - h.cos\phi.\dot{\phi}\dot{\vec{k}} \tag{1.14}$$

If ϕ is very small, then $sin\phi \approx \phi$, $cos\phi \approx 1$, $p = \dot{\phi}$. Note that $\vec{p}$ is the roll velocity about the roll axis.

Then,

$$\vec{V_r} = \vec{V_s} = [u - h.\phi.r]\vec{i} + [v + cr + hp]\vec{j} + h.\phi.p.k \tag{1.15}$$

$$\vec{\omega}_u = \vec{\omega}_{NR} = \begin{bmatrix} 0 \\ 0 \\ r \end{bmatrix} \tag{1.16}$$

Note that $r = \dot{\psi}$ is the z component.

$$\vec{\omega}_R = \vec{\omega}_S = \begin{bmatrix} p.cos\theta_R \\ 0 \\ r + p.sin\theta_R \end{bmatrix} \tag{1.17}$$

The velocity of non-rolling mass is as follows:

$$\vec{V}_{NR} = \vec{V}_0 - e.\dot{\vec{i}}$$
$$\vec{V}_{NR} = u\vec{i} + [v - er]\vec{j} \tag{1.18}$$

The accelerations of rolling and non-rolling masses are as follows:

$$\vec{a}_r = \vec{a}_s = \frac{d\vec{V}_r}{dt}$$
$$\vec{a}_{NR} = \vec{a}_u = \frac{d\vec{V}_{NR}}{dt} \tag{1.19}$$

$$\sum F_y = ma_y$$
$$\sum F_y = m_s a_{sy} + m_u a_{uy} \tag{1.20}$$

$$a_{sy} \cong ur + \dot{v} + c\dot{r}h\ddot{\phi}$$
$$a_{uy} = ur + \dot{v} - e\dot{r} \tag{1.21}$$

If we substitute Equation 1.21 into Equation 1.20 , we obtain:

$$\sum F_y = Mu[r + \dot{\beta}] + m_s.h.\dot{p}$$

Note that $\beta = \frac{v}{u}$, and $\dot{\beta} = \frac{\dot{v}}{u}$

$$\sum F_y = Mu[r \cdot \beta] + m_s hp \tag{1.22}$$

While finding the forces and moments we assume that solid rear axle does not roll, an independent front suspension which causes the front wheels to incline as the spring mass rolls and rear suspension kinematic properties cause the rear axle to steer as the sprung mass rolls.

Lateral force in y-direction:

$F_{y\alpha}$ and $F_{y\gamma}$ are the tire forces due to slip angle and camber change, respectively.

$$\begin{gathered}\sum F_y = F_{y\alpha f} + F_{y\alpha r} + F_{y\gamma} \\ = C_{\alpha f}\alpha_f + C_{\alpha r}\alpha_r + C_{\gamma f}\frac{\partial \gamma_f}{\partial \phi}\phi\end{gathered} \tag{1.23}$$

$$\alpha_f = \delta_f - (\beta + \frac{ar}{u}) \tag{1.24}$$

$$\alpha_r = \delta_r + \frac{br}{u} - \beta \tag{1.25}$$

$$\begin{aligned}\sum F_y =& C_{\alpha f}[\delta_f - \beta - \frac{ar}{u}] + C_{\alpha r}[\frac{\partial \delta_r}{\partial \phi}\phi - \beta + \frac{br}{u}] + C_{\gamma f}\frac{\partial \gamma_f}{\partial \phi}\phi \\ =& Mu[r + \dot{\beta}] + m_s h\dot{p}\end{aligned} \tag{1.26}$$

The moments about z axis:

Moments in yaw direction due to cornering force, roll induced camber thrust and self aligning moments will be considered.

$$\sum M_z = a[C_{\alpha f}\alpha_f + C_{\gamma f}\frac{\partial \gamma_f}{\partial \phi}\phi] - bc_{\alpha r}\alpha_r + \frac{\partial M_z}{\partial \alpha_f}\alpha_f + \frac{\partial M_z}{\partial \alpha_r}\alpha_r \tag{1.27}$$

Finally, governing equations for yaw-roll model can be written as follows:

$$
\begin{bmatrix} mu & 0 & m_R h & 0 \\ 0 & I_{zz} & I_{xz} & 0 \\ m_R hu & I_{xz} & I_{xx} & 0 \\ 0 & 0 & 0 & 1 \end{bmatrix} \begin{bmatrix} \dot{\beta} \\ \dot{r} \\ \dot{p} \\ \dot{\phi} \end{bmatrix} +
$$

$$
\begin{bmatrix} C_{\alpha f} + C_{\alpha r} & C_{\alpha f}\frac{a}{u} - C_{\alpha r}\frac{b}{u} + mu & 0 & -(C_{\alpha r}\frac{\partial \delta_r}{\partial \phi} + C_{\gamma f}\frac{\partial \gamma_f}{\partial \phi}) \\ aC_{\alpha f} - bC_{\alpha r} & \frac{a^2 C_{\alpha f}}{u} + b^2 \frac{C_{\alpha r}}{u} & 0 & -aC_{\gamma f}\frac{\partial \gamma_f}{\partial \phi} - bC_{\alpha r}\frac{\partial \delta_r}{\partial \phi} \\ 0 & m_R.h.u & C_R & k_R - m_R.g.h \\ 0 & 0 & -1 & 0 \end{bmatrix} \begin{bmatrix} \beta \\ r \\ p \\ \phi \end{bmatrix}
$$

$$
= \begin{bmatrix} C_{\alpha f}\delta \\ aC_{\alpha f}\delta \\ 0 \\ 0 \end{bmatrix} \tag{1.28}
$$

The time response data of a yaw roll model is plotted for side slip angle, yaw velocity, roll velocity, and roll angle in Figure 1.5.

As seen in Figure 1.5, the input is step steering. So, in the first 1 second time yaw velocity of the vehicle increases as the steering angle increases. After the step steer input, the roll velocity firstly increases, then it oscillates and comes to steady state position with zero roll velocity. The roll angle also makes the same response to step steer input. Side slip angle firstly increases slightly, then decreases and comes to steady state position at a negative value.

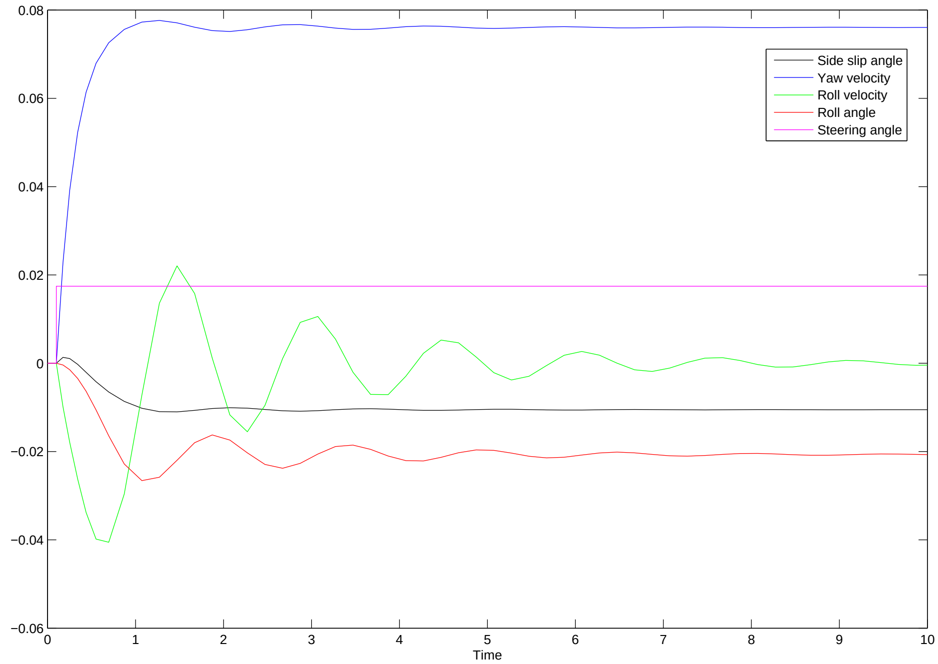

Figure 1.5. Yaw-roll model time response data

1.3.3. 7-DOF Vehicle Model

7-DOF mathematical model is developed to obtain ride characteristics [29]. The model of 7-DOF vehicle is shown in Figure 1.6. The seven degrees of freedom are defined as the sprung mass vertical motion (Z_c), sprung mass pitch and roll motions (θ, ϕ), and vertical motions of 4 wheels (Z_1, Z_2, Z_3, Z_4). Besides, independent front and rear suspensions are used and anti-roll bars are introduced both in the rear and in the front which the vehicle sprung mass is assumed to be a rigid body. This model enables us to investigate the effect of chassis design factors such as stabilizer bars, suspension stiffness, and mass ratio on the vehicle ride quality. The ride quality of the three dimensional vehicle that includes bounce, pitch, roll and unsprung masses motion can be studied using this model.

In this model the followings denote the vehicle parameters:

M=Vehicle mass (970 kg)

M_s=Sprung mass (1773 kg)

M_{uf}=Front unsprung mass (98.5 kg)

M_{ur}=Rear unsprung mass (98.5 kg)

K_{SF}=Front suspension stiffness (24 kN/m)

K_{SR}= Rear suspension stiffness (24.57 kN/m)

B_{SF}=Front suspension damping coefficient (3918 Ns/m)

B_{SR}=Rear suspension damping coefficient (4310 Ns/m)

K_T=Tire stiffness (216 kN/m)

L=Wheelbase (2.889 m)

T_F=Front track width (1.547 m)

T_R=Rear track width (1.554 m)

K_{ARBF}=Front anti-roll bar stiffness (300 N/deg)

K_{ARBR}=Rear anti-roll bar stiffness (300 N/deg)

I_{yy}=Sprung mass pitch inertia about the CG (3669.9 kg/m^2)

I_{xx}=Sprung mass roll inertia about the CG (1140 kg/m^2)

Z_1, Z_2, Z_3, Z_4= Front-left, front-right, rear-left, rear-right tires' vertical displacements.

$Z_{01}, Z_{02}, Z_{03}, Z_{04}$= Front-left, front-right, rear-left, rear-right sinusoidal ground inputs

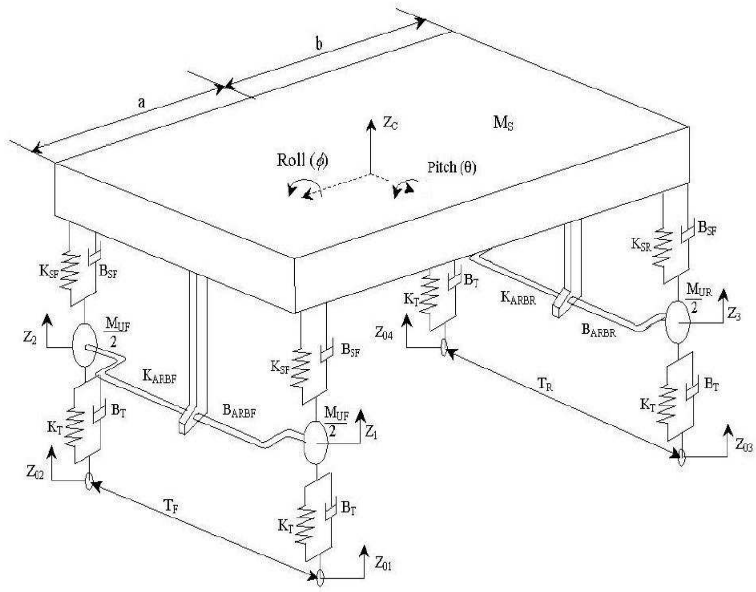

Figure 1.6. 7-dof vehicle model

[29]

The equations of motion for 7-degree of freedom model are as follows:

$$M_s\ddot{Z}_c + K_{SF}(Z_c - a\theta + \frac{T_F}{2}\phi - Z_1) + K_{SF}(Z_c - a\theta - \frac{T_F}{2\phi - Z_2}) +$$

$$K_{SR}(Z_c - b\theta + \frac{T_R}{2\phi - Z_3}) + K_{SR}(Z_c - b\theta - \frac{T_R}{2\phi - Z_4}) +$$

$$b_{SF}(\dot{Z}_c - a\dot{\theta} + \frac{T_F}{2}dot\phi - Z_1) + b_{SF}(\dot{Z}_c - a\dot{\theta} - \frac{T_F}{2}dot\phi - Z_2) + \tag{1.29}$$

$$b_{SR}(\dot{Z}_c + b\dot{\theta} - \frac{T_R}{2}dot\phi - Z_4) = 0$$

$$I_{yy}^{cg}\dot{\theta} - K_{SF}a(Z_C - a\theta + \frac{T_F}{2}\phi - Z_1) - K_{SF}a(Z_C - a\theta - \frac{T_F}{2}\phi - Z_2) +$$

$$K_{SR}b(Z_C + b\theta + \frac{T_R}{2}\phi - Z_3) + K_{SR}b(Z_C + b\theta - \frac{T_R}{2}\phi - Z_4) - b_{SF}a(\dot{Z}_C -$$

$$a\dot{\theta} + \frac{T_F}{2}\dot{\phi} - \dot{Z}_1) - b_{SF}a(\dot{Z}_C - at\dot{h}eta - \frac{T_F}{2}\dot{\phi} - \dot{Z}_2) + \tag{1.30}$$

$$b_{SR}b(\dot{Z}_C + b\dot{\phi} + \frac{T_R}{2}\dot{\phi} - \dot{Z}_3) + b_{SR}b(\dot{Z}_C + b\dot{\theta} - \frac{T_R}{2}\dot{\phi} - Z_4) = 0$$

$$I_{xx}^{cg}\ddot{\theta} + K_{SF}\frac{T_F}{2}(Z_C - a\theta + \frac{T_F}{2}\phi - Z_1) - K_{SF}\frac{T_{SF}}{2}\phi - Z_2 +$$

$$K_{SR}\frac{T_R}{2}(Z_C + b\theta + \frac{T_R}{2}\phi - Z_3) - K_{SR}\frac{T_R}{2}(Z_C + b\theta - \frac{T_R}{2}\phi - Z_4) -$$

$$K_{ARBF}(\frac{Z_1 - Z_2}{T_F} - \phi) - K_{ARBR}(\frac{Z_3 - Z_4}{T_R} - \phi) + b_{SF}\frac{T_F}{2}(\dot{Z}_C - a\dot{\theta} + \frac{T_F}{2}\dot{\phi} - \dot{Z}_1) -$$

$$b_{SF}\frac{T_F}{2}(\dot{Z}_C - a\dot{\theta} - \frac{T_F}{2}\dot{\theta} - \dot{Z}_2) + b_{SR}\frac{T_R}{2}(\dot{Z}_C + b\dot{\theta} + \frac{T_R}{2}\dot{\phi} - \dot{Z}_3) -$$

$$b_{SR}\frac{T_R}{2}(\dot{Z}_C + b\dot{\theta} - \frac{T_R}{2}p\dot{h}i - \dot{Z}_4) - b_{ARBF}(\frac{\dot{Z}_1 - \dot{Z}_2}{T_F} - \dot{\phi}) - b_{ARBR}(\frac{\dot{Z}_3 - \dot{Z}_4}{T_R} - \phi) = 0 \tag{1.31}$$

$$(\frac{M_{UF}}{2})\ddot{Z}_1 - K_{SF}(Z_C - a\theta + \frac{T_F}{2}\phi - Z_1)+$$

$$K_T(Z_1 - Z_{01}) + \frac{K_{ARBF}}{T_F}(\frac{Z_1 - Z_2}{T_F} - \phi) - b_{SF}(\dot{Z}_C - a\dot{\theta} + \frac{T_F}{2}\dot{\phi} - \dot{Z}_1)+$$

$$b_r(\dot{Z}_1 - \dot{Z}_{01}) + \frac{b_{ARBF}}{T_F}(\frac{\dot{Z}_1 - \dot{Z}_2}{T_F} - \dot{\phi}) = 0 \tag{1.32}$$

$$(\frac{M_{UF}}{2})\ddot{Z}_2 - K_{SF}(Z_C - a\theta - \frac{T_F}{2}\phi - Z_2)+$$

$$K_T(Z_2 - Z_{02}) - \frac{K_{ARBF}}{T_F}(\frac{Z_1 - z_2}{T_F} - \phi) - b_{SF}(\dot{Z}_C - a\dot{\theta} - \frac{T_F}{2}\dot{\phi} - \dot{Z}_2)+$$

$$b_T(\dot{Z}_2 - \dot{Z}_{02}) - \frac{b_{ARBF}}{T_F}(\frac{\dot{Z}_1 - \dot{Z}_2}{T_F} - \dot{\phi}) = 0 \tag{1.33}$$

$$(\frac{M_{UR}}{2})\ddot{Z}_3 - K_{SR}(Z_C + b\theta + \frac{T_R}{2}\phi - Z_3) +$$

$$K_T(Z_3 - Z_{03}) + \frac{K_{ARBR}}{T_R}(\frac{Z_3 - Z_4}{T_R} - \phi) - b_{SR}(\dot{Z}_C +$$

$$b\theta + \frac{T_R}{2}\dot{\phi} - \dot{Z}_3)b_T(\dot{Z}_3 - \dot{Z}_{03}) + \frac{b_{ARBR}}{T_R}(\frac{\dot{Z}_3 - \dot{Z}_4}{T_F} - \dot{\phi}) = 0$$

(1.34)

$$\frac{M_{UR}}{2}\ddot{Z}_4 - K_{SR}(Z_C + b\theta - \frac{T_R}{2}\phi - Z_4) +$$

$$K_T(Z_4 - Z_{04}) - \frac{K_{ARBR}}{T_R}(\frac{Z_3 - Z_4}{T_R} - \phi) -$$

$$b_{SR}(\dot{Z}_C + b\dot{\theta} - \frac{T_R}{2}\dot{\phi} - \dot{Z}_4) +$$

$$b_T(\dot{Z}_4 - \dot{Z}_{04}) - \frac{b_{ARBR}}{T_R}(\frac{\dot{Z}_3 - Z_4}{T_F} - \dot{\phi}) = 0$$

(1.35)

The equations obtained above are second order linear differential equations. These equations can be converted into first order differential equations by defining the following state space variables.

$$X_1 = Z_c, \quad X_2 = \theta, \quad X_3 = \phi, \quad X_4 = Z_1,$$

$X_5 = Z_2, \quad X_6 = Z_3, \quad X_7 = Z_4, \quad X_8 = \dot{Z}_c,$

$X_9 = \dot{\theta}, \quad X_{10} = \dot{\phi}, \quad X_{11} = \dot{Z}_1, \quad X_{12} = \dot{z}_2,$

$X_{13} = \dot{Z}_3, \quad X_{14} = \dot{Z}_4$

$U_1 = Z_{01}, \quad U_2 = Z_{02}, \quad U_3 = Z_{03}, \quad U_4 = Z_{04}, \quad U_5 = Z_{05}, \quad U_6 = Z_{06},$

$U_7 = Z_{07}, \quad U_8 = Z_{08}$

The state space equations are transformed into matrix form by defining a state vector, characteristic matrix and input vector.

$$\frac{dX}{dt} = AX + BU \tag{1.36}$$

The matrix A (14x14 matrix) is called the state transition matrix and the matrix B(14x1 matrix) is defined as the the input coefficient matrix.

Matrix A is obtained as follows:

$A = 1.e + 004*$

Columns 1 through 7

$$\begin{bmatrix} 0 & 0 & 0 & 0 & 0 & 0 & 0 \\ 0 & 0 & 0 & 0 & 0 & 0 & 0 \\ 0 & 0 & 0 & 0 & 0 & 0 & 0 \\ 0 & 0 & 0 & 0 & 0 & 0 & 0 \\ 0 & 0 & 0 & 0 & 0 & 0 & 0 \\ 0 & 0 & 0 & 0 & 0 & 0 & 0 \\ 0 & 0 & 0 & 0 & 0 & 0 & 0 \\ -0.0055 & 0.001 & 0 & 0.0014 & 0.0014 & 0.0014 & 0.0014 \\ 0.0005 & -0.0057 & 0 & -0.0011 & -0.0011 & 0.0008 & 0.0008 \\ -0.0016 & 0 & -0.0065 & -0.0026 & -0.0026 & 0.0029 & 0.0007 \\ 0.0487 & -0.0804 & 0.0151 & -0.4727 & -0.0146 & 0 & 0 \\ 0.0487 & -0.0804 & -0.0603 & 0.0146 & -0.5019 & 0 & 0 \\ 0.0499 & 0.0733 & 0.00612 & 0 & 0 & -0.5029 & 0.0145 \\ 0.0499 & 0.0624 & -0.0612 & 0 & 0 & 0.0145 & -0.5029 \end{bmatrix}$$

Columns 8 through 14

$$
\begin{bmatrix}
0.0001 & 0 & 0 & 0 & 0 & 0 & 0 \\
0 & 0.0001 & 0 & 0 & 0 & 0 & 0 \\
0 & 0 & 0.0001 & 0 & 0 & 0 & 0 \\
0 & 0 & 0 & 0.0001 & 0 & 0 & 0 \\
0 & 0 & 0 & 0 & 0.0001 & 0 & 0 \\
0 & 0 & 0 & 0 & 0 & 0.0001 & 0 \\
0 & 0 & 0 & 0 & 0 & 0 & 0.0001 \\
0.0001 & 0 & 0.0002 & 0.0002 & 0.0002 & 0.0002 & -0.0009 \\
-3.4802 & 0 & -0.0002 & -0.0002 & 0.0001 & 0.0001 & 0.0001 \\
0 & -0.0007 & 0.0002 & 0.0002 & 0.0001 & 0.0002 & 0 \\
-0.0131 & 0.0075 & -0.0009 & -0.3500 & 0 & 0 & 0.0080 \\
-0.0131 & -0.0075 & 0.0008 & -0.0088 & 0 & 0 & 0.0080 \\
0 & 0.0081 & 0 & 0 & -0.0096 & 0.0008 & 0.008 \\
0.0109 & -0.0081 & 0 & 0 & 0.0008 & -0.0096 & 0.0088
\end{bmatrix}
$$

Matrix B is obtained as follows:

$B = 1.0e + 003*$

$$\begin{bmatrix} 0 & 0 & 0 & 0 & 0 & 0 & 0 & 0 \\ 0 & 0 & 0 & 0 & 0 & 0 & 0 & 0 \\ 0 & 0 & 0 & 0 & 0 & 0 & 0 & 0 \\ 0 & 0 & 0 & 0 & 0 & 0 & 0 & 0 \\ 0 & 0 & 0 & 0 & 0 & 0 & 0 & 0 \\ 0 & 0 & 0 & 0 & 0 & 0 & 0 & 0 \\ 0 & 0 & 0 & 0 & 0 & 0 & 0 & 0 \\ 0 & 0 & 0 & 0 & 0 & 0 & 0 & 0 \\ 0 & 0 & 0 & 0 & 0 & 0 & 0 & 0 \\ 0 & 0 & 0 & 0 & 0 & 0 & 0 & 0 \\ 4.3858 & 0 & 0 & 0 & 0.0002 & 0 & 0 & 0 \\ 0 & 4.3858 & 0 & 0 & 0 & 0.0002 & 0 & 0 \\ 0 & 0 & 4.3858 & 0 & 0 & 0 & 0.0002 & 0 \\ 0 & 0 & 0 & 4.3858 & 0 & 0 & 0 & 0.0002 \end{bmatrix}$$

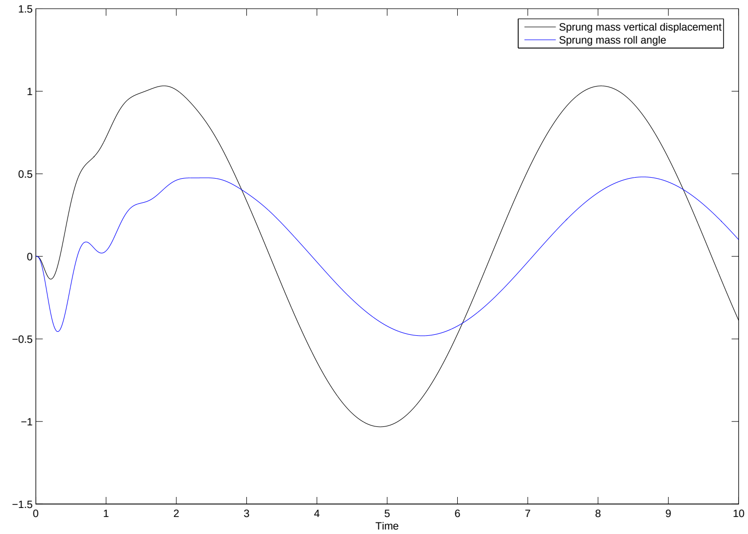

Figure 1.7. 7-dof model time response data

Inputs that are taken from the tires are sinusoidal. As seen in Figure 1.7, the vertical motion of the sprung mass is sinusoidal. Besides, the inputs from left and right tires differ from each other. So, the vehicle make roll motion. Sprung mass does not make pitch motion. This is due to the inputs from tires that are same for front and rear tires. However, this vehicle make vertical motion with an increasing velocity as the sinusoidal inputs continue during simulation.

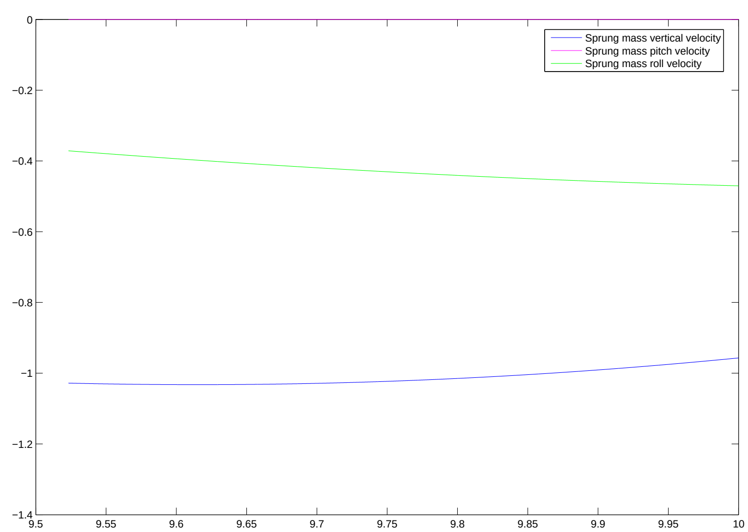

Figure 1.8. 7-dof model time response data

1.3.4. 13-DOF Vehicle Model

The thirteen degree of freedom vehicle model is derived under the following assumptions [30].

1. Ride motions do not influence the lateral motions of the vehicle.

2. Roll axis is horizontal.

3. Only front steering input is considered.

4. Tire slip angles and lateral velocity are small.

5. The effect of tire self aligning torque is small.

The definition of the coordinate system and parameters used in deriving the 13 DOF vehicle handling model is illustrated in Figure 1.9. Under the assumptions above, equations of motion with respect to the roll center are obtained.

Longitudinal Force, F_x:

$$F_x = m \cdot (\dot{v_x} - r \cdot v_y - r \cdot p \cdot \frac{m_s \cdot h}{m}) \tag{1.37}$$

Lateral Force, F_y:

$$F_y = m \cdot (\dot{v_y} + r \cdot v_x + \dot{p} \cdot \frac{m_s \cdot h}{m}) \tag{1.38}$$

Yaw Moment, T_z:

$$T_z = I_z \cdot \dot{r} - I_{xz} \cdot \dot{p} \tag{1.39}$$

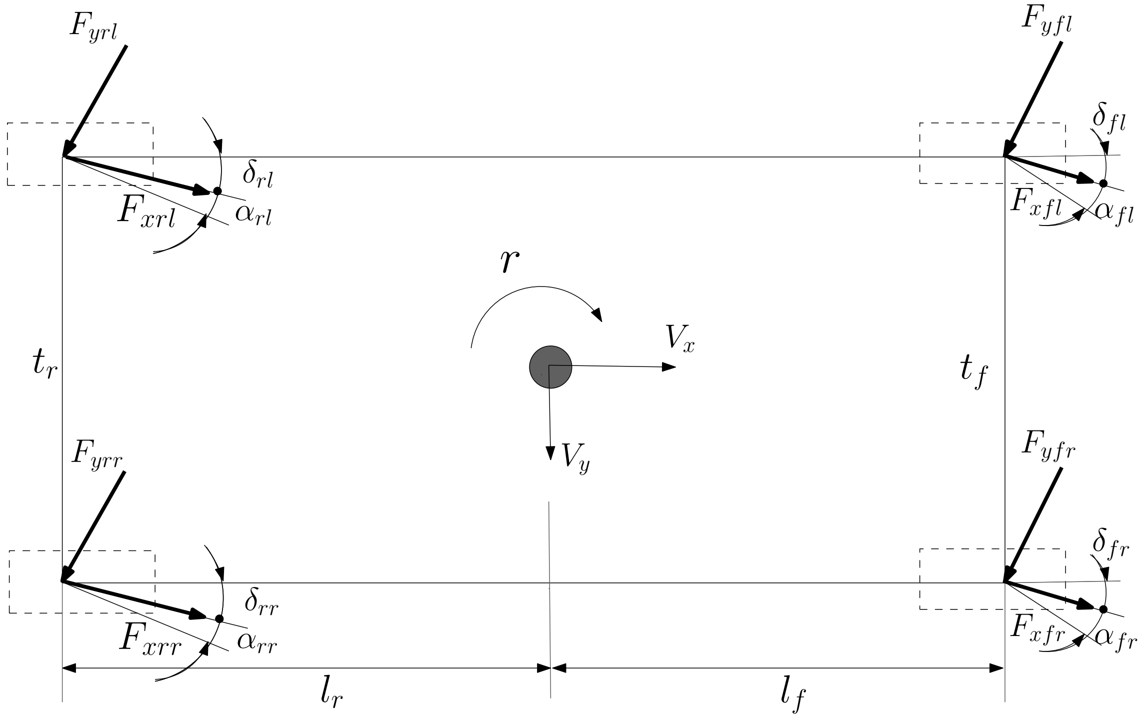

Figure 1.9. 13-dof vehicle model

[30]

Roll moment, T_x:

$$T_x = I_x \cdot \dot{p} - I_{xz} \cdot \dot{r} + m_s \cdot h \cdot (\dot{v_y} + r \cdot v_x) \tag{1.40}$$

The equation for roll angle and equations for the slip angles and slip ratios are formulated as follows:

Longitudinal velocity, v_x:

$$\dot{v_x} = \frac{F_x}{m} + r \cdot v_y + r \cdot p \cdot \frac{m_s \cdot h}{m} \tag{1.41}$$

Lateral velocity, v_y:

$$\dot{v_y} = -r \cdot v_x - \frac{1}{K_{vy}} \cdot [F_y \cdot (I_{xz}^2 - I_x \cdot I_z) + m_s \cdot h \cdot (I_z \cdot T_x + I_{xz} \cdot T_z)] \tag{1.42}$$

Yaw Rate, r:

$$\dot{r} = \frac{1}{K_{vy}} \cdot [(m \cdot I_x - m_s^2 \cdot h^2) \cdot T_z + m \cdot I_{xz} \cdot T_x - m_s \cdot h \cdot I_{xz} \cdot F_y] \tag{1.43}$$

Roll Rate, p:

$$\dot{p} = \frac{1}{K_{vy}} \cdot [m \cdot (I_z \cdot T_x + I_{xz} \cdot T_z) - m_s \cdot h \cdot I_z \cdot F_y] \tag{1.44}$$

Roll Angle, ϕ:

$$\dot{\phi} = p \tag{1.45}$$

Slip Angles, α:

$$\dot{\alpha}_{fl} = \frac{V_x}{\sigma_y}(\alpha_{fl_{ss}} - \alpha_{fl}) \tag{1.46}$$

$$\dot{\alpha}_{fr} = \frac{V_x}{\sigma_y}(\alpha_{fr_{ss}} - \alpha_{fr}) \tag{1.47}$$

$$\dot{\alpha}_{rl} = \frac{V_x}{\sigma_y}(\alpha_{rl_{ss}} - \alpha_{rl}) \tag{1.48}$$

$$\dot{\alpha}_{rr} = \frac{V_x}{\sigma_y}(\alpha_{rr_{ss}} - \alpha_{rr}) \tag{1.49}$$

Slip Ratio, s:

$$\dot{s_{fl}} = \frac{V_x}{\sigma_x}(s_{fl_ss} - s_{fl}) \tag{1.50}$$

$$\dot{s_{fr}} = \frac{V_x}{\sigma_x}(s_{fr_ss} - s_{fr}) \tag{1.51}$$

$$\dot{s_{rl}} = \frac{V_x}{\sigma_x}(s_{rl_ss} - s_{rl}) \tag{1.52}$$

$$\dot{s_{rr}} = \frac{V_x}{\sigma_x}(s_{fr_rr} - s_{rr}) \tag{1.53}$$

In these equations σ_y and σ_x are lateral and longitudinal relaxation lengths in meters respectively.

The constant K_{vy} is introduced in the above equations and plays a role of an inertia for the uncoupled lateral velocity. It is defined as:

$$K_{vy} = m \cdot I_x \cdot I_z - m \cdot I_{xz}^2 - m_s^2 \cdot h^2 \cdot I_z \tag{1.54}$$

The steady state values, α_{ss} of the slip angles and steer angles, δ for each tire are also defined as:

$$\alpha_{fl_{ss}} = -\delta_{fl} + \frac{v_y + l_f \cdot r}{V_x} \tag{1.55}$$

$$\alpha_{fr_{ss}} = -\delta_{fr} + \frac{v_y + l_f \cdot r}{V_x} \tag{1.56}$$

$$\alpha_{rl_{ss}} = -\delta_{rl} + \frac{v_y - l_r \cdot r}{V_x} \tag{1.57}$$

$$\alpha_{rr_{ss}} = -\delta_{rr} + \frac{v_y - l_r \cdot r}{V_x} \tag{1.58}$$

$$\delta_{fl} = \delta_{fo} + K_{rsf} \cdot \phi - K_{csf} \cdot F_{yfl} \tag{1.59}$$

$$\delta_{fr} = \delta_{fo} + K_{rsf} \cdot \phi - K_{csf} \cdot F_{yfr} \tag{1.60}$$

$$\delta_{rl} = K_{rsr} \cdot \phi - K_{csr} \cdot F_{yrl} \tag{1.61}$$

$$\delta_{rr} = -K_{rsr} \cdot \phi - K_{csr} \cdot F_{yrr} \tag{1.62}$$

Here;

δ_{fo}: Steer angle input[rad]

K_{rsf} and K_{rsr}: Roll steer coefficient of front and rear [rad]

K_{csf} and K_{csr}: Cornering stiffness of front and rear [rad/N], which represent the lateral force compliance steer of the suspension systems and tires.

F_{yfl},F_{yfr},F_{yrl},F_{yrr}: Lateral force of each tire [N].

The steady state values, (s_{ss}), of the slip ratios are as follows:

$$S_{fl_{ss}} = 1 - \frac{V_x}{R_w \cdot \omega_{fl}} \tag{1.63}$$

$$S_{fr_{ss}} = 1 - \frac{V_x}{R_w \cdot \omega_{fr}} \tag{1.64}$$

$$S_{fl_{ss}} = 1 - \frac{V_x}{R_w \cdot \omega_{rl}} \tag{1.65}$$

$$S_{fl_{ss}} = 1 - \frac{V_x}{R_w \cdot \omega_{rr}} \tag{1.66}$$

R_w: Dynamic rolling radius [m],

ω_{fl}, ω_{fr}, ω_{rl}, ω_{rr}:Wheel angular velocity inputs [rad/s],

The resultant external forces and torques are obtained as the following equations:

$$F_x = F_{xf} + F_{xr} \tag{1.67}$$

$$F_y = F_{yf} + F_{yr} \tag{1.68}$$

$$T_z = l_f F_{yf} - l_r F_{yr} + \frac{t_f}{2}[F_{xfl} - F_{yfl}\delta_{fl} - (F_{xfr - F_{yfr}\delta_{fr}})] + \frac{t_r}{2}[F_{xrl} - F_{yrl}\delta_{rl} - (F_{xrr} - F_{yrr}\delta rr)] \tag{1.69}$$

$$T_x = m_s \cdot h \cdot g - (K_r \cdot \phi + B_r \cdot p) \tag{1.70}$$

t_f and t_r: Front and rear tread [m],

K_r: Sum of front and rear roll stiffness $[N \cdot m/rad]$

B_r: Sum of front and rear roll damping $[N \cdot m \cdot /rad]$

$$F_{xf} = F_{xfl} + F_{xfr} - F_{yfl} \cdot \delta_{fl} - F_{yfr} \cdot \delta_{fr} \tag{1.71}$$

$$F_{xr} = F_{xrl} + F_{xrr} - F_{yrl} \cdot \delta_{rl} - F_{yrr} \cdot \delta_{rr} \tag{1.72}$$

$$F_{yf} = F_{yfl} + F_{yfr} + F_{xfl} \cdot \delta_{fl} - F_{xfr} \cdot \delta_{fr} \tag{1.73}$$

$$F_{yr} = F_{yrl} + F_{yrr} - F_{xrl} \cdot \delta_{rl} - F_{xrr} \cdot \delta_{rr} \tag{1.74}$$

The longitudinal force and lateral force of the tire are assumed to be a linear function of the slip quantities; slip angles and slip ratios. This assumed relation may be modified to more accurate one in high slip condition.

$$F_{xfl} = C_{xf} \cdot s_{fl} \tag{1.75}$$

$$F_{xfr} = C_{xf} \cdot s_{fr} \tag{1.76}$$

$$F_{xrl} = C_{xr} \cdot s_{rl} \tag{1.77}$$

$$F_{xrr} = C_{xr} \cdot s_{rr} \tag{1.78}$$

$$F_{yfl} = -C_{yf} \cdot \alpha_{fl} \tag{1.79}$$

$$F_{yfr} = -C_{yf} \cdot \alpha_{fr} \tag{1.80}$$

$$F_{yrl} = -C_{yr} \cdot \alpha_{rl} \tag{1.81}$$

$$F_{yrr} = -C_{yr} \cdot \alpha_{rr} \tag{1.82}$$

C_{xf} and C_{xr}: Front and rear longitudinal force stiffness [N],

C_{yf} and C_{yr}: Front and rear cornering stiffness [N/rad].

The mathematical model is constructed in Simulink using the Equation 1.37 through 1.75 as shown in Figure 1.10 through Figure 1.16.

The Subsystems that are used in the full simulink model are shown in Figure 1.11, Figure 1.12, Figure 1.13, Figure 1.14, Figure 1.15, and Figure 1.16.

The input for these simulations is step steering as shown in Figure 1.17.

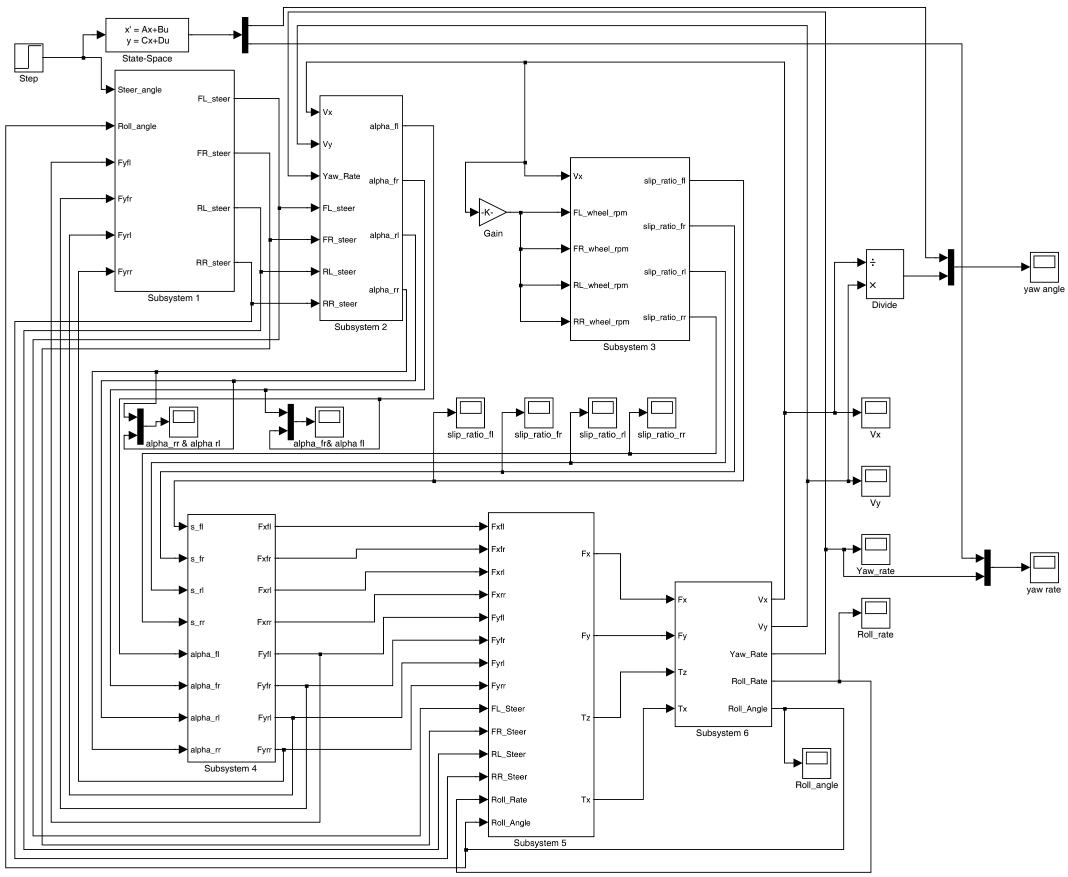

Figure 1.10. 13-dof vehicle simulink model

In Figure 1.18 while the yaw velocity of 13-DOF freedom model is decreasing, yaw velocity of 3-DOF model and single track model does not change. The reason for this difference is a result of longitudinal velocity change during simulation. In 13-DOF the initial velocity is 20 m/s. However, we do not set it to that value. So it starts to decrease as the vehicle steers to one side. In single track model and 3-DOF freedom model longitudinal velocity is set to 20 m/s initially and it does not change as seen in Figure 1.20.

In Figure 1.19 13-DOF model, 3-DOF model and 7-DOF model roll velocity values are compared. The roll velocity of 7-DOF model less than 3-DOF model and 13-DOF model. Also, the oscillation time for 7-DOF model is less than the 3-DOF model. This difference is a result of anti-roll bar that is used in 7-DOF freedom model but in 13-DOF model in spite of high roll velocity value within one second, its oscillation

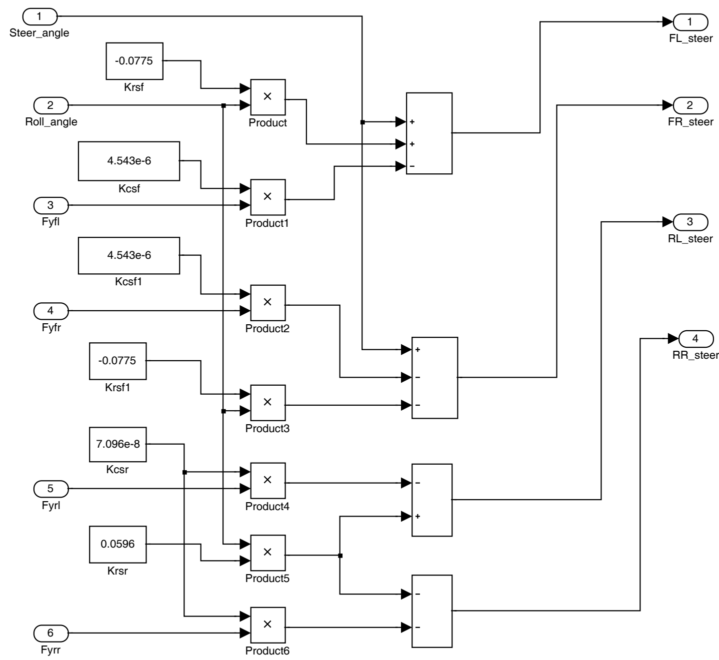

Figure 1.11. Subsystem 1

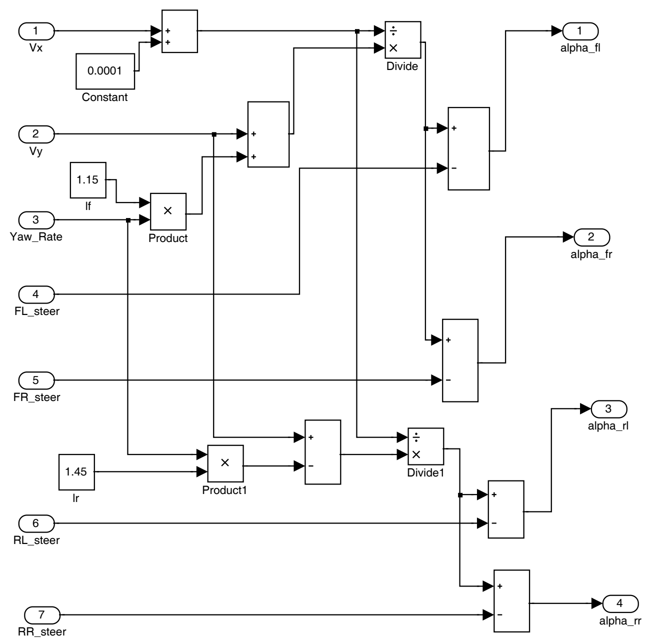

Figure 1.12. Subsystem 2

does not last long because the longitudinal velocity of this vehicle decreases as the time passes.

In Figure 1.21 and Figure 1.22 show the front and rear slip angle change. The

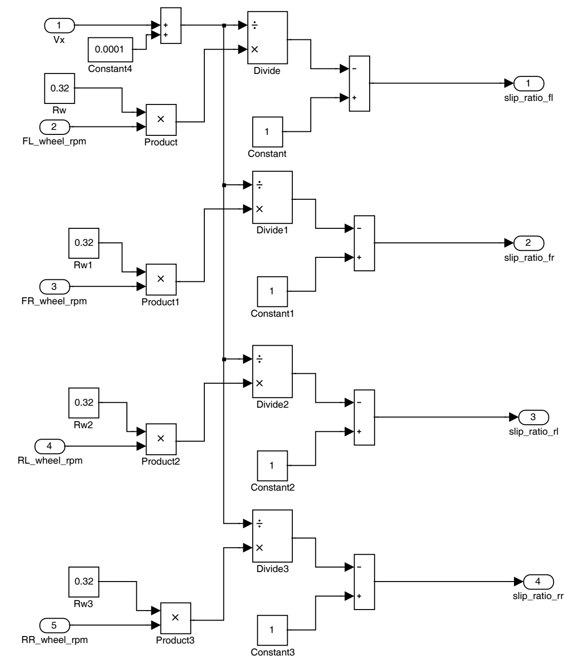

Figure 1.13. Subsystem 3

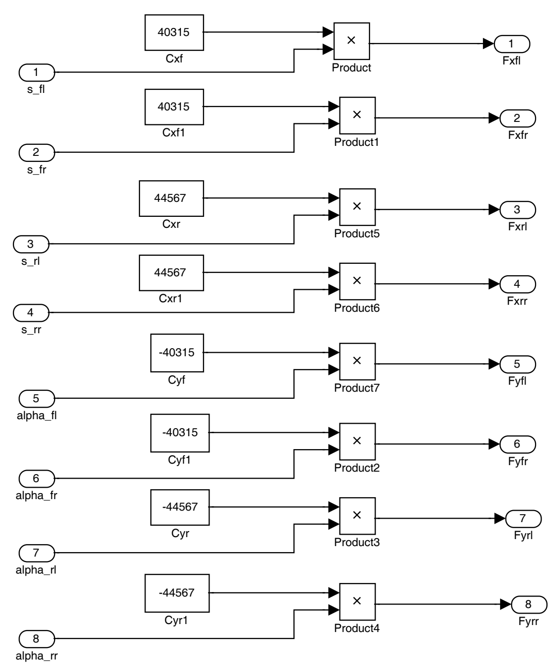

Figure 1.14. Subsystem 4

difference between left and right tire side slip angles for both front and rear tires is because of the steering direction. In our analysis steering is to the right hand-side. So rear right tire and front left tire slip quantities are more than the other two tires.

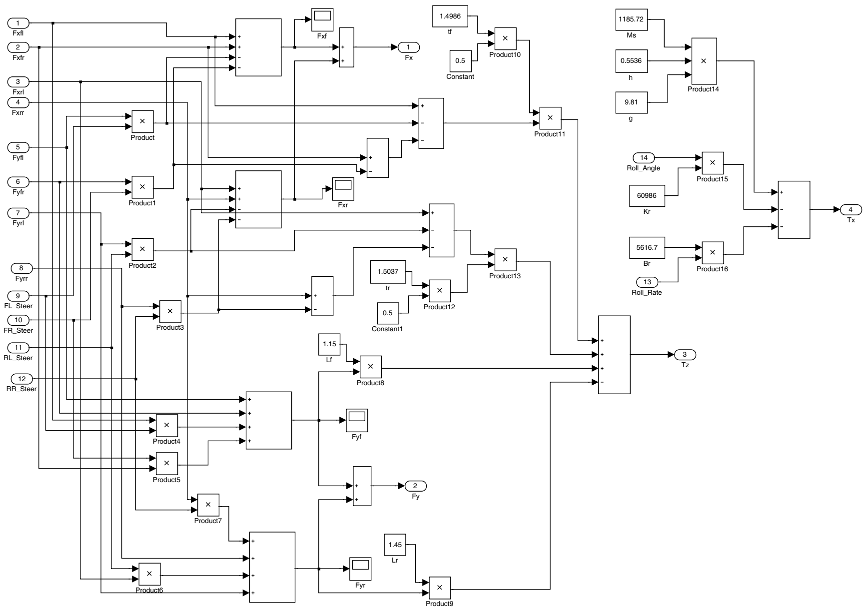

Figure 1.15. Subsystem 5

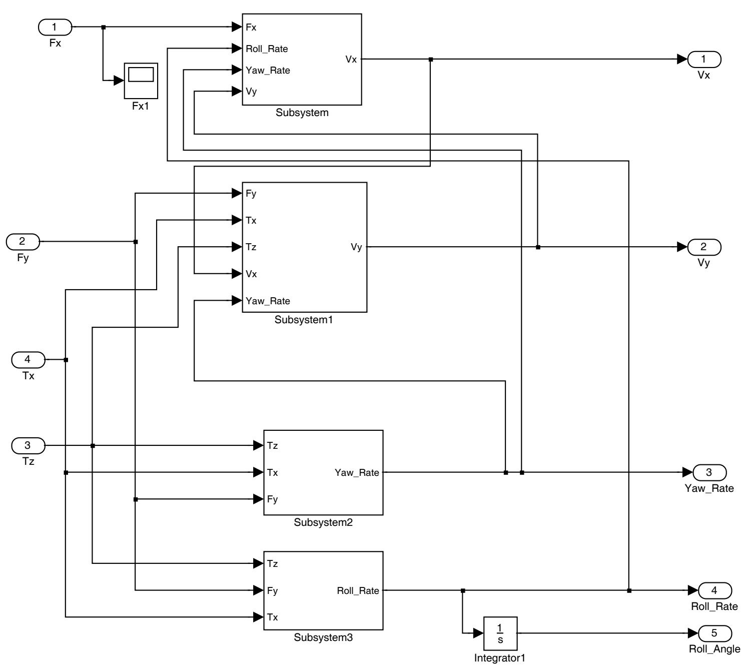

Figure 1.16. Subsystem 6

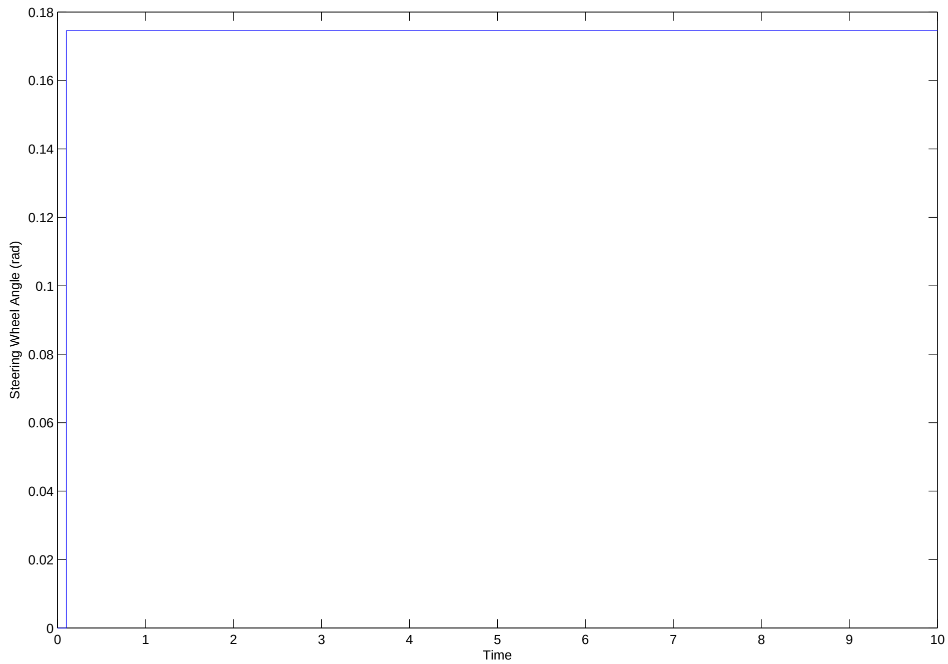

Figure 1.17. Steering input for 13-dof model

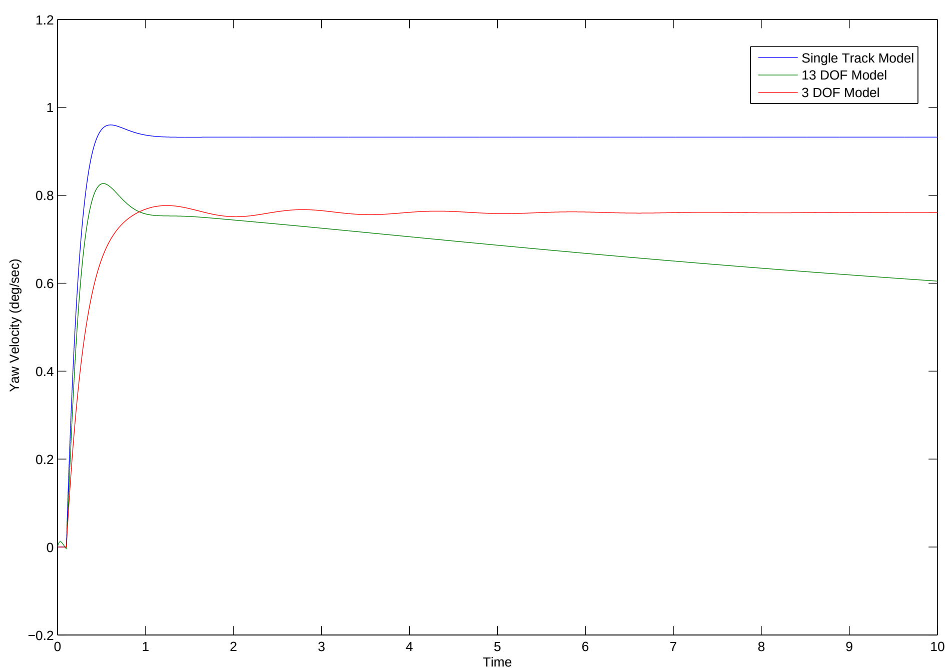

Figure 1.18. Comparison of yaw velocity time response between 13-dof model, single track model and yaw-roll model

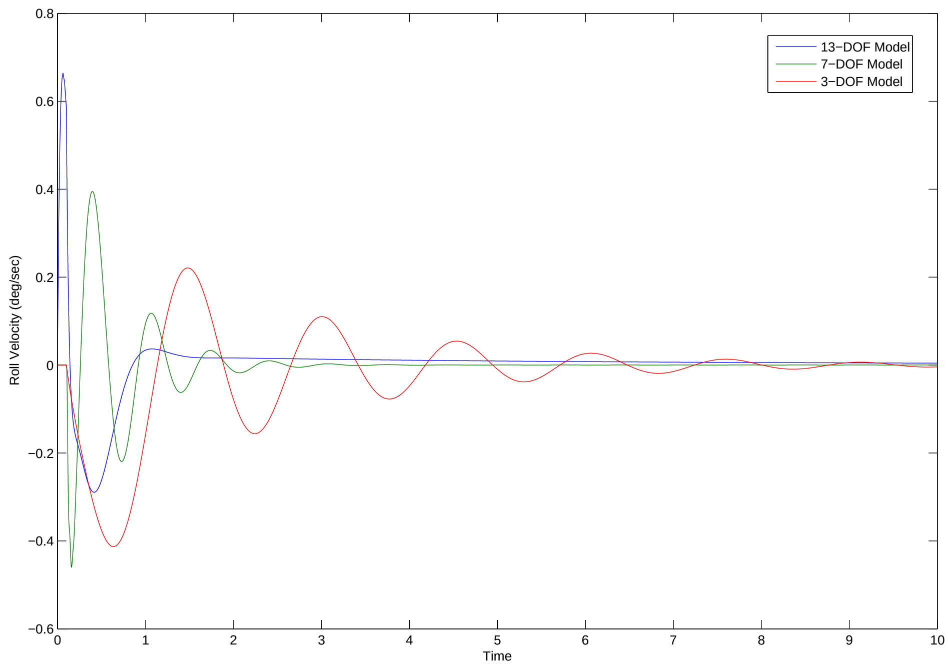

Figure 1.19. Comparison of roll velocity time response between 13-dof model, 7-dof model and 3-dof model

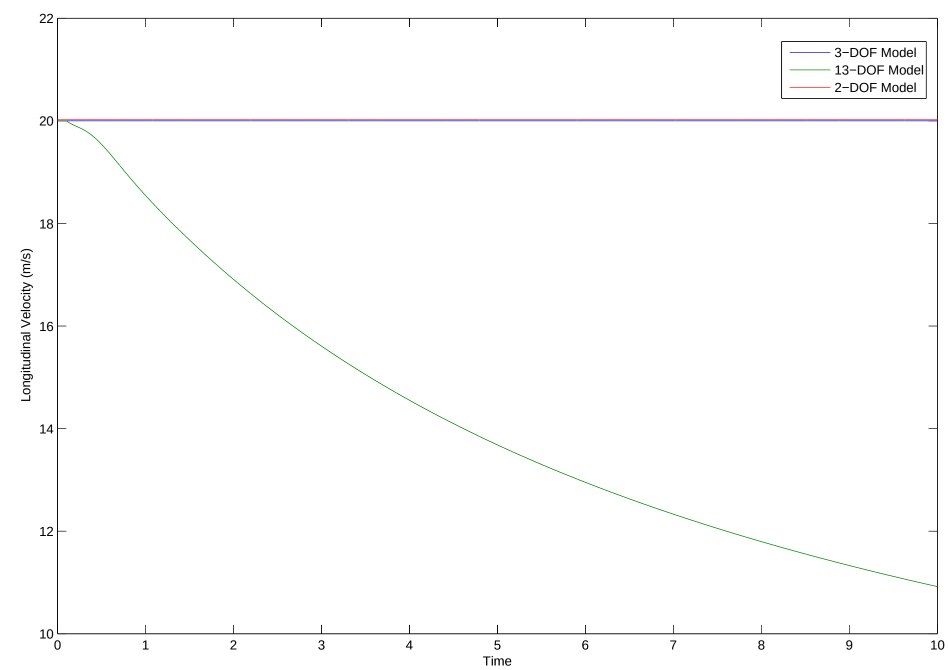

Figure 1.20. 13-dof longitudinal velocity change time response

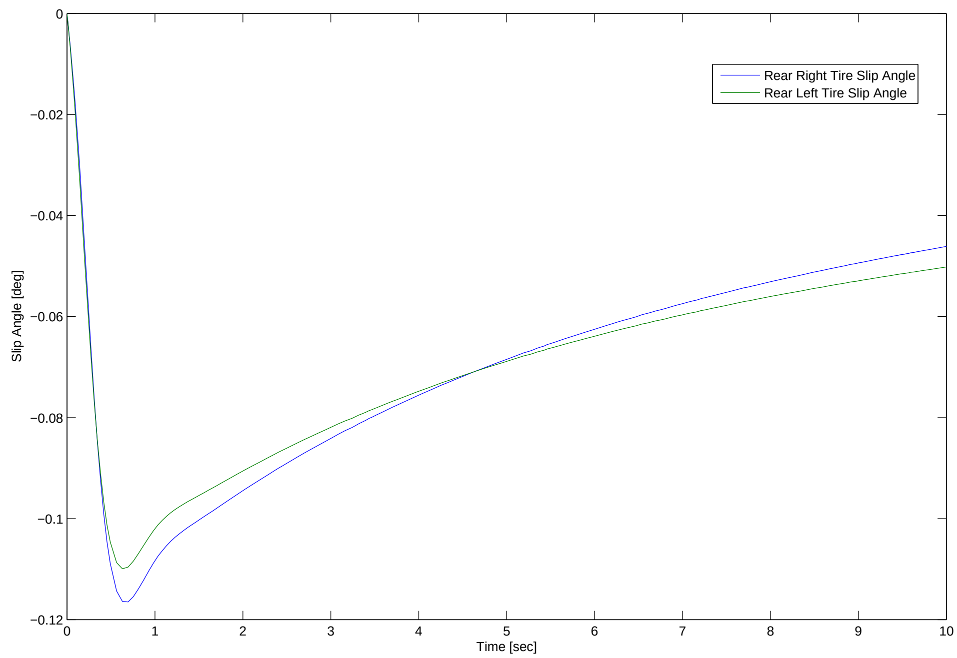

Figure 1.21. Comparison of rear right tire and rear left tire slip angles time response in 13-dof model

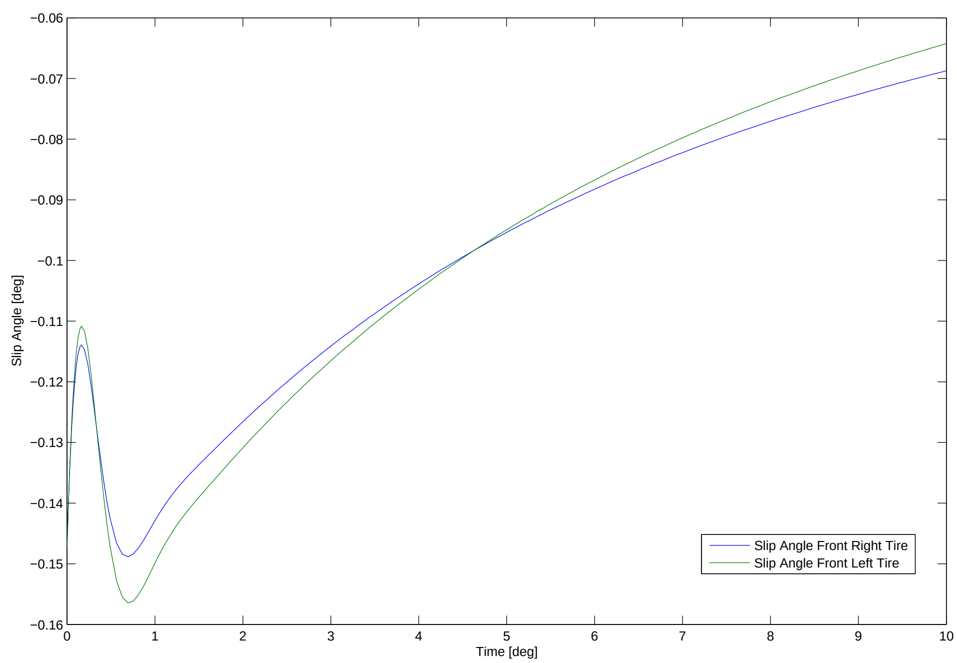

Figure 1.22. Comparison of front right tire and front left tire slip angles time response in 13-dof model

2. ADAMS MODEL OF A LIGHT COMMERCIAL VEHICLE

2.1. ADAMS Solution Methodology

The first step in the simulation is to prepare the specifications of the vehicle that will be modeled. The specifications include rigid parts, connecting joints and forces. For the rigid body part it is necessary to define the mass, the location of the center of mass, moments of inertias of the mass. Each part has a mark to define its center of mass location, joint location, orientation, force location and direction. In the model the ground should also be included as a non-moving part. Parts are connected to each other by using standard joints defined by ADAMS. The general body has six degrees of freedom in space. Three components for the position of center of mass and three for orientations. So three cartesian coordinates and three Euler angles are used. Equations of motion are obtained using Lagrange dynamics. Six equations of motion are obtained for a body with six DOF.

The next step is external and internal forces. External forces can be torsional and translational, and constant or functionally time dependent. Four types of loadings are considered: gravity, torque, translational force and ground force. For each tire on the vehicle, ADAMS calculates three forces and three torques acting at wheel center. In order to perform these calculations it is necessary to update the position, velocity and orientation of the wheel by using the position of wheel center. ADAMS always makes integration to find new position and orientation of the vehicle [31]. In the pre-processor, hardpoint locations of each rigid part is defined. The hardpoint locations give the position of each part with respect to ground reference frame, joint location, orientation and force location. The differential equations representing the system are numerically integrated to calculate positions, velocities, accelerations and forces. Pre-processor and post-processor allow users to define models and evaluate results using the graphical environment.

The model is assembled in ADAMS by defining the hardpoints and mass properties of each part and when the model is assembled by ADAMS, the program can be used to carry out kinematic, static or dynamic analyses. ADAMS uncouples the equations of motion and solves them separately for displacements, velocities, accelerations and forces. For static analysis, initial velocities and accelerations are taken to be zero. Then equilibrium is searched. Static analysis is often performed as a preliminary step for dynamic analysis. In ADAMS, inputs are defined as velocity or acceleration. The velocity or the acceleration that are initially defined should satisfy the constraint equations and equations of motion. If the input values do not satisfy these two equations then ADAMS try to find the closest input to the one you have defined by using Newton Raphson iteration method. Then it solves the equations of motion. There are four kinds of fundamental constraint elements in ADAMS, namely atpoint, inplane, perpendicular, and angular. Initial values must satisfy the constraints. Newton-Raphson method is used in determining an initial value which is close to the input value that satisfies constraint equations.

Example:

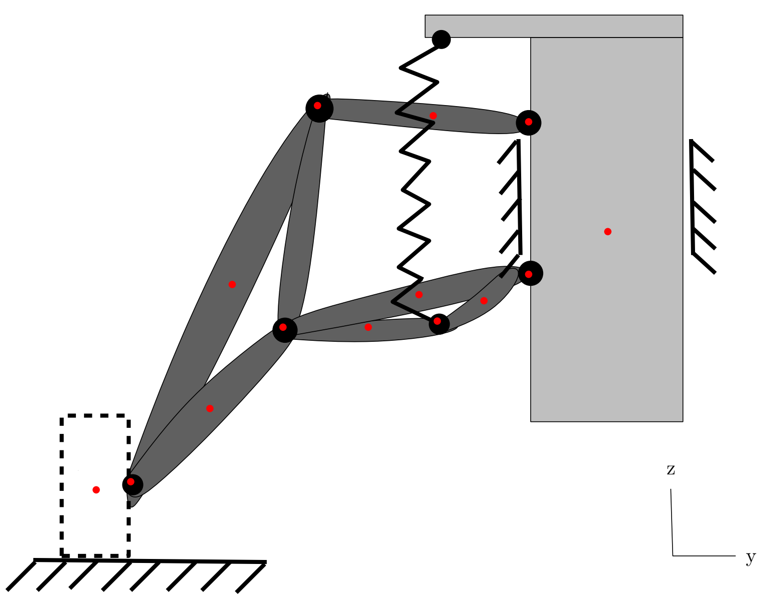

Figure 2.1. Double wishbone suspension model

The red points in Figure 2.1 indicate the hardpoint locations. The black points are the joints between the suspension parts. In ADAMS these joints and the hardpoint locations must be defined with mass properties of each part. There is a coordinate frame attached to each moving part on the suspension and a ground reference frame which is not moving. The position of each part is defined with respect to the ground reference frame. After defining the initial position of each part, the velocities and accelerations are calculated by taking derivatives of positions. ADAMS configuration of two rigid parts connected to each other is shown in Figure 2.2.

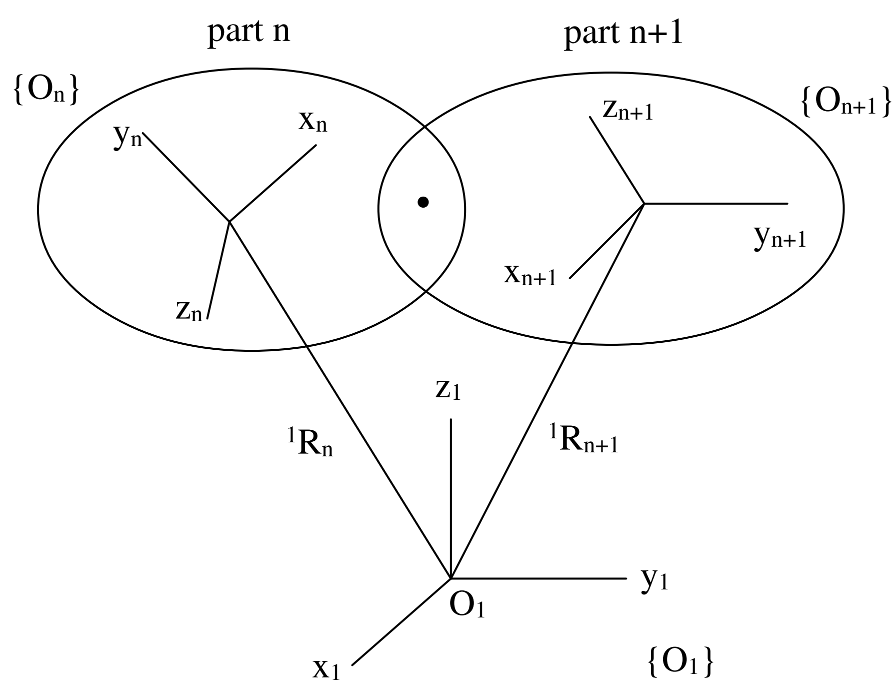

Figure 2.2. ADAMS configuration of two rigid parts connected to each other

2.2. ADAMS Model

A light commercial vehicle, Ford Transit Connect, was selected as a case model. This vehicle has McPherson strut for the front suspension and rack and pinion type of front steering system. The rear suspension is consisted of leaf spring and damper. All the wheels have $195/65R15$ tire. A full vehicle model is assembled with the subsystems including front and rear suspension, front steering, wheels and tires. Tires used in this model are Pacejka 2002 tire model. The vehicle model is created in ADAMS by defining the harpoint locations of each point of each part. Hardpoints define the x-y-z position of a point on a vehicle part. These points are taken from the CAD data of the full vehicle. Then these points are exported to ADAMS for specific front and rear suspensions, and steering system. When the templates do not have the required parts in the software's library as the rear suspension of our model, then this part is created using ADAMS/View which enables us to draw new part. This drawing will also include the hardpoint locations. In our model the vehicle body is not taken into consideration because it is out of our concern and does not affect lateral drift of the vehicle. The most important hardpoint locations in our model belong to the suspension parts and steering geometry.

The hardpoint locations of the model are given as follows:

Table 2.1. Vehicle body hardpoint locations

Name	LeftX	LeftY	LeftZ	RightX	RightY	RightZ
$controller\ ref^{*}$	2597.17	0.0	916.1			
$test\ gyro^{**}$	2597.17	0.0	916.1			
$bodymount1$	1000	-100	1000	1000	100	1000
$bodymount2$	1500	-100	1000	1500	100	1000
$bodymount3$	2000	-100	1000	2000	100	1000
$bodymount4$	2500	-100	1000	2500	100	1000
$bodymount5$	3000	-100	1000	3000	100	1000
$boxmount1$	0.0	0.0	0.0	0.0	0.0	0.0
$boxmount2$	0.0	0.0	0.0	0.0	0.0	0.0
$boxmount3$	0.0	0.0	0.0	0.0	0.0	0.0

* Traction/Braking reference point.

** Test equipment.

Table 2.2. Front suspension hardpoint locations

Name	LeftX	LeftY	LeftZ	RightX	RightY	RightZ
$bumper - lower$	1765.48	-567.35	880.24	1765.48	567.35	880.24
$bumper - upper$	1769.26	-555.27	957.97	1769.26	555.27	957.97
$contactpatch$	1745.82	-753.76	154.97	1745.82	753.76	154.97
$lca - front$	1760.3	-363.6	365.8	1760.3	363.6	365.8
$lca - rear$	2030.9	-366.9	369.3	2030.9	366.9	369.3
$lower - ball - joint$	1735.0	-712.8	364.25	1735.0	712.8	364.25
$rebound - lower$	1748.73	-621.41	525.86	1748.73	621.41	526.86
$rebound - upper$	1748.73	-621.41	526.86	1748.73	621.41	526.86
$spindle - align$	1745.45	-647.75	440.82	1745.45	647.75	440.82
$spring - seat - lower$	1761.15	-611.49	785.86	1761.15	611.49	785.86
$spring - seat - upper$	1769.24	-555.27	965.97	1769.24	555.27	965.97
$strut - knuckle$	1751.3	-612.95	557.25	1751.3	612.95	557.25
$subframe - front$	1792.98	-470.39	558.87	1792.98	470.39	558.87
$subframe - mid - 1$	0.0	0.0	0.0	0.0	0.0	0.0
$subframe - mid - 2$	0.0	0.0	0.0	0.0	0.0	0.0
$subframe - rear$	2127.0	-355.0	352.28	2127.0	355.0	352.28
$tierod - inner$	1912.0	-324.0	439.1	1912.0	324.0	439.0
$tierod - outer$	1862.73	-687.4	451.55	1862.73	687.4	451.55
$top - mount$	1769.92	-553.09	981.4	1769.92	553.09	981.4
$wheel - center$	1745.8	-747.73	442.91	1745.8	747.73	442.91

Table 2.3. Rear suspension hardpoint locations

Name	LeftX	LeftY	LeftZ	RightX	RightY	RightZ
$leaf - spring$	4410.5	0.0	400.0			
$panhard - axle$	4275.0	-410.0	400.0			
$panhard - frame$	4250.0	410.0	380.0			
$bumper - lower$	4416.14	-484.92	466.51	4416.14	484.92	466.51
$bumper - upper$	4416.13	-485.0	541.89	4416.13	485.0	541.89
$contact - patch$	4410.5	-776.1	155	4410.5	776.1	155.0
$damper - lower$	4381.5	-600	304	4381.5	600	304
$damper - upper$	4102.0	-600	591.76	4102.0	600	591.76
$front - leaf - eye$	3716.5	-515.25	354.16	3716.5	515.25	354.16
$front - torsional - joint$	4059.98	-515.25	363.27	4059.98	515.25	363.27
$leaf - to - shackle$	4967.84	-515.25	457.23	4967.84	515.25	457.23
$rear - torsional - joint$	4660.06	-515.25	473.21	4660.06	515.25	473.21
$rebound - lower$	4344.72	-600	310.71	4344.72	600	310.71
$rebound - upper$	4090.91	-600	535.47	4090.91	600	535.47
$second - stage - axle$	4407.77	-485.1	440.75	4407.77	485.1	440.75
$second - stage - frame$	4407.77	-485.0	414.89	4407.77	485.0	414.89
$shackle - to - frame$	4912.45	-515.25	540.61	4912.45	515.25	540.61
$spindle - align$	4410.5	-661.03	443.0	4410.5	661.03	443
$subframe - mid1$	0.0	0.0	0.0	0.0	0.0	0.0
$subframe - mid2$	0.0	0.0	0.0	0.0	0.0	0.0
$wheel - center$	4410.5	-776.1	443	4410.5	776.1	443

The front and rear suspensions and steering system of the vehicle designed in

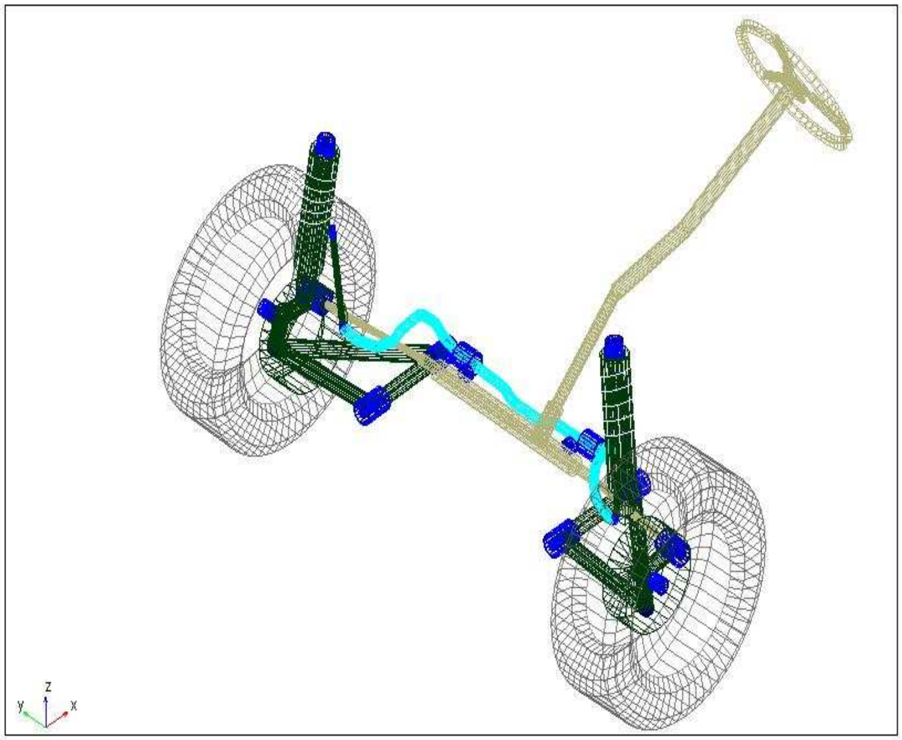

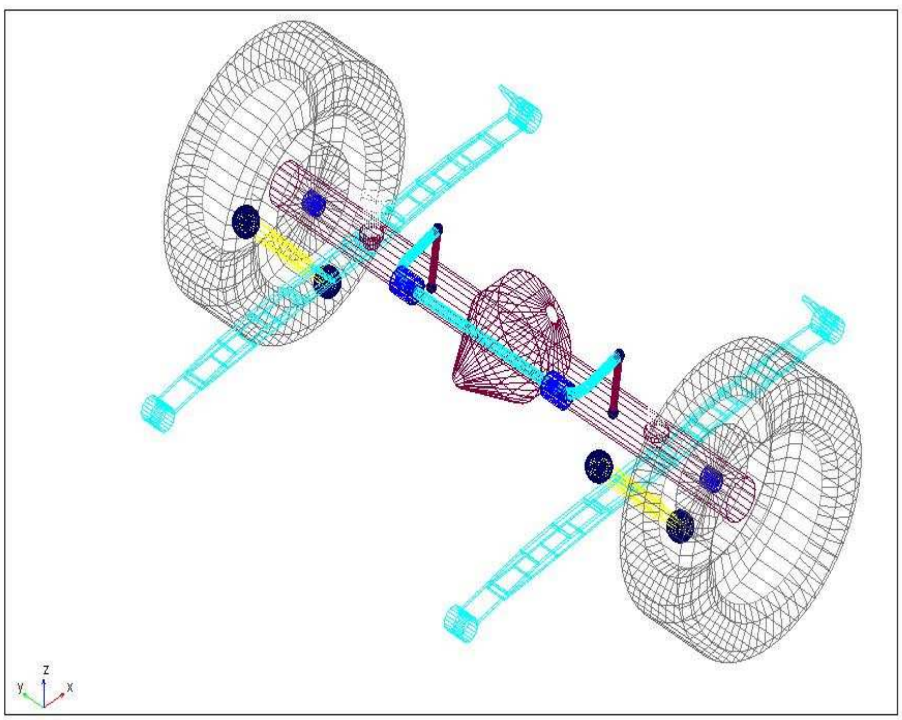

Figure 2.4. Rear suspension and tire model in ADAMS

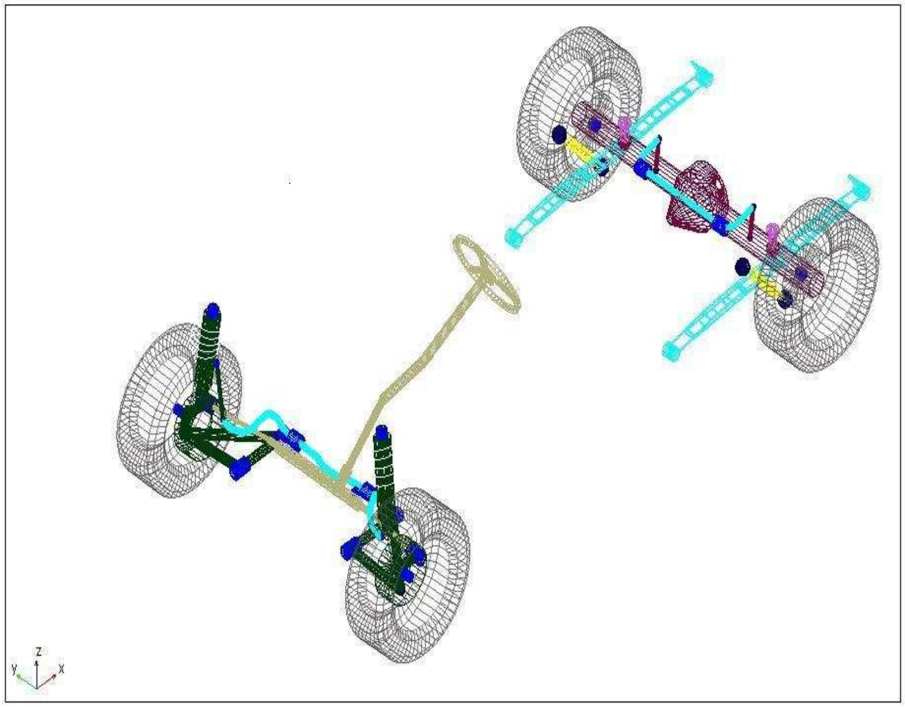

Figure 2.5. Full vehicle model in ADAMS

The vehicle and its suspension and steering parts that are modeled in IDEAS are

Figure 2.6. Full vehicle model in IDEAS

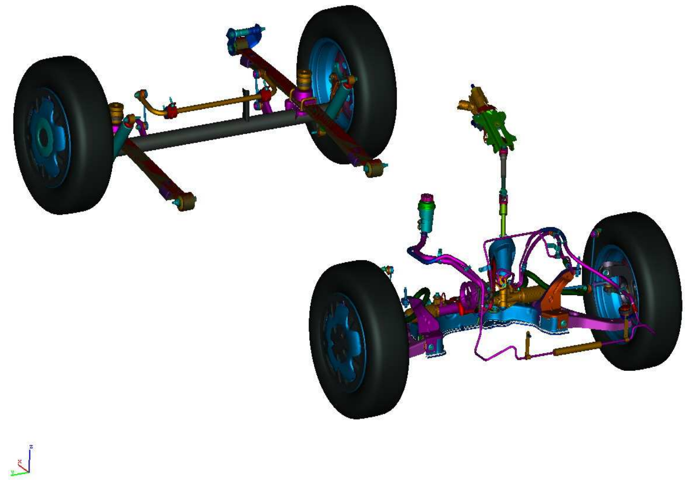

Figure 2.7. Suspension and steering components of the vehicle

2.3. Front and Rear Suspension Model Parts and Suspension Geometries

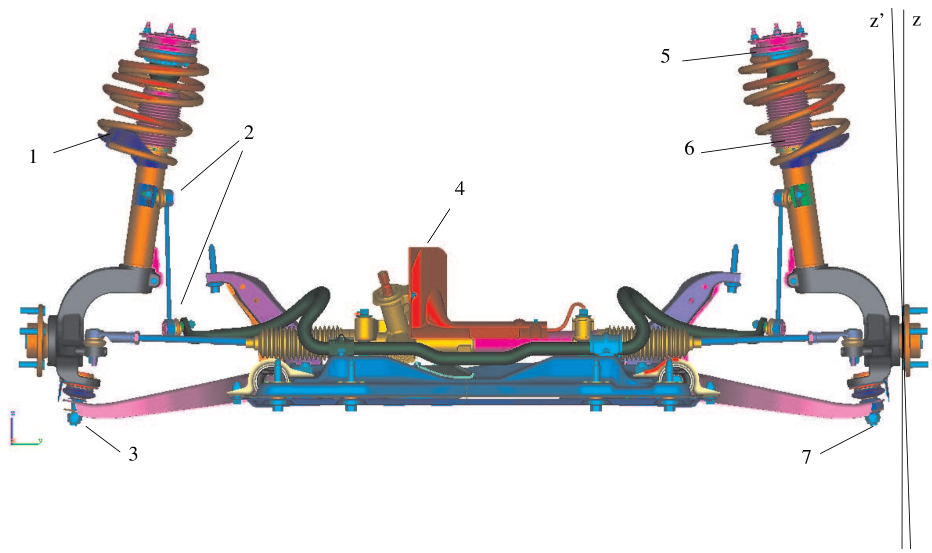

Figure 2.8. Front suspension components and camber angle. (1- Shock absorber spring plate, 2- Ball-joint, 3- Ball-joint, 4- Heat shield, 5- Bearing, 6- Gaitor, 7- Ball-joint)

Figure 2.11 shows the components of front suspension and camber angle. The type of front suspension is McPherson. The angle between z (vertical axis) and $z\prime$ shows the camber angle. Shock absorber spring plate works in which the vehicle passes a bump or a cavity to support the spring. Ball joints are used at point 2 and 3 to have rotational motion in all directions. Heat shield protects the steering and the components of front suspension close to exhaust pipe because the temperature of exhaust gasses are approximately 125 ^{0}F.

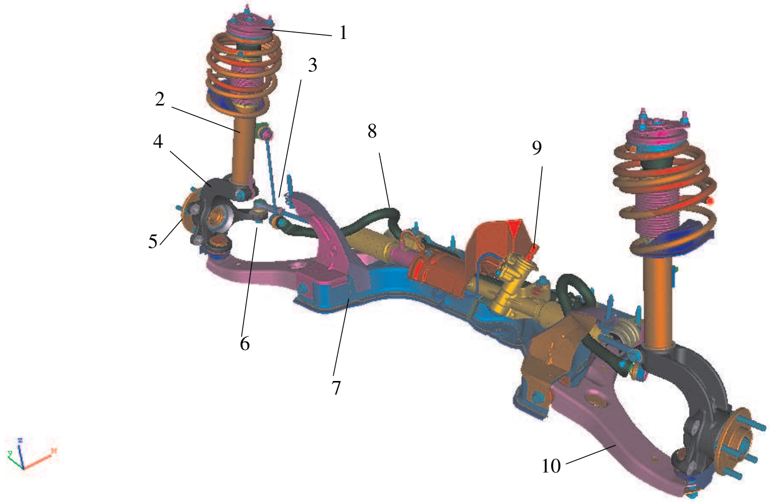

Figure 2.9. Front suspension components. (1- Top mount, 2- Shock absorber, 3- Tie rod, 4- Knuckle, 5- Hub, 6- Toe adjuster, 7- Cross-member, 8- Anti-Roll bar, 9- Steering column, 10- L-arm)

In Figure 2.9 iso view of front suspension is seen. Top mount is the part in which the front suspension is attached to the vehicle. Tie rod is the part of steering system that transmits the steering wheel's motion to the wheels. Knuckle carries the shock absorber and hub is attached to the knuckle and the tires are attached to the hub. Toe adjuster is used to align front wheel toe angles. Anti-roll bar is attached to the suspension to resist roll motion. The steering column transmits torque input from the steering wheel. L-arm is the body of front suspension that carries the components.

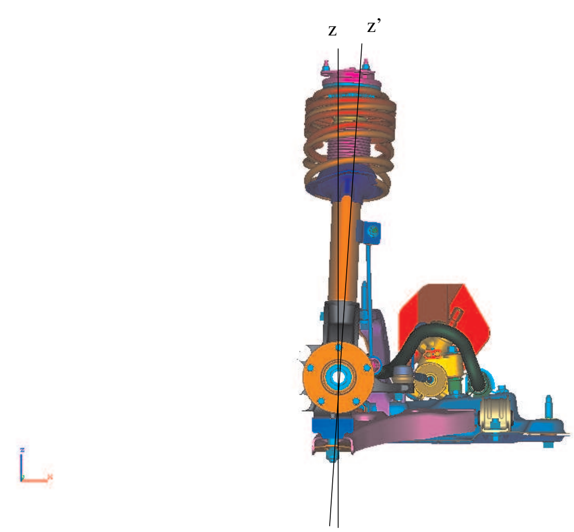

Figure 2.10. Front suspension caster angle

Caster angle is defined as the angle between z-axis (vertical axis) and z'-axis.

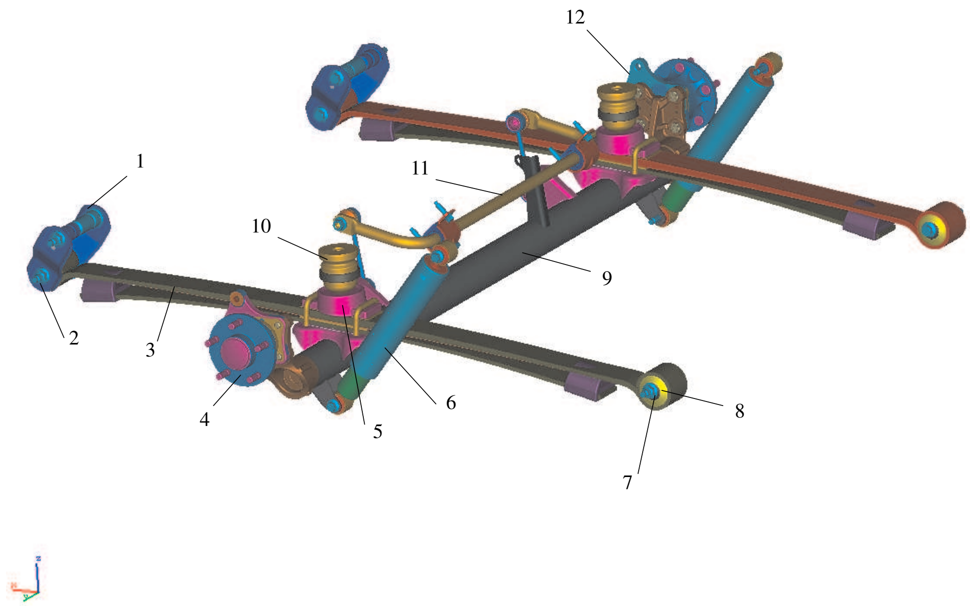

Figure 2.11. Rear suspension components.(1- Shackle, 2- Bush, 3- Leaf spring, 4- Hub, 5- Clamp plate, 6- Shock absorber, 7- Front eye, 8- Bush, 9- Rear axle, 10- Bump stop, 11- Anti-roll bar, 12- Spindle)

The

rear stop

work

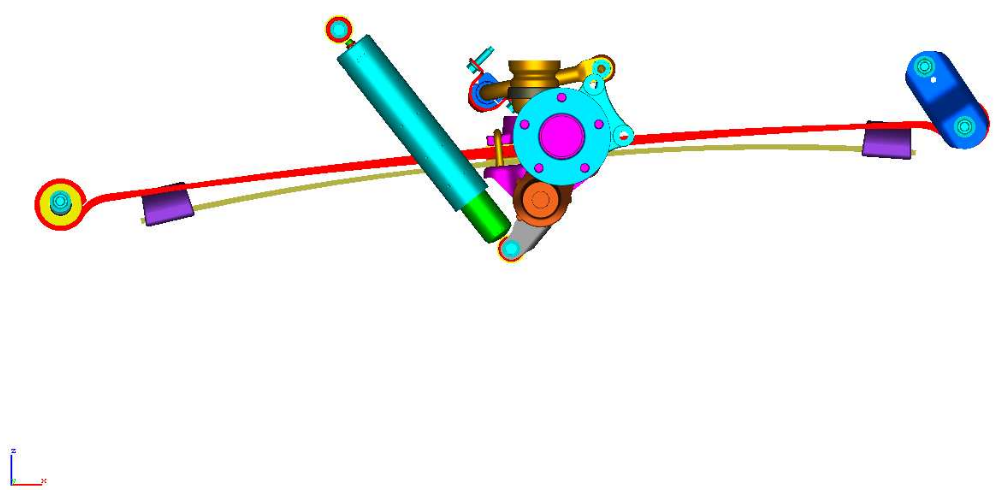

Figure 2.12. Rear suspension side view

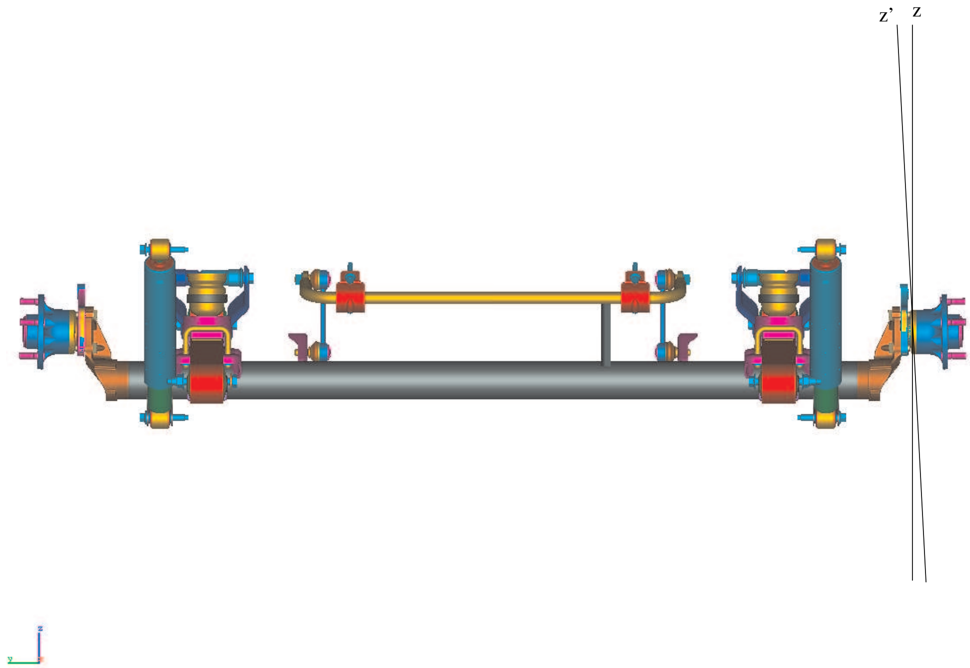

Figure 2.13. Rear suspension camber angle

Rear suspension has also camber value. This angle is created in the production stage of the spindle. Spindle has the required angle on its surface to have that camber value.

Figure 2.14. Rear suspension bottom view

Toe adjustment is a post production process. The only adjustable parameter is

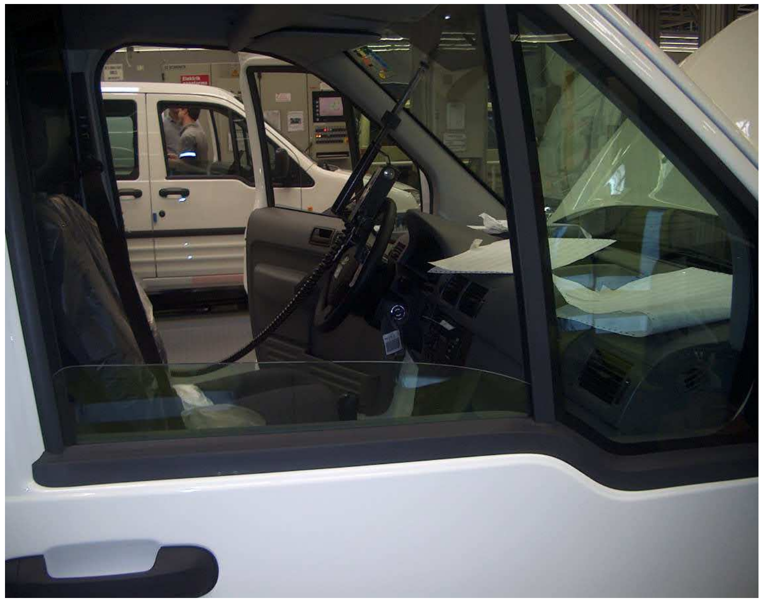

Figure 2.15. Toe adjustment process with a fastened steering wheel

the toe value. As seen in Figure 2.15 steering wheel is set to zero steering angle. Then the toe angles are aligned. Toe alignment is done by adjusting the length of the tie rod as seen in Figure 2.16.

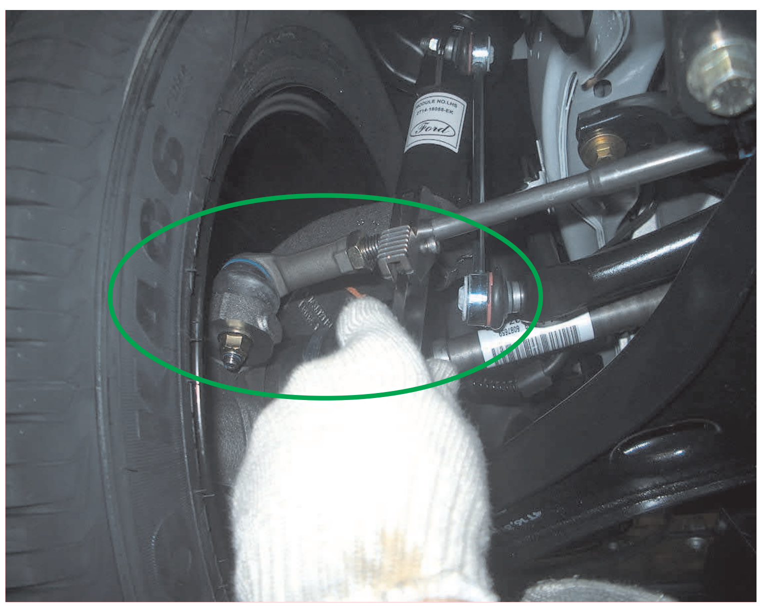

Figure 2.16. Front wheel toe adjustment

Figure 2.17. Front suspension L-arm

Figure 2.18. Front wheel alignment

In the following chapter field tests are done in Ford Otosan Inc. Kocaeli Plant. The results obtained from field tests are compared to ADAMS steady state drift results. Steady drift test is done at constant velocity and zero steering angle. It is assumed that road camber is also zero. The vehicle is driven at 80 kph for 10 seconds. These tests are repeated for 65 times with various suspension parameters. Then the results of the analysis and the field tests are compared.

3. RESULTS

3.1. Field Test Procedures and Results

The vehicle is driven at 80 kph in the test road that has no camber angle. At initial time step the steering wheel is set to zero steering angle and the speed of the vehicle is constant. Then the steering wheel is left free for some time until the vehicle has a drift of one lane to one side of the road. These tests are repeated for randomly selected vehicles for a couple of times. In fact, all the vehicles on roads have a drift problem because of vehicle asymmetry. However, to call it a problem according to Ford Inc. criteria, the drift time must be above the limits that is less than 7 seconds per lane change at 80 kph. If drift time is between 7 and 10 seconds, it is in the acceptable range but that indicates a problem which is not serious. The vehicles that drift above 10 seconds are assumed to be perfect. The test road that is used in Ford-Otosan Inc. Kocaeli Plant is shown in Figure 3.1. The parameters from Table 3.1 to Table 3.9

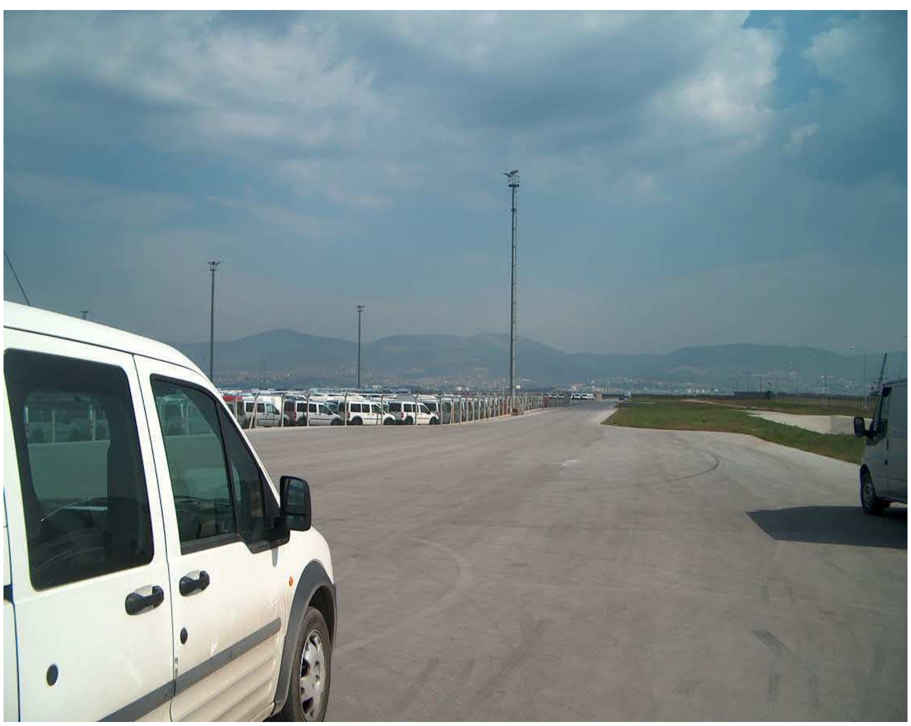

Figure 3.1. Test road

Table 3.1. Vehicle parameters

Vehicles	Front Toe		Front Camber		Front Caster	
	LH	RH	LH	RH	LH	RH
1	0,17	0,15	-0,95	-0,32	1,60	1,67
2	0,18	0,13	-0,80	-0,30	1,45	1,75
3	0,10	0,07	-0,62	-0,52	1,57	1,73
4	0,08	0,08	-0,98	-0,50	0,98	1,35
5	0,08	0,12	-0,92	-0,40	1,38	1,77
6	0,07	0,07	-0,87	-0,85	1,55	1,37
7	0,12	0,13	-1,17	-0,18	1,37	1,95
8	0,12	0,12	-0,67	-0,35	1,28	1,57
9	0,12	0,05	-0,78	-0,03	1,47	1,50
10	0,12	0,13	-1,03	-0,40	1,07	1,10
11	0,08	0,10	-0,48	-0,48	1,67	1,47
12	0,12	0,08	-0,67	-0,23	1,47	1,37
13	0,22	0,12	-0,60	-0,47	1,37	1,33
14	0,10	0,15	-0,65	-0,13	1,25	1,27
15	0,13	0,18	-0,83	-0,37	1,33	1,30
16	0,13	0,13	-0,67	-0,80	1,08	0,93
17	0,08	0,00	-0,65	-0,68	1,60	1,40
18	0,07	0,03	-0,82	-0,25	1,53	1,63
19	0,17	0,18	1,08	0,42	1,67	1,68
20	0,07	0,07	-0,82	-0,20	1,18	1,45
21	0,07	0,13	-0,72	-0,43	1,32	0,95
22	0,03	0,05	-0,82	-0,27	1,65	1,60
23	0,07	0,07	-0,77	-0,28	1,38	1,05
24	0,00	0,05	-0,87	-0,17	1,65	1,52
25	0,08	0,13	-0,97	-0,42	1,35	1,25
26	0,08	0,23	-0,60	-0,62	1,60	1,78
27	0,03	0,07	-0,87	-0,48	1,72	1,87

Table 3.2. Vehicle parameters

Vehicles	Front Toe		Front Camber		Front Caster	
	LH	RH	LH	RH	LH	RH
28	0,17	0,13	-0,80	-0,35	1,75	1,57
29	0,13	0,08	-0,85	-0,33	0,72	0,70
30	0,05	0,07	-0,88	-0,30	1,57	1,73
31	0,10	0,07	-0,52	-0,70	1,23	1,23
32	0,02	0,10	-0,68	-0,68	1,30	1,32
33	-0,03	-0,02	-0,62	-0,62	1,38	1,38
34	0,07	0,03	-0,75	-0,45	1,83	1,87
35	-0,03	-0,08	-0,77	-0,60	1,57	1,23
36	0,10	0,17	-1,07	-0,28	1,40	1,37
37	-0,02	-0,12	-0,85	-0,43	1,60	1,35
38	-0,05	-0,07	-0,88	-0,45	1,18	1,68
39	-0,07	-0,10	-0,83	-0,48	1,45	1,53
40	0,08	0,18	-1,03	-0,45	1,55	1,83
41	0,02	0,03	-0,85	-0,18	1,73	1,63
42	0,07	-0,02	-0,93	-0,17	1,52	1,77
43	0,13	0,12	-0,72	-0,52	1,75	1,35
44	-0,03	-0,03	-0,57	-0,38	1,33	1,53
45	0,05	0,13	-0,87	-0,40	1,43	1,77
46	0,05	0,03	-0,70	-0,50	1,32	1,30
47	0,15	0,20	-0,80	-0,52	1,65	1,68
48	0,07	0,13	-0,75	-0,50	1,28	1,55
49	-0,12	-0,07	-0,63	-0,30	1,05	1,23
50	0,05	0,08	-0,97	-0,17	0,78	1,18
51	0,18	0,15	-0,85	-0,32	1,53	1,57
52	0,02	0,12	-0,67	-0,57	1,47	1,60
53	0,00	-0,08	-0,72	-0,32	1,57	1,62
54	-0,07	-0,03	-0,78	-0,67	1,58	1,73

Table 3.3. Vehicle parameters

Vehicles	Front Toe		Front Camber		Front Caster	
	LH	RH	LH	RH	LH	RH
55	-0,08	-0,02	-0,63	-0,65	1,65	1,40
56	0,15	0,10	-0,77	-0,28	1,33	1,62
57	0,13	0,08	-0,87	-0,37	1,00	1,55
58	-0,03	0,00	-1,02	-0,13	1,28	1,87
59	-0,05	-0,05	-0,88	-0,57	1,62	1,45
60	-0,17	-0,07	-1,05	-0,18	1,32	1,77
61	0,08	0,13	-0,80	-0,43	1,20	1,25
62	0,12	0,02	-0,68	-0,42	1,53	1,37
63	-0,02	0,02	-0,77	-0,37	1,35	1,58
64	0,08	0,07	-0,78	-0,57	1,38	1,47
65	0,07	0,05	-0,50	-0,38	1,38	1,60

3.2. Individual Effects of Suspension Parameter Analysis in ADAMS

Figure 3.2 shows that as the negative front camber increases the lateral drift of the vehicle decreases. However, the difference in front left camber and front right camber does not affect lateral drift of the vehicle much.

In Figure 3.3 it is seen that as the positive front caster increases, lateral drift of the vehicle decreases. Small caster changes do not affect the lateral drift of the vehicle so much.

In Figure 3.4 toe angles are varied from positive value to negative value (toe-out to toe-in). As the positive toe (toe in) values increase, the lateral drift of the vehicle decreases. However, the negative toe (toe-out) has more effect on lateral drift of the vehicle than the toe-in value.

Besides the front suspension alignments, the rear suspension alignments have also an effect on lateral drift of the vehicle. As rear negative camber increases in Figure

Table 3.4. Vehicle parameters

Vehicles	Rear Toe		Rear Camber	
	LH	RH	LH	RH
1	0,22	0,05	-0,77	-0,57
2	0,33	0,00	-0,88	-0,63
3	0,23	-0,05	-0,67	-0,65
4	0,42	-0,02	-0,75	-0,62
5	0,20	0,13	-0,75	-0,68
6	0,15	0,05	-0,73	-0,65
7	0,12	0,13	-0,58	-0,82
8	0,50	-0,02	-0,70	-0,92
9	0,08	0,23	-0,72	-0,82
10	0,47	-0,03	-0,58	-0,88
11	0,25	0,12	-0,82	-0,75
12	0,30	0,05	-0,68	-0,85
13	0,33	0,08	-0,83	-0,65

3.5, the lateral drift of the vehicle increases. If we use positive camber values for rear suspension the lateral drift decreases as the positive camber increases.

In Figure 3.6, as positive rear toe increases, the lateral drift of the vehicle decreases. By the way, the rear toe has less effect than the front toe on the lateral displacement of the vehicle. When we use negative toe (toe-out) for rear wheels the lateral drift of the vehicle increased.

In Figure 3.7 it is seen that the road crown has an obvious effect on the lateral displacement of the vehicle. The vehicle drift to a side in which the vehicle has road crown. The road crown effect is more than any other suspension alignment.

These tests show only the individual effects of suspension alignments. However, the suspension alignments can not be considered separately, because all alignments are dependent to each other. So lateral drift analysis should be done taking all the most

Table 3.5. Vehicle parameters

Vehicles	Rear Toe		Rear Camber	
	LH	RH	LH	RH
14	0,33	-0,07	-0,75	-0,80
15	0,30	0,12	-0,83	-0,72
16	0,28	0,03	-0,55	-0,90
17	0,22	0,10	-0,72	-0,78
18	0,15	0,15	-0,63	-0,78
19	0,18	0,12	-0,78	-0,77
20	0,43	-0,10	-0,62	-0,87
21	0,08	0,17	-0,72	-0,77
22	0,22	0,05	-0,73	-0,78
23	0,27	0,12	-0,75	-0,82
24	0,13	0,18	-0,95	-0,63
25	0,28	0,03	-0,63	-0,65
26	0,32	-0,10	-0,73	-0,50
27	0,12	0,20	-0,70	-0,60
28	0,18	0,05	-0,98	-0,62
29	0,15	0,12	-0,90	-0,80
30	0,32	-0,05	-0,93	-0,52
31	0,22	0,08	-0,58	-0,82
32	0,27	-0,02	-0,67	-0,70
33	0,17	0,18	-0,65	-0,77
34	0,17	0,07	-0,68	-0,67
35	0,13	0,03	-0,78	-0,57
36	0,15	0,25	-0,78	-0,60
37	0,33	0,02	-0,80	-0,63
38	0,18	0,13	-0,85	-0,62
39	0,28	0,03	-0,82	-0,80
40	0,20	0,10	-0,82	-0,55

Table 3.6. Vehicle parameters

Vehicles	Rear Toe		Rear Camber	
	LH	RH	LH	RH
41	0,28	-0,05	-0,80	-0,57
42	0,28	-0,02	-0,95	-0,57
43	0,08	0,13	-0,87	-0,67
44	0,20	0,27	-0,85	-0,62
45	0,37	0,02	-0,85	-0,68
46	0,32	0,02	-0,67	-0,55
47	0,32	-0,07	-0,78	-0,82
48	0,12	0,23	-0,72	-0,68
49	0,22	0,13	-0,85	-0,70
50	0,30	0,20	-0,78	-0,72
51	0,32	0,02	-0,82	-0,70
52	0,27	0,13	-0,73	-0,75
53	0,20	0,02	-0,88	-0,50
54	0,30	0,03	-0,80	-0,55
55	0,03	0,30	-0,87	-0,82
56	0,15	0,15	-0,85	-0,68
57	0,20	0,08	-0,90	-0,57
58	0,25	0,08	-0,92	-0,78
59	0,07	0,20	-0,82	-0,65
60	0,20	0,03	-0,85	-0,63
61	0,08	0,10	-0,90	-0,67
62	0,32	0,07	-0,78	-0,58
63	0,27	-0,02	-0,90	-0,70
64	0,22	0,08	-0,85	-0,68
65	0,17	0,15	-0,78	-0,68

effective parameters into account such as toe, camber and caster for both front and rear suspensions. In section 3.1, these parameters are considered together.

Table 3.7. Drift time/lane change (sec)

Vehicles	Experimental Results
1	8
2	9
3	13
4	7
5	13
6	9
7	17
8	9
9	11
10	10
11	10
12	10
13	9
14	9
15	9
16	14
17	10
18	12
19	18
20	7
21	9
22	9
23	8
24	7
25	9
26	11
27	10
28	5

Table 3.8. Drift time/lane change (sec)

Vehicles	Experimental Results
29	10
30	5
31	14
32	10
33	10
34	10
35	5
36	9
37	4
38	9
39	7
40	10
41	4
42	5
43	6
44	9
45	8
46	7
47	11
48	12
49	8
50	10
51	9
52	11
53	5
54	6
55	9
56	12

Table 3.9. Drift time/lane change (sec)

Vehicles	Experimental Results
57	12
58	10
59	8
60	8
61	10
62	7
63	8
64	10
65	11

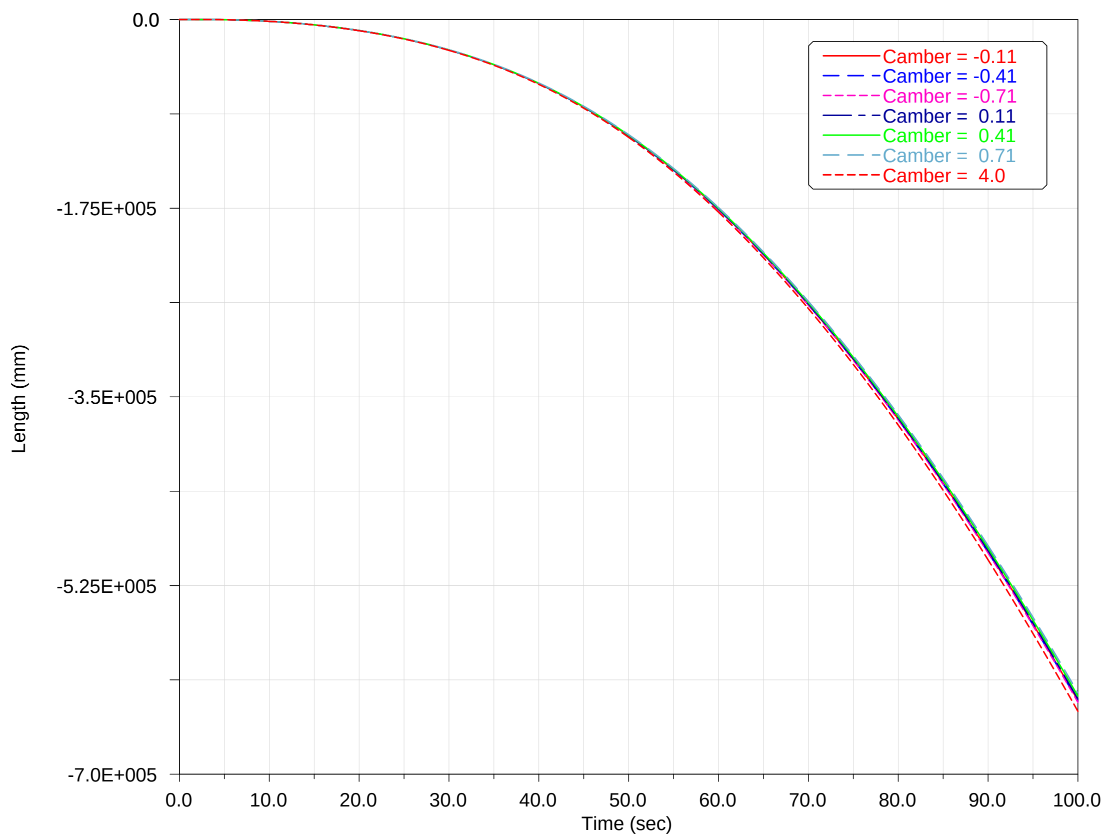

Figure 3.2. Steady state drift test front camber effect

3.3. Steady State Drift Tests in ADAMS

Steady state drift tests are done by setting suspension parameters such as camber, caster, toe according to Table 3.1, Table 3.2, Table 3.3, Table 3.4, Table 3.5, Table 3.6.

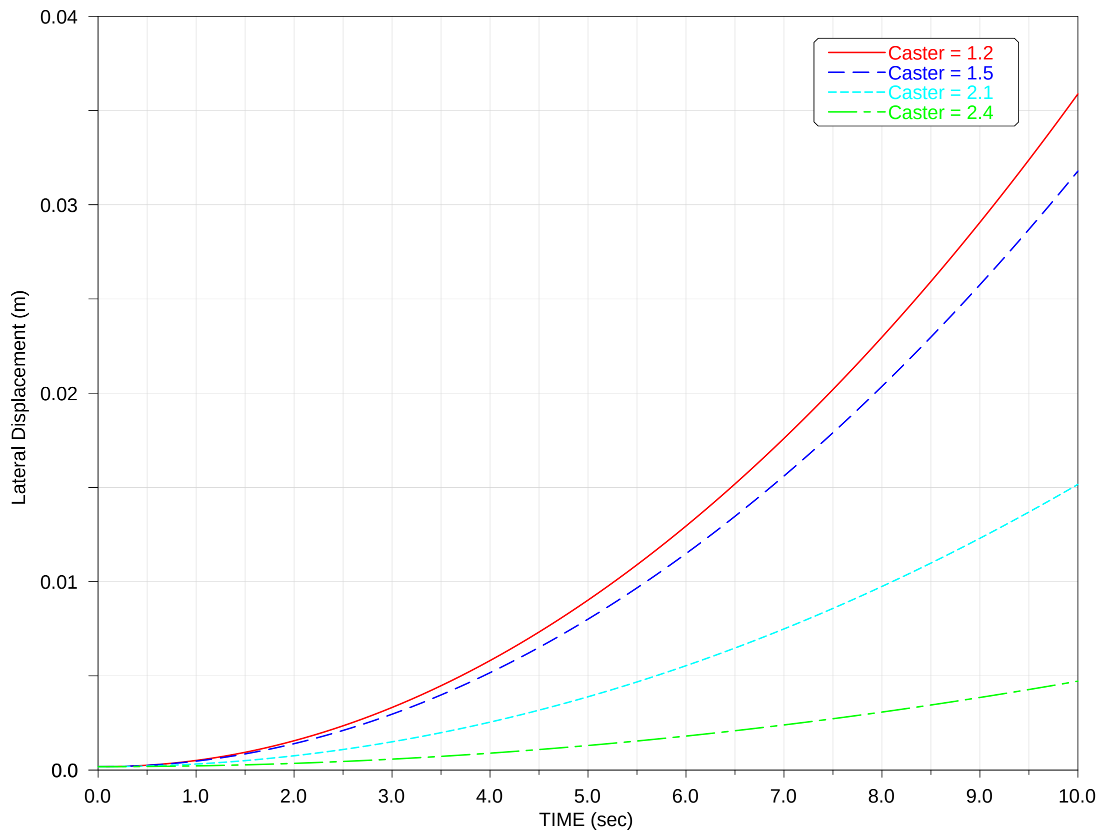

Figure 3.3. Steady state drift test front caster effect

Table 3.10. Nominal suspension values and tolerance range

Front wheel single toe angle	0.11	0.04 to 0.18
Front camber angle	-0.61	-1.11 to -0.11
Front caster angle	1.6	1.35 to 1.85
Rear wheel single toe angle	0.15	0 to 0.3
Rear camber angle	-1.0	-0.75 to -1.25

Drift time of each vehicle in ADAMS analysis will be compared to the real vehicle road tests. The initial velocity of each vehicle is 80 kph during tests.

Nominal values for front toe, front camber, front caster, rear toe and rear camber alignments are shown in Table 3.10.

Figure 3.8, Figure 3.9, Figure 3.10, Figure 3.11, Figure 3.12, Figure 3.13, Figure 3.14, Figure 3.15, Figure 3.16, Figure 3.17 and Figure 3.18 show the steady state drift test results that are done in ADAMS according to real car suspension parameters.

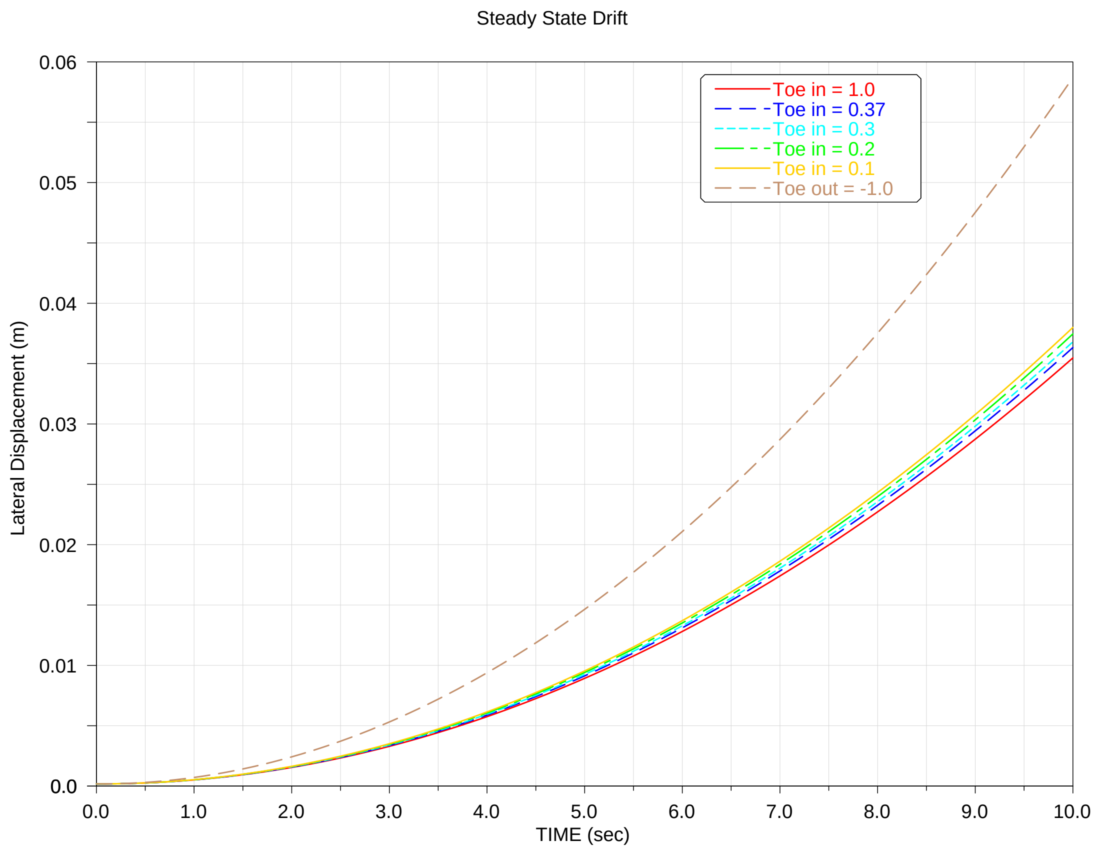

Figure 3.4. Steady state drift test front toe effect

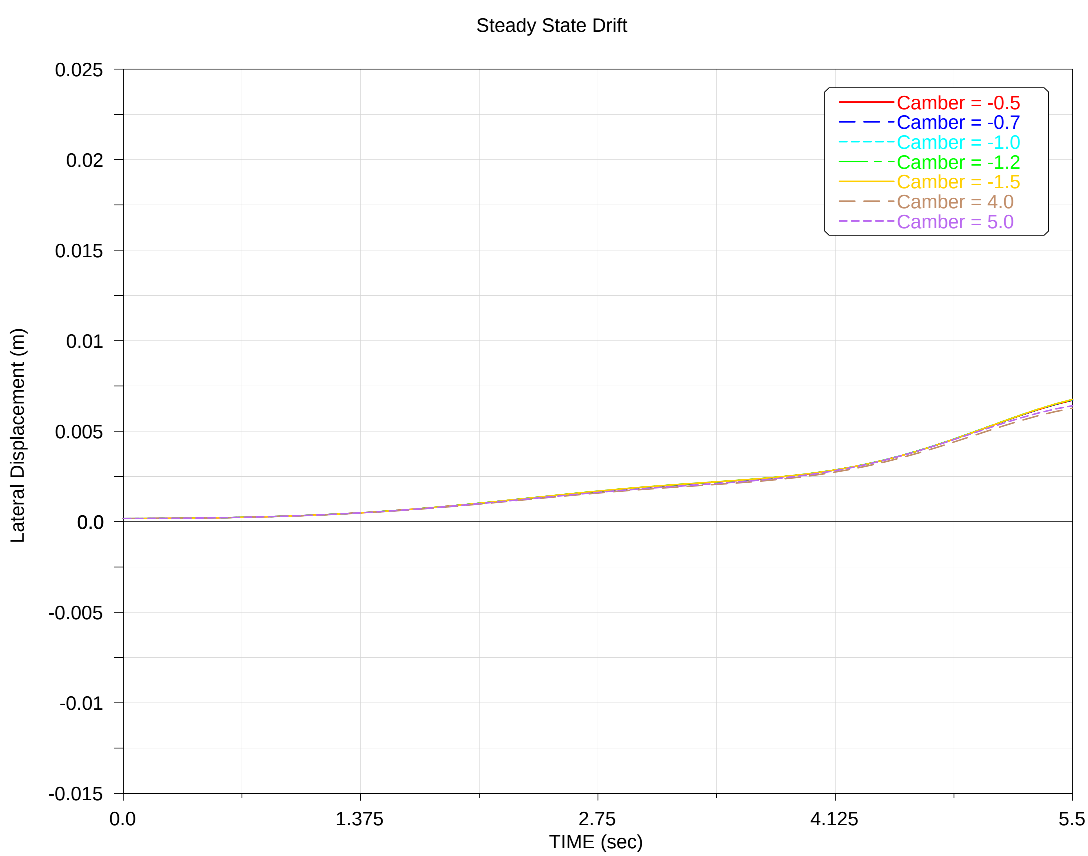

Figure 3.5. Steady state drift test rear camber effect

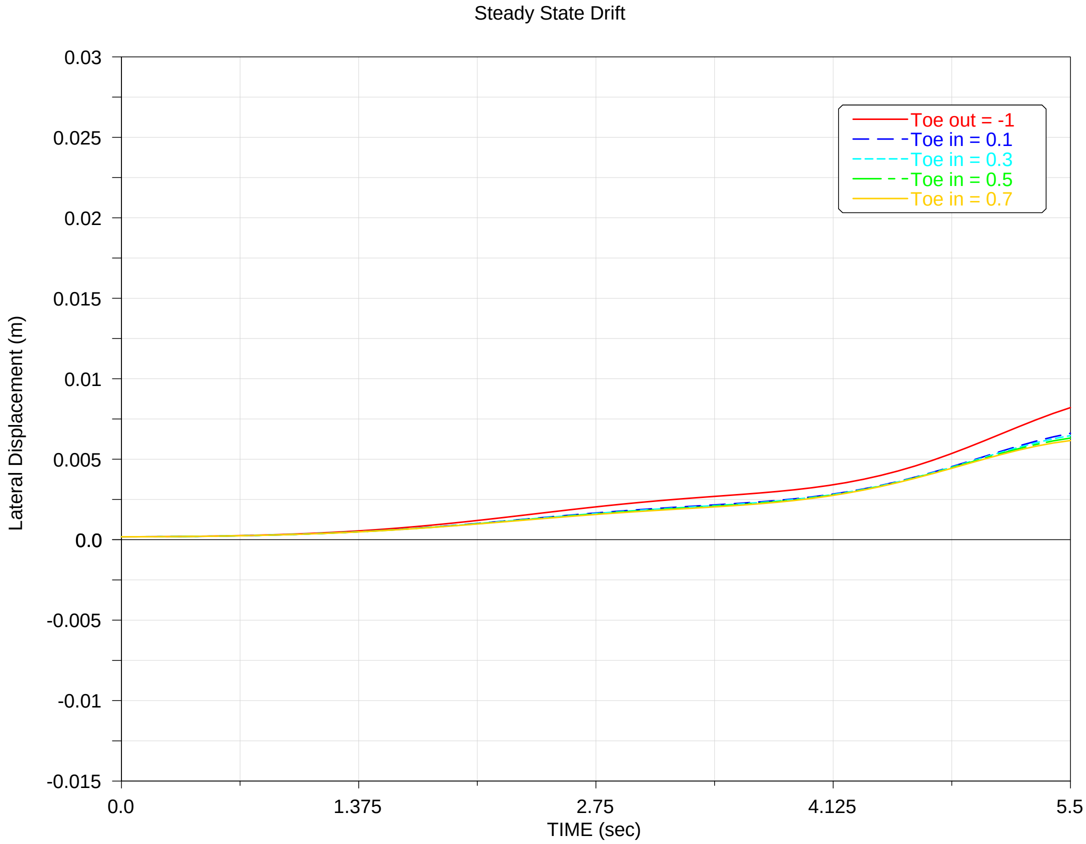

Figure 3.6. Steady state drift rear toe effect

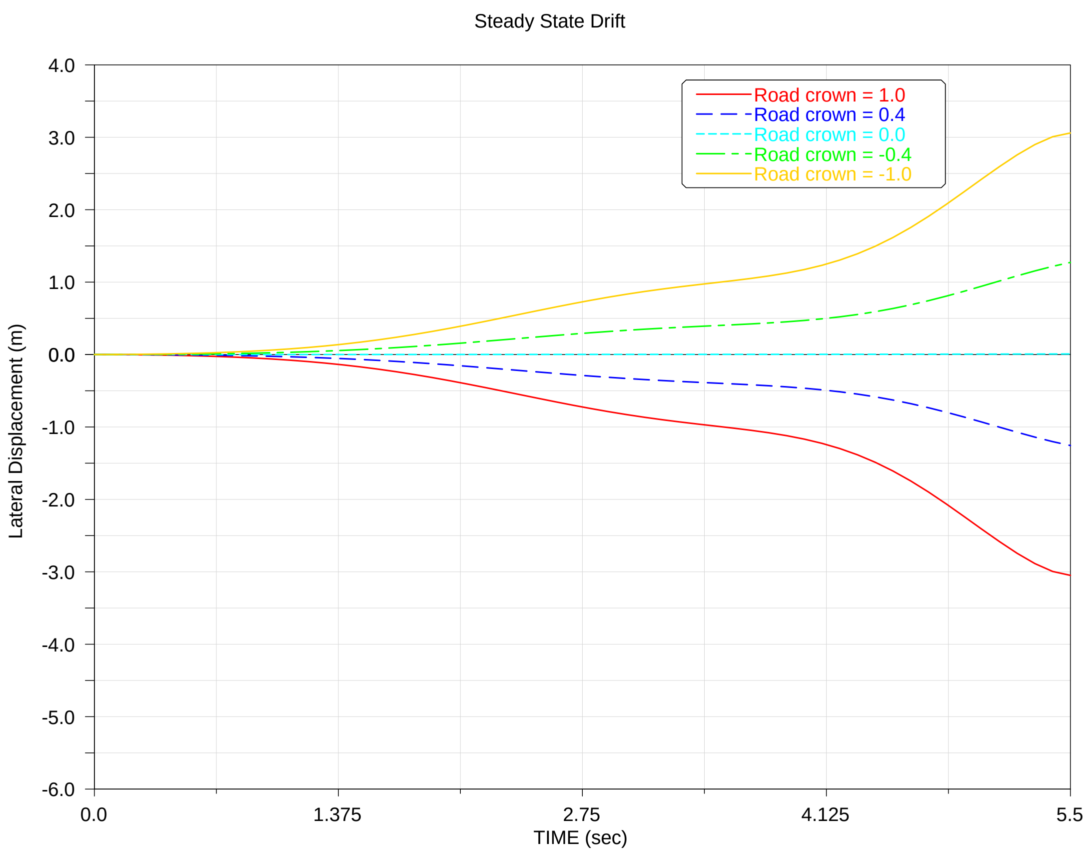

Figure 3.7. Steady state drift road crown effect

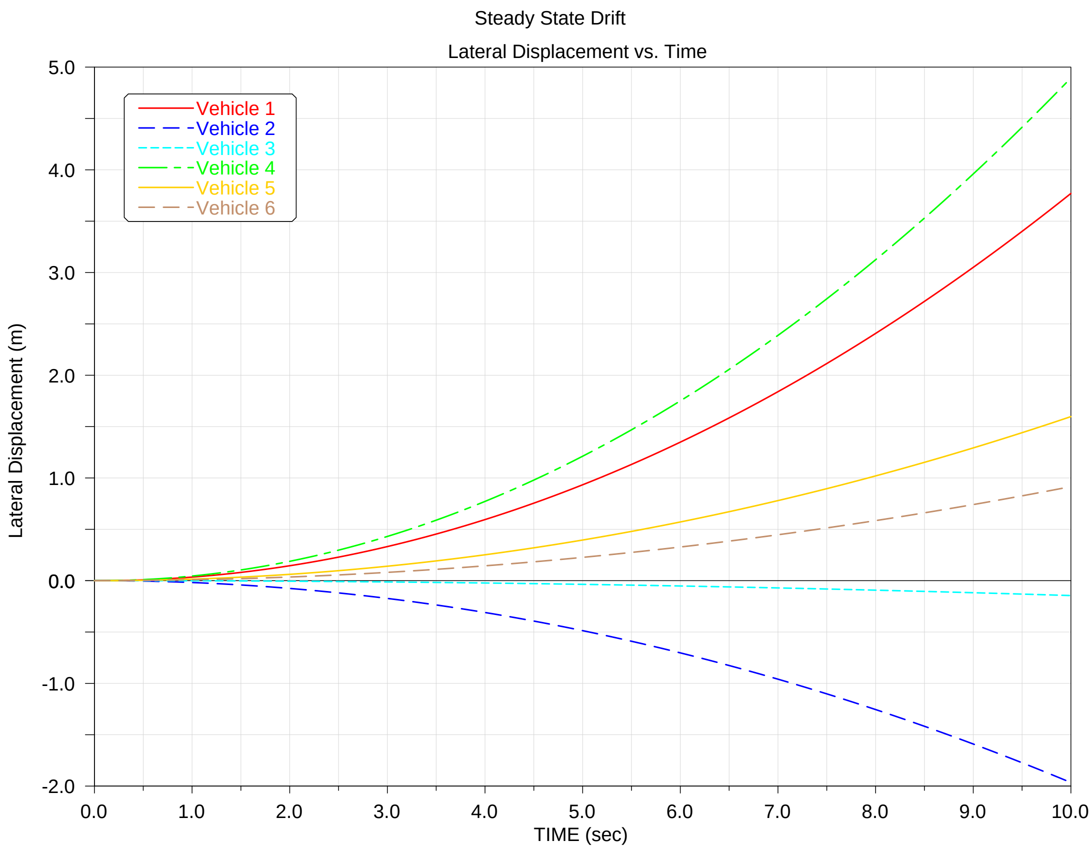

Figure 3.8. Steady state drift test for vehicles 1-2-3-4-5-6

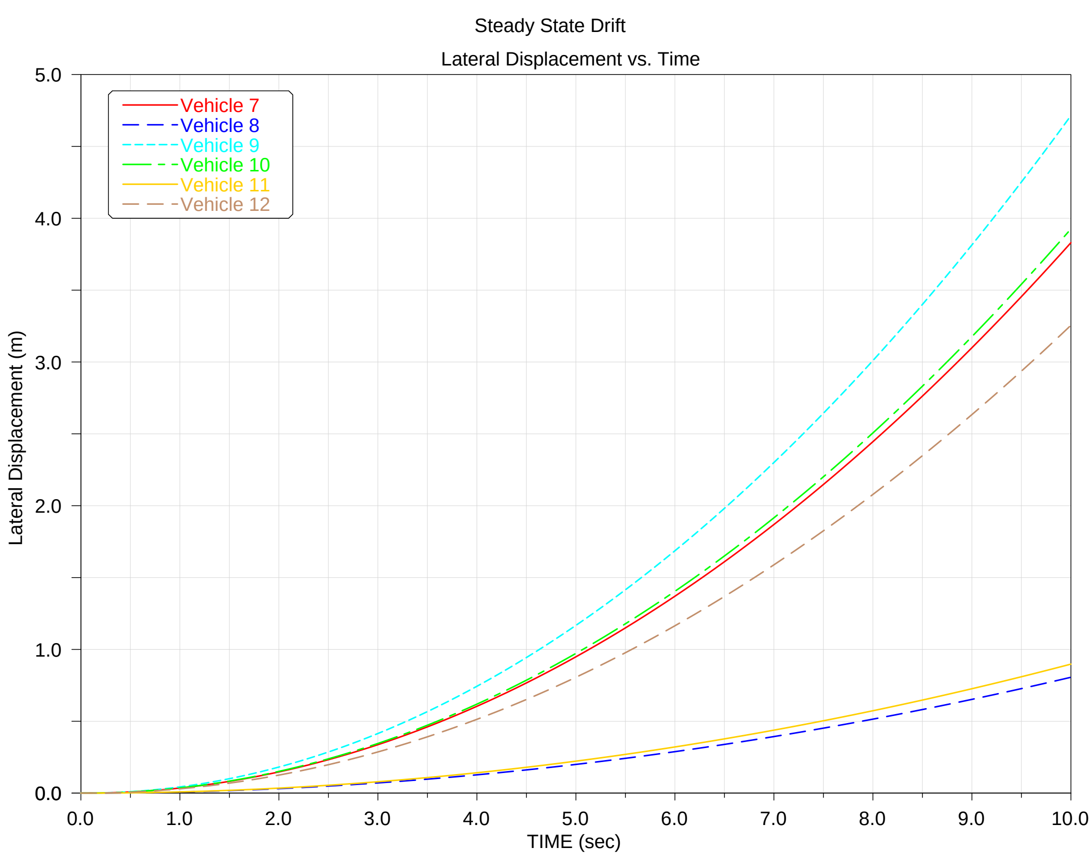

Figure 3.9. Steady state drift test for vehicles 7-8-9-10-11-12

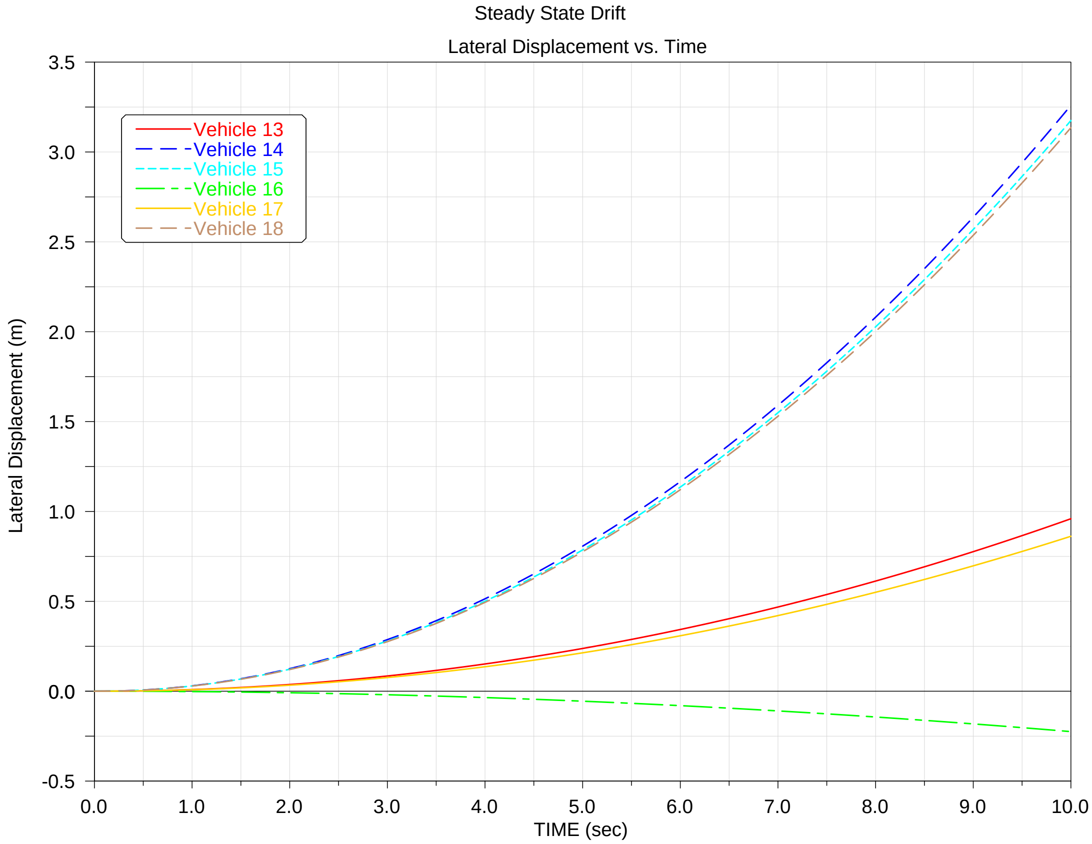

Figure 3.10. Steady state drift test for vehicles 13-14-15-16-17-18

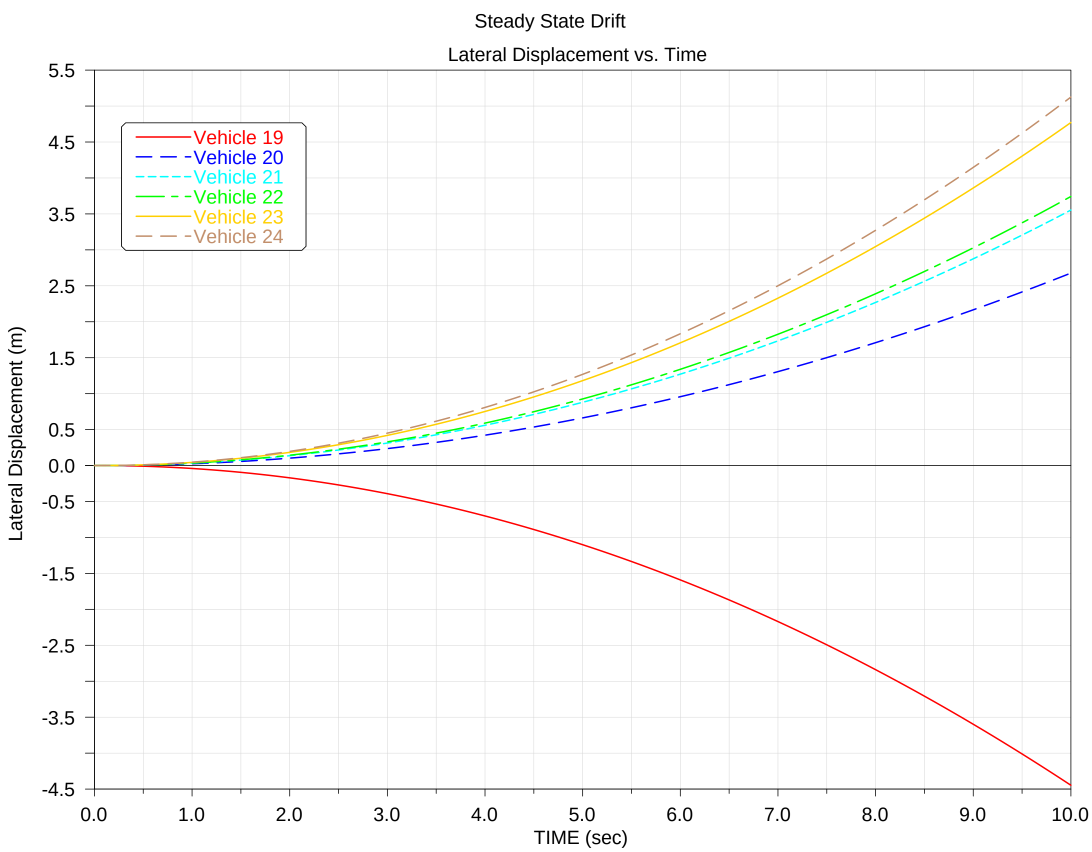

Figure 3.11. Steady state drift test for vehicles 19-20-21-22-23-24

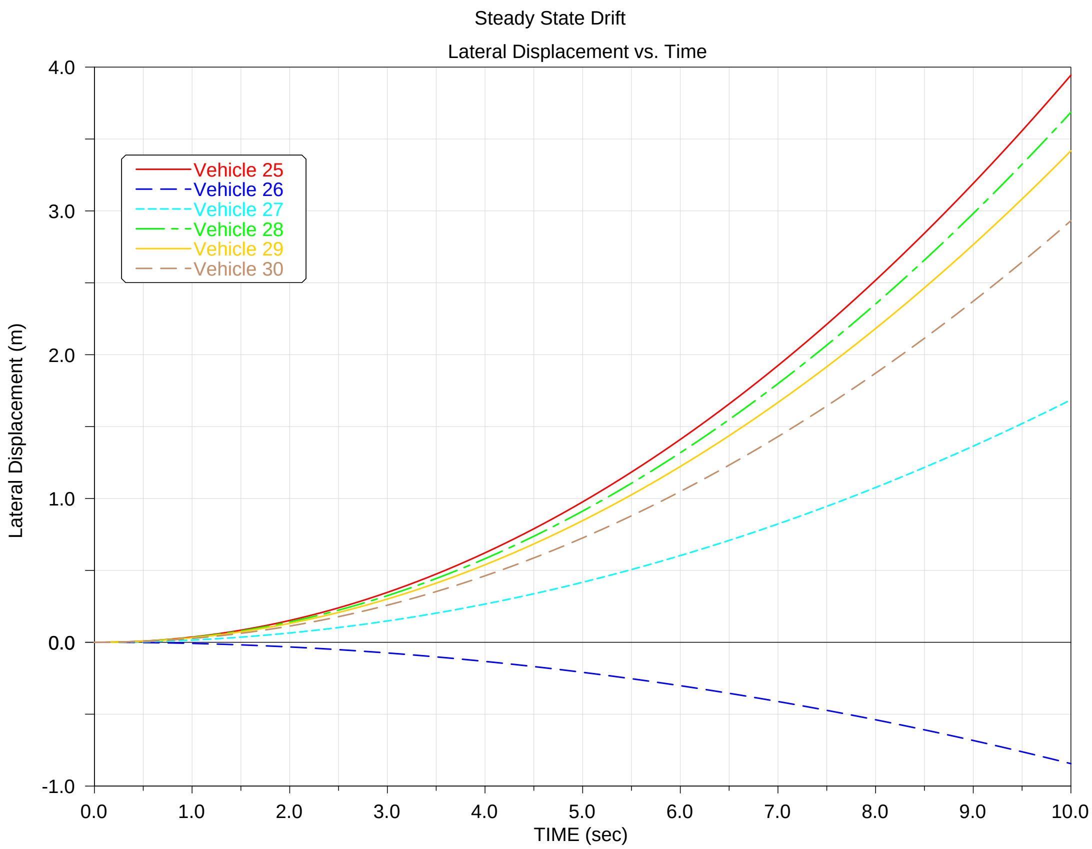

Figure 3.12. Steady state drift test for vehicles 25-26-27-28-29-30

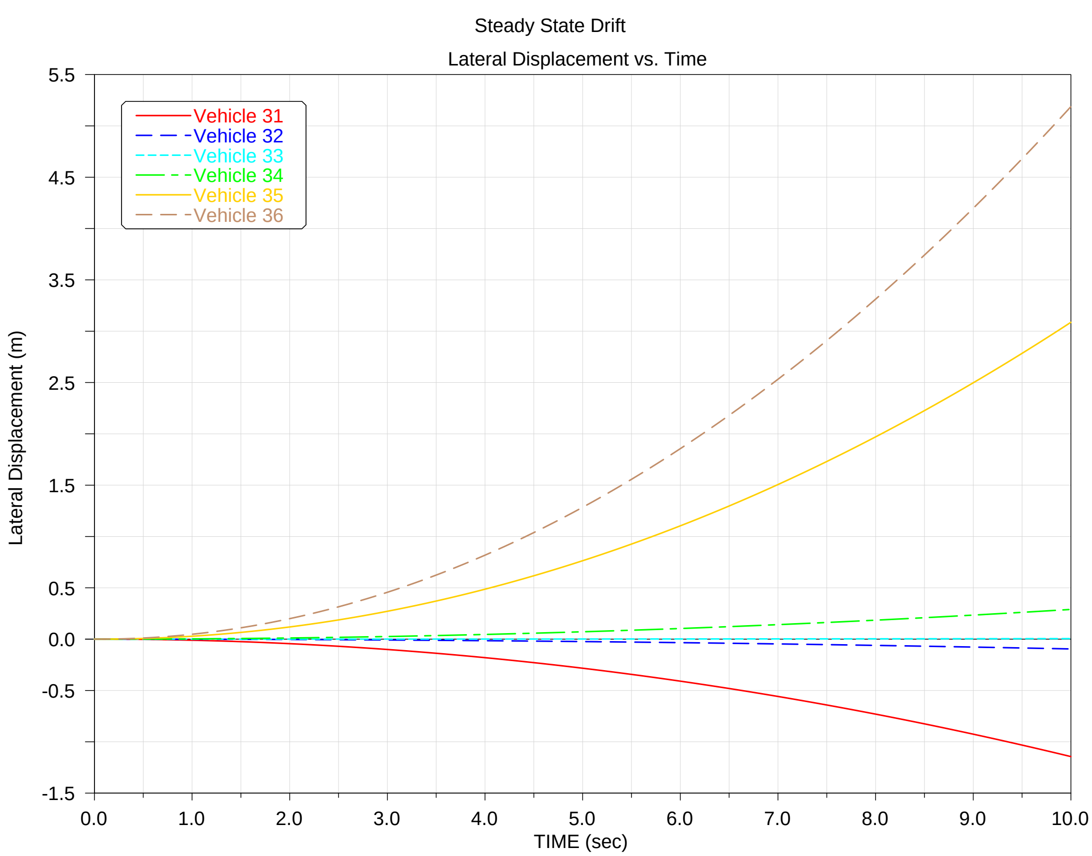

Figure 3.13. Steady state drift test for vehicles 31-32-33-34-35-36

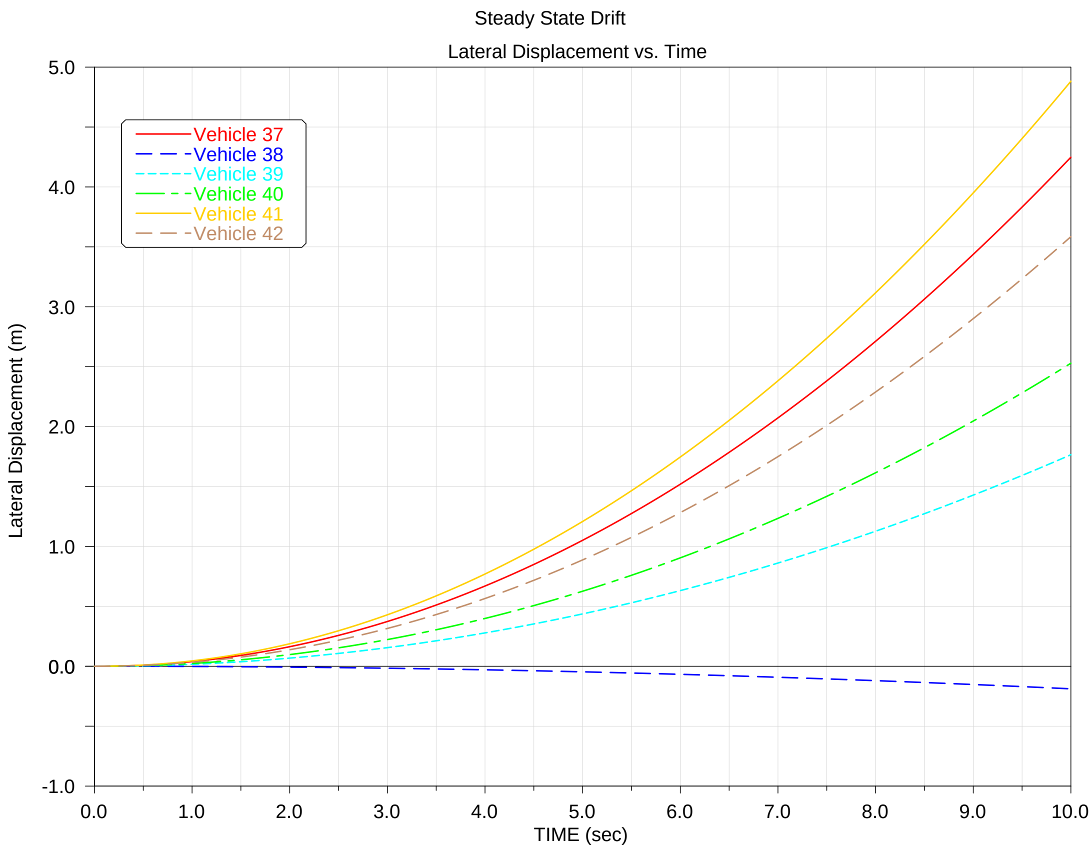

Figure 3.14. Steady state drift test for vehicles 37-38-39-40-41-42

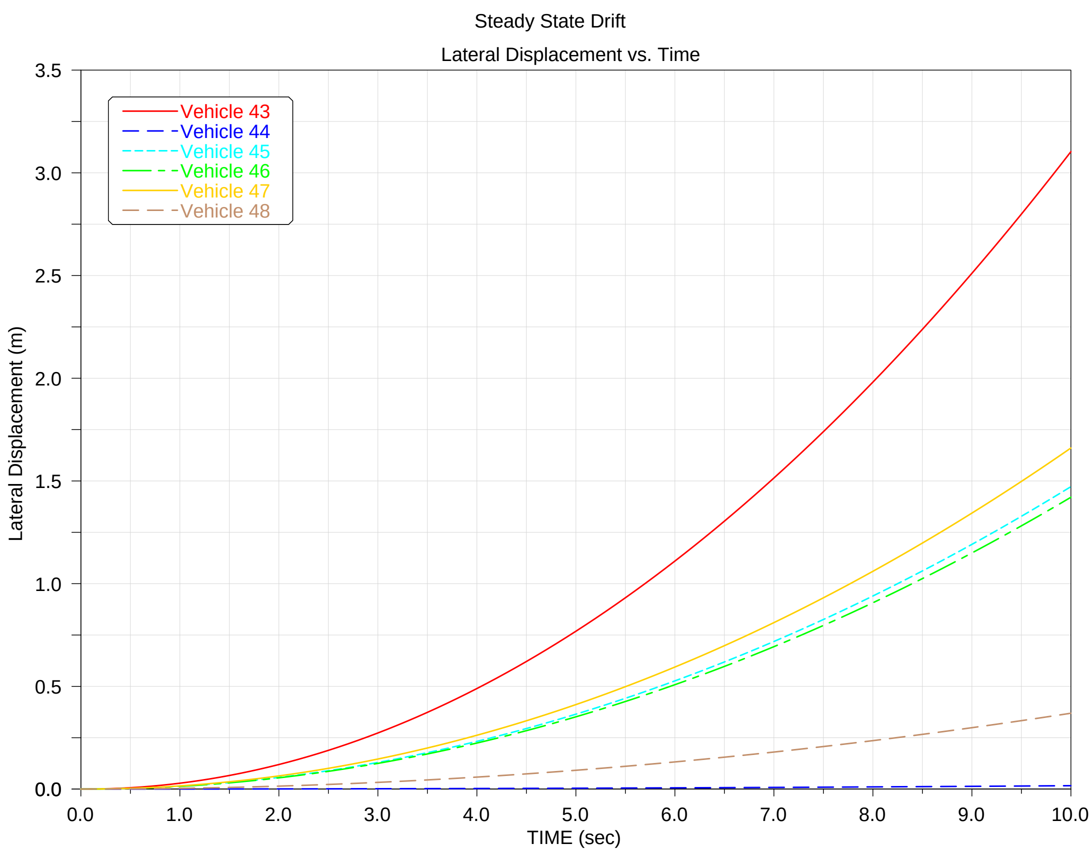

Figure 3.15. Steady state drift test for vehicles 43-44-45-46-47-48

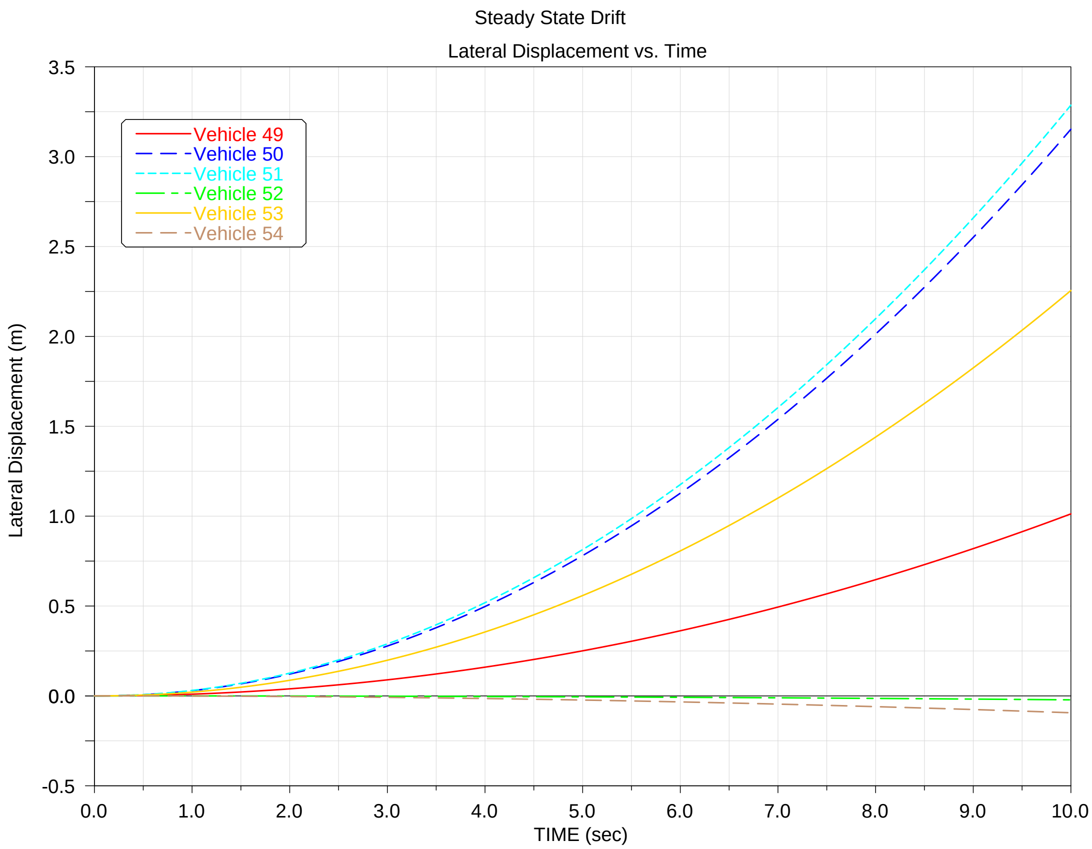

Figure 3.16. Steady state drift test for vehicles 49-50*51-52-53-54

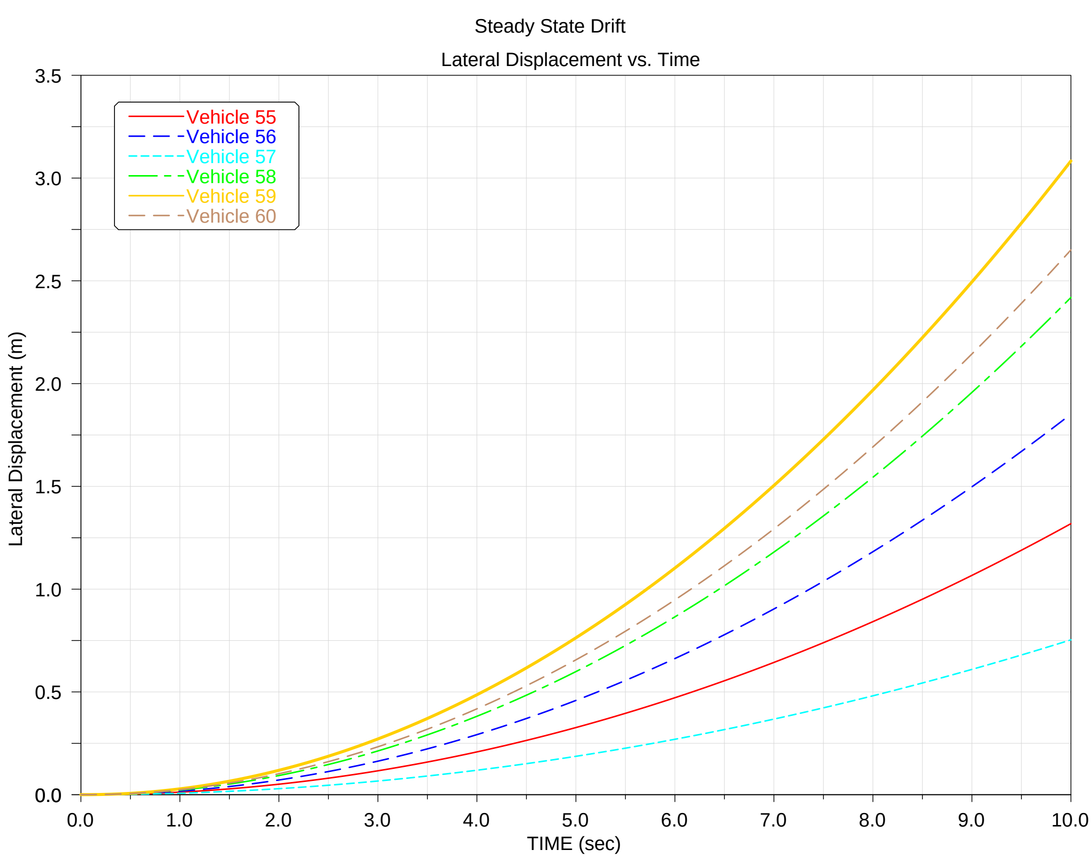

Figure 3.17. Steady state drift test for vehicles 55-56-57-58-59-60

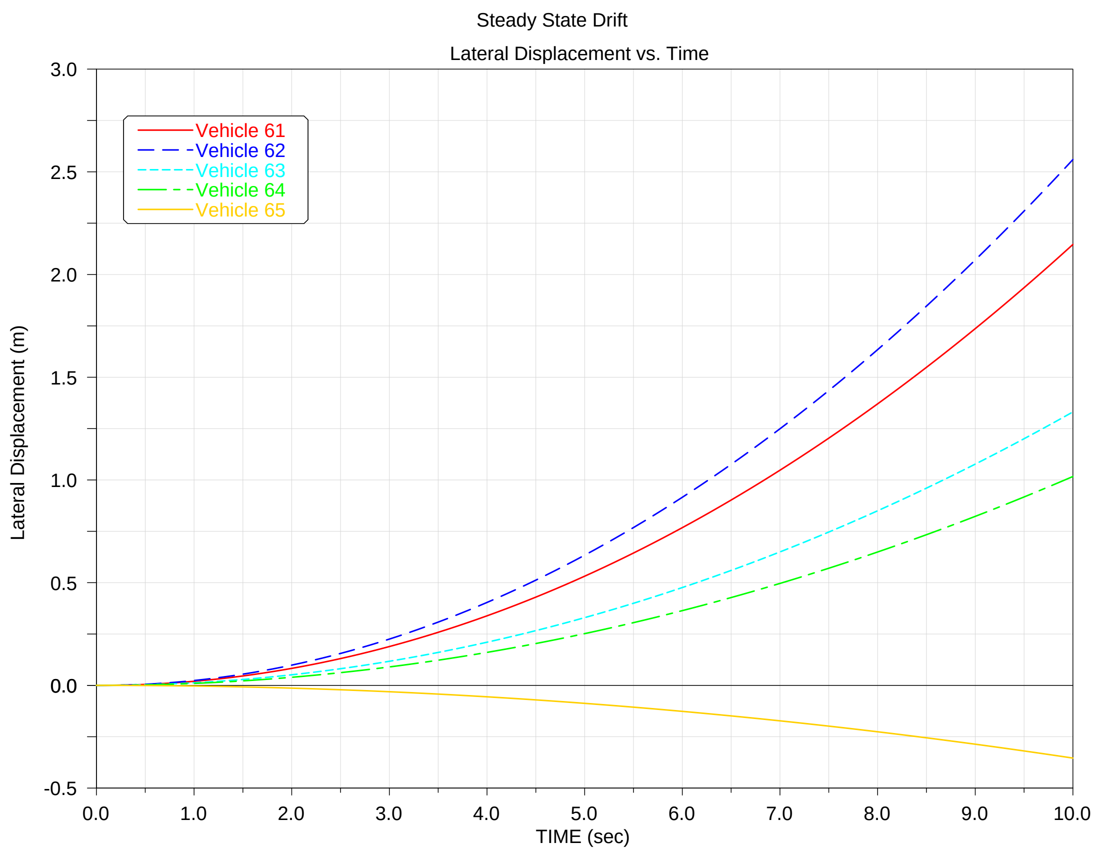

Figure 3.18. Steady state drift test for vehicles 61-62-63-64-65

3.4. Comparison of Road Test and ADAMS Results

In Figure 3.19 road test results and ADAMS results are plotted for 65 different vehicles studied. The trend of results that are obtained from both road tests and ADAMS are consistent with each other. At test vehicles number $3-16-32-33-44-52$ the ADAMS drift time results have peak values. When the vehicles number $3-16-32-33-44-52$, the misalignment in the suspension parameters of these vehicles are at tolerance limits. In general, ADAMS results for one lane change time are consistently higher than the measurements obtained at road tests. This might have occurred as a result of two reasons. One of them is the sensitivity of road tests to external effects such as wind, unbalanced tire pressures and road crown. The other reason can be the lack of precision in measurements. On the other hand, the software requests some inputs such as the suspension geometry (camber, caster, toe) and the initial values for position, velocity, acceleration with which it starts to solve equations of motion obtained by Lagrange dynamics, and these inputs should satisfy all constraint equations. If the constraints are not satisfied, new initial values that satisfy constraint equations are used by the program that are obtained by using Newton-Raphson iteration method. The difference between user's actual input and the input modified and used can cause a difference in results by the program. The changed parameters should be checked if there is a big difference between the parameter values that are changed by ADAMS and the input values.

ADAMS results vs road test results are plotted in Figure 3.20. When a trend line is fitted, the R^2 value is 0.45. This shows the difference between ADAMS results and road test results plotted in Figure 3.19. The difference can be due to noise effects such as wind and road crown that are present on Ford-Otosan's test area. In general, the data in the left bottom region of Figure 3.20 are close to each other. However, there are some results that affect the consistency more. The road tests should be repeated on a road with zero wind and road crown. In Section 3.5, steady state drift test results are evaluated for statistically to see which parameters are more effective on drift time of the vehicle. MINITAB is used as the statistical analysis tool to search for the relation between suspension parameters.

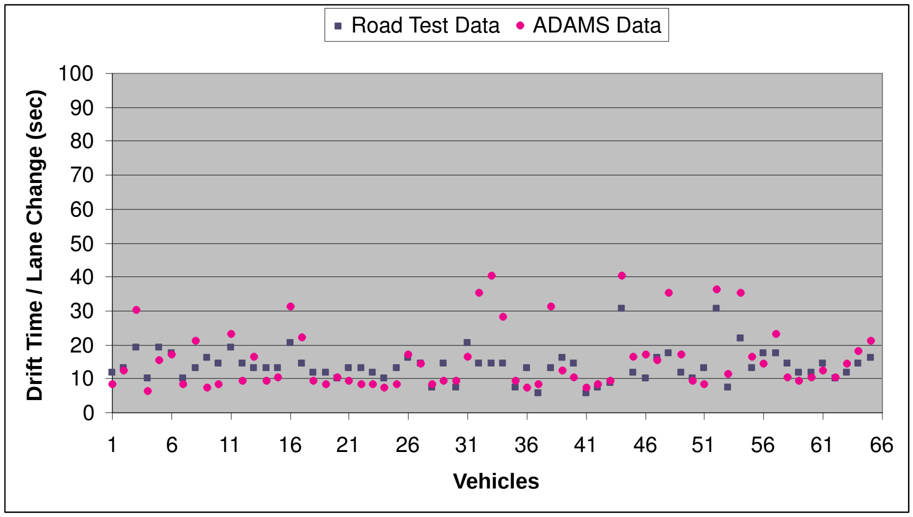

Figure 3.19. Comparison of ADAMS data and experimental data

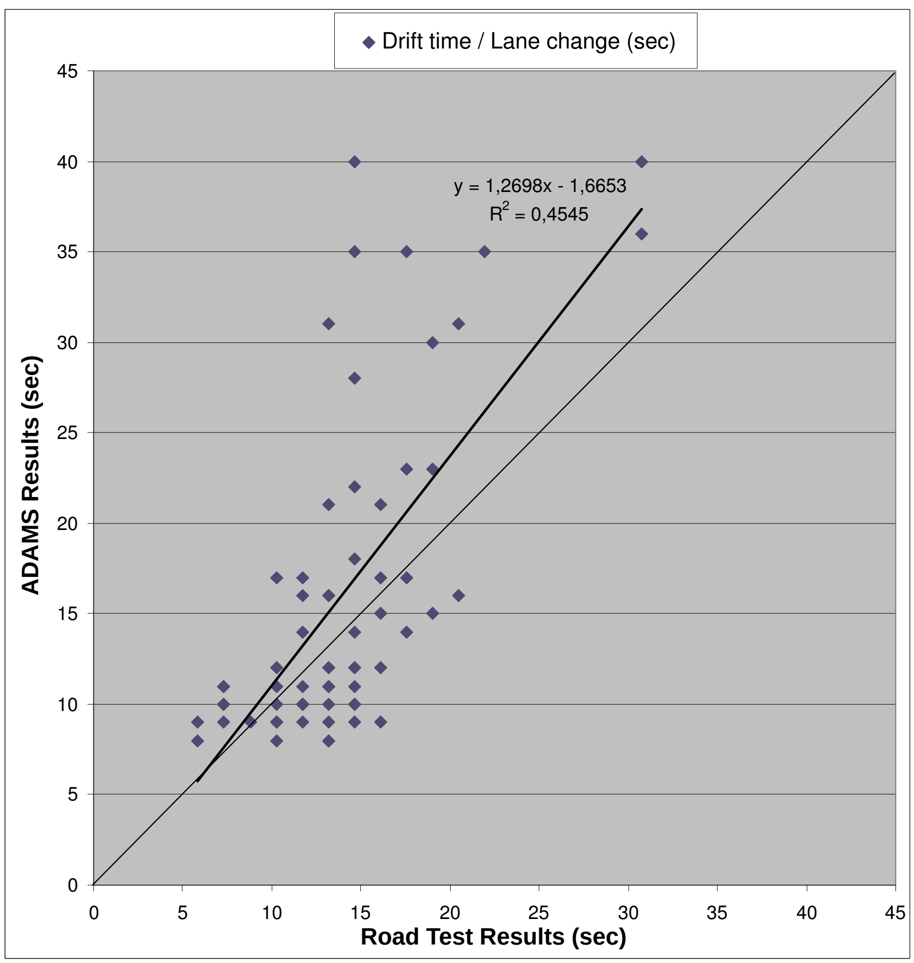

Figure 3.20. Comparison of ADAMS data and experimental data

3.5. Statistical Analysis of Steady State Drift Tests

In Minitab, the reliability parameter α is selected to be 0.1 to obtain a confidence of 90 percent. The regression data in Table 3.11 are obtained using MINITAB. If probability value, p, in Table 3.11 is smaller than the selected α, then this parameter is regarded as significant. In Table 3.11 p values for parameters are smaller than 0.1 except for front caster, front camber, front toe and front camber, front toe and rear toe, front camber and rear camber. In Table 3.12 analysis of variance is shown for the regression analysis. The p values in Table 3.12 are all smaller than α. Using the regression analysis results the coefficients for lateral drift time equation is derived. This shows us that regression analysis fits a curve that is close to our road test results as shown in Figure 3.21.

According to p values and T values in Table 3.11, front toe, rear camber, front camber and front caster interaction, front caster and rear toe interactions are selected as the significant parameters on lateral drift. These parameters are ordered according to their importance using stepwise regression analysis in Table 3.13-3.14. The regression is established using field test data of Tables 3.1-3.9. The result of stepwise regression that uses two steps are tabulated in Table 3.13 where front toe, rear camber and front caster-rear toe interaction are significant parameters. In Table 3.14 stepwise regression results where six steps are shown. The dominant parameter is seen to be the rear toe. The second important parameter is front toe, the third parameter is front camber, fourth parameter is front caster and the least important parameter is rear camber, among the parameters used.

Table 3.11. Estimated effects and coefficients for drift time

Term	Coefficient	T	P
Constant	7.171	49.739	0
F1	0.525	4.211	0,00
F2	-0.106	-0.345	0,739
F3	0,125	0.627	0,548
F4	1.068	2.087	0,070
F5	0,708	3.556	0,007
F1*F2	0,076	0.251	0.808
F1*F3	1.012	4.364	0,002
F1*F4	-0.488	-0.966	0.362
F1*F5	-0.654	-2.820	0,022
F2*F3	1.363	3.714	0.006
F2*F4	-1.396	-0.798	0.448
F2*F5	0.863	2.351	0.047
F3*F4	-3.729	-6.098	0.000
F3*F5	0.630	1.912	0.092
F4*F5	-0.593	-2.283	0.052

F1: Front toe difference, F2: Front camber difference,

F3: Front caster difference, F4: Rear toe difference, F5: Rear camber difference

Table 3.12. Analysis of variance for drift time

Source	DF	Seq SS	Adj SS	Adj MS	F	P
Regression	15	20.7944	20.7944	1.38629	9.91	0.001
Linear	5	6.0448	5.3437	1.06873	7.64	0.006
Interaction	10	14.7496	14.7496	1.47496	10.55	0.001
Residual error	8	1.1190	1.1190	0.13987		
Total	23	21.9133				

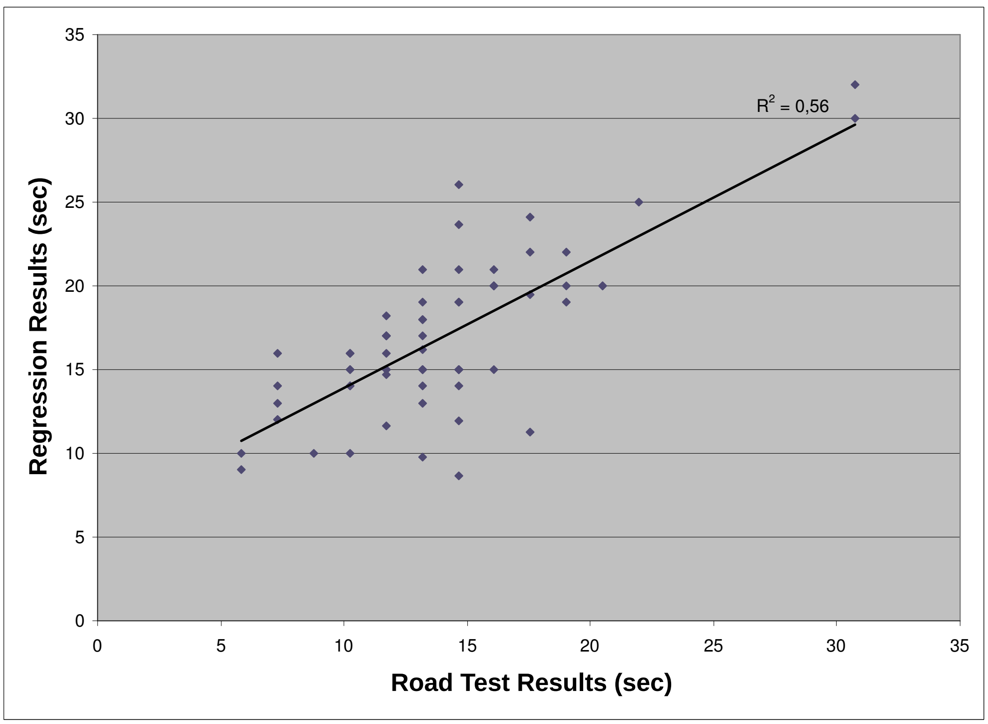

Figure 3.21. Comparison of road test results and regression results

Table 3.13. Stepwise regression table

Step	1	2
Constant	7.237	7.172
Front Toe	0.37	0.44
T-Value	1.63	2.06
P-Value	0.119	0.053
Rear camber	0.24	0.23
T-Value	0.70	0.72
P-Value	0.491	0.477
Front caster*Rear toe	-3.6	-3.4
T-Value	-3.13	-3.20
P-Value	0.005	0.005
Rear Toe	1.08	
T-Value	2.01	
P-Value	0.059	
S	0.829	0.773
R-Sq	37.24	48.22
R-Sq(adj)	27.83	37.32

Table 3.14. Stepwise regression

Step	1	2	3	4	5	6
Constant	7,140	7,133	7,119	7,184	7,391	7,417
Front Toe	0,47	0,47	0,47	0,40		
T-Value	1,73	1,78	1,80	1,56		
P-Value	0,100	0,091	0,087	0,134		
Front Camber	-0,46	-0,46	-0,46			
T-Value	-1,08	-1,11	-1,13			
P-Value	0,295	0,282	0,273			
Front Caster	0,31	0,31				
T-Value	0,80	0,82				
P-Value	0,433	0,424				
Rear Toe	1,49	1,49	1,50	1,20	1,03	
T-Value	2,11	2,17	2,19	1,90	1,60	
P-Value	0,049	0,043	0,040	0,072	0,124	
Rear Camber	0,14					
T-Value	0,37					
P-Value	0,717					

4. CONCLUSIONS

Road tests and computations showed that the combination of front toe difference, front caster difference and rear toe difference dominate the lateral drift of the vehicle. If the parameters are taken into account one by one, the importance of parameters from the most important one to the least important one can be ordered as rear camber difference, front toe difference, front camber difference, rear toe difference and front caster difference. However, when these parameters are taken into account individually, they do not have much effect on lateral drift. Therefore, the combined effect of these parameters should be analyzed. Because effect of combination of three parameters is difficult to model. One should check the interaction between two suspension parameters that has an effect close to the effect of three combined suspension parameters. As a result, a stepwise regression with two steps is done and the results are tabulated in Table 3.13; front toe, rear camber, front caster and rear toe interaction are determined to be the significant parameters. In Table 3.14 results of a stepwise regression with six steps are shown. According to results in Table 3.14, the dominant parameter is rear toe. The second important parameter is front toe, the third parameter is front camber, forth parameter is front caster and the least important parameter is rear camber.

Misalignment of the suspension parameters arises from the production stage. According to information obtained from manufacturer, the misalignment in camber angle is based on the production failure of knuckle and hardpoint location of top mount. The other parameter is the toe angle which is the only adjustable parameter in front suspension after the production of the vehicle; the misalignment in toe angle can be corrected. However, toe angle in rear suspension is not adjustable. The spindle geometry has the toe and camber angles. Lastly, the least important parameter affecting drift within the ones that have been investigated is caster. This parameter depends on the hardpoint location of top mount depending on bolt joint location tolerances on the chassis. As a result, correction of only one parameter is not sufficient in improving lateral drift motion of a vehicle. Combination of these parameters provides us a better handling performance.

In this study, the only parameters of interest that affect vehicle handling are camber, caster and toe. However, there are several other effects such as front ride height difference, center of gravity height, wheelbase, track width, conicity, ply-steer residual aligning torque, tire pressure side-to-side difference, road crown, and lateral forces resulting from vehicle aerodynamics that should be analyzed on handling of a vehicle. The combination of these effects will definitely give us a better vehicle handling performance. So, a future study may focus on considering the effects of these parameters that have not been investigated in this study.

REFERENCES

1. Becker, G., H. Fromm and H. Maruhn,"Vibrations of the Steering Systems of Automobiles", Berlin, 1931.

2. Oley, M., "Stable and Unstable Steering", General Motors Corp., 1937.

3. Segel, L., "Research in the Fundamentals of Automobile Control and Stability", *SAE National Summer Meeting*, Atlantic City, 1956.

4. Whitcomb, D.W. and F.M. William, "Design Implications of a General Theory of Automobile Stability and Control", *Proceeding of Automobile Division*; The Institution of Mechanical Engineers, (7):367-391, 1956.

5. Radt, H.S., and W.F. Milliken, "Exactly What Happens When An Automobile Skids?", *SAE Journal*, pp. 27-33, 1960.

6. Goland, M. and F. Jindra, "Car Handling Characteristics", *Automobile Engineer*, 51(8):296-302, 1961.

7. Weir, D.H. and T.M. Duane, "Dynamics of The Automobile Related to Driver Control", *Transactions of The Society of Automotive Engineers*, SAE 680194.

8. Tiffany, N.O., G.A. Cornell and R.L. Code, "A Hybrid Simulation of Vehicle Dynamics and Subsytems", *SAE Technical Paper Series*, 700155.

9. McHenry, R. and N. Deleys, "Vehicle Dynamics in Single Vehicle Accidents", *Cornell Aeronautical Laboratory Inc.*, Technical Report CAL No. VJ-2251-V-3, 1968.

10. Okada, T., T. Takiguchi, M. Nishioka and G. Utsumomiya, "Evaluation of Vehicle Handling and Stability by Computer Simulation at First Stage of Vehicle Planning", *SAE Technical Paper Series*, 730525.

11. Speckhart, F.H., "A Computer Simulation for Three-Dimensional Vehicle Dynamics", *SAE Technical Paper Series*, 730526.

12. Morman, K.N., "Non-Linear Model Formulation for The Static and Dynamic Analysis of Front Suspensions", *SAE Technical Paper Series*, 770052.

13. Allen, R.W., T. Szostak, T.J Rosenthal and D.E. Johnston, "Test Methods and Computer Modeling for The Analysis of Ground Vehicle Handling", *SAE Technical Paper Series*, 861115.

14. Nalecz, A.G., "Investigation into The Effects of Suspension Design on Stability of Light Vehicles", *SAE Techinical Paper Series*, 870497.

15. Nalecz, A.G., "Development and Validation of Light Vehicle Dynamics Simulation (LVDS)", *SAE Technical Paper Series*, 920056.

16. Allen, R.W., T.J. Rosenthal, D.H. Klyde, K.J. Owens and T.H. Szostak, "Validation of Ground Vehicle Computer Simulations Developed for Dynamics Stability Analysis", *SAE Technical Paper Series*, 920054.

17. Allen, R.W., T.J. Rosenthal, D.H. Klyde, K.J Owens and H.T Szostak, "Characteristics Influencing Ground Vehicle Lateral/Directional Stability", *SAE Technical Paper Series*, 910234.

18. Allen, R.W. and T.J. Rosenthal, "A Computer Simulation Analysis of Safety Maneuvers for Assesing Ground Vehicle Dynamic Stability", *SAE Technical Paper Series*, 930760.

19. Heydinger, G.J., W.R Garrot, J.P Chrstos, D.A Guenther, "A Methodology for Validating Vehicle Dynamics Simulations", *SAE Technical Paper Series*, 900128.

20. Heydinger, G.J., P.A Grygier and S. Lee, "Pulse Testing Techniques Applied to Vehicle Handling Dynamics", *SAE Technical Paper Series*, 930828.

21. Clover, C.L. and E. Bernard, "The Influence of Lateral Load Transfer Distribution on Directional Response", *SAE Technical Paper Series*, 930763.

22. Allen, R.W., T.J Rosenthal, D.H Klyde, K.J Owens and H.T Szostak, "Characteristics Influencing Ground Vehicle Lateral/Directional Stability", *SAE Technical Paper Series*, 910234.

23. Antoun, R.J., P.B Hackert, M.C O'Leary and A. Sitchin, "Vehicle Dynamic Handling Computer Simulation-Model Development, Correlation, and Application Using ADAMS", *SAE Technical Paper Series*, 860574.

24. Yoshinori, M. and H. Matsushita, "A Simulation System for Vehicle Dynamics Control", *SAE Technical Paper Series*, 910240.

25. Hegazy, S., H. Rahnejat and K. Hussain, "Multi-Body Dynamics in Full-Vehicle Handling Analysis", *Proceedings Institution of Mechanical Engineers*, ,Volume 213, Part K., 1999.

26. Allen, R.W., T.J Rosenthal, D.H Klyde and J.R Hogue, "Computer Simulation Analysis of Light Vehicle Lateral Directional Dynamic Stability", *SAE Technical Paper Series*, 1999-01-0124.

27. Gillespie, T.D., "Fundementals of Vehicle Dynamics", *Warrandale, PA: Society of Automotive Engineers*, 1992.

28. Longoria, R.G., "Extended Vehicle Handling Models, 3-DOF Model, Roll Stability Course Notes", Department of Mechanical Engineering, The University of Texas at Austin, 2003.

29. Barak, P., N. Panakanti and T. Desai, "Effect of Chassis Design Factors (CDF) on the Ride Quality Using a Seven Degree of Freedom Vehicle Model", *SAE Technical Paper Series*, 2004-01-1555.

30. Park, J., "Enhancement of Vehicle Handling Dynamics Model Using Global Search-

ing Algorithm and Estimation Theory", PhD Dissertation, Ohio State University, 2002.

31. Blundell, M.V., "The Modeling and Simulation of Vehicle Handling Part 1:Analysis Methods", *Proceedings Institution of Mechanical Engineers*, 1999, Volume 213.